UNIVERSITAT POLITÈCNICA DE CATALUNYA
BARCELONATECH

Functionalization of titanium with integrin-selective ligands for orthopedic and dental applications

Roberta Fraioli

ADVERTIMENT La consulta d'aquesta tesi queda condicionada a l'acceptació de les següents condicions d'ús: La difusió d'aquesta tesi per mitjà del repositori institucional UPCommons (http://upcommons.upc.edu/tesis) i el repositori cooperatiu TDX (http://www.tdx.cat/) ha estat autoritzada pels titulars dels drets de propietat intel·lectual **únicament per a usos privats** emmarcats en activitats d'investigació i docència. No s'autoritza la seva reproducció amb finalitats de lucre ni la seva difusió i posada a disposició des d'un lloc aliè al servei UPCommons o TDX.No s'autoritza la presentació del seu contingut en una finestra o marc aliè a UPCommons (*framing*). Aquesta reserva de drets afecta tant al resum de presentació de la tesi com als seus continguts. En la utilització o cita de parts de la tesi és obligat indicar el nom de la persona autora.

ADVERTENCIA La consulta de esta tesis queda condicionada a la aceptación de las siguientes condiciones de uso: La difusión de esta tesis por medio del repositorio institucional UPCommons (http://upcommons.upc.edu/tesis) y el repositorio cooperativo TDR (http://www.tdx.cat/?locale-attribute=es) ha sido autorizada por los titulares de los derechos de propiedad intelectual **únicamente para usos privados enmarcados** en actividades de investigación y docencia. No se autoriza su reproducción con finalidades de lucro ni su difusión y puesta a disposición desde un sitio ajeno al servicio UPCommons No se autoriza la presentación de su contenido en una ventana o marco ajeno a UPCommons (*framing)*. Esta reserva de derechos afecta tanto al resumen de presentación de la tesis como a sus contenidos. En la utilización o cita de partes de la tesis es obligado indicar el nombre de la persona autora.

WARNING On having consulted this thesis you're accepting the following use conditions: Spreading this thesis by the institutional repository UPCommons (http://upcommons.upc.edu/tesis) and the cooperative repository TDX (http://www.tdx.cat/?locale-attribute=en) has been authorized by the titular of the intellectual property rights **only for private uses** placed in investigation and teaching activities. Reproduction with lucrative aims is not authorized neither its spreading nor availability from a site foreign to the UPCommons service. Introducing its content in a window or frame foreign to the UPCommons service is not authorized (framing). These rights affect to the presentation summary of the thesis as well as to its contents. In the using or citation of parts of the thesis it's obliged to indicate the name of the author.

PhD thesis

Functionalization of titanium with integrin-selective ligands for orthopedic and dental applications

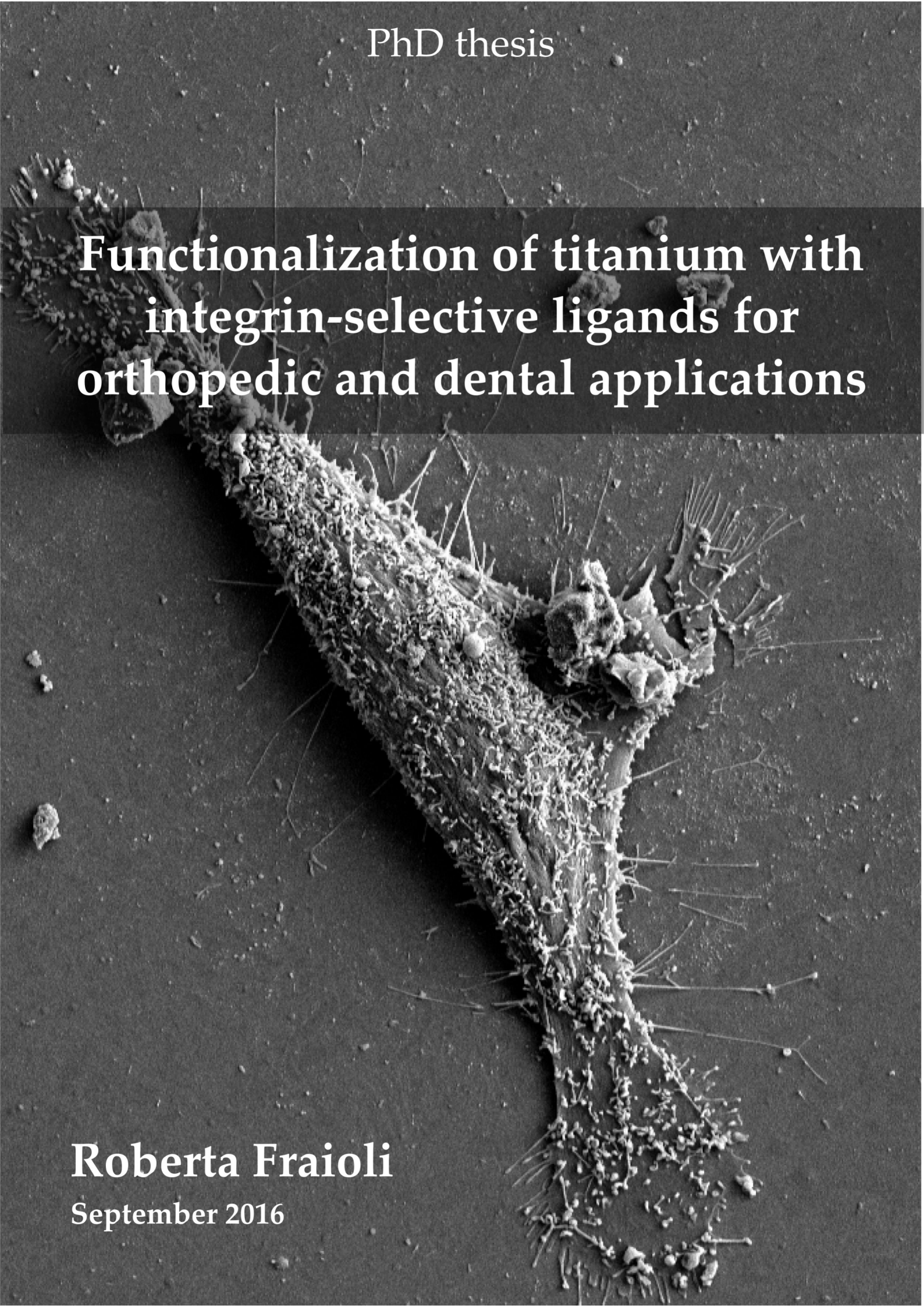

Roberta Fraioli

September 2016

Functionalization of titanium with integrin-selective ligands for orthopedic and dental applications

Roberta Fraioli

A dissertation submitted in partial fulfillment of the requirements
for the degree of Doctor of Philosophy

Department of Materials Science and Metallurgical Engineering
Doctoral Program in Materials Science and Engineering
Universitat Politècnica de Catalunya – Barcelona Tech

Supervisors:

Dr. Jose María Manero Planella

Dr. Carlos Mas Moruno

Barcelona, September 2016

Front cover: hMSC on smooth Ti surface
Back cover: hMSC on nanorough Ti surface

Acknowledgments

I've postponed writing these acknowledgements so many times. Mainly because writing them is somehow admitting that this period of life is coming to an end. Surely these years were full of moments in which I wished to be a doctor already or never to be one, but I carried on and never fully imagined that I would once cross the finishing line until now, that I see it just in front of me. Now, the idea of losing those precious bits of satisfaction, disillusion, excitement, drama, discovery and misery that make up any PhD is slightly puzzling. Ups and downs are PhD students' everyday food; young researchers follow the daily moments of success and failure of their experiments just like they were on a roller coaster. But I guess this (apart from making PhD students utterly moody, depending on the color of the cell-culture plate, the image in the microscope or the results of hours of data processing…) make this training period so special and unforgettable.

Sharing such intense emotions with others inevitably makes relationships very strong. And now I find myself saying that truly not a single day of these four years would have been the same without my colleagues and friends. So thank you to all the people at the UPC, starting from my directors Jose Maria and Carles for their support. Carles, tu vas viure el meu doctorat en real time, cada dia compartir despatx amb els teus doctorands no és gens fàcil, però vas fer-ho i molt bé! Thank you also to all other UPC collegues, PhD students, Postdocs, Professors and Technicians: Anna, Judit, Joanna, Mònica, Elia, Priya, María Isabel, David, Albert, Jordi, Cristina, Marta, Daniel, Maria Pau, Xavier, Elisa, Clara, Cristina, Montse E., Pablo, Trifon and Montse D. for their help during these years.

Thank to the people at the CEE in Glasgow! Thank you Matt for being very welcoming and letting me join the lab without hesitation, and Monica for following my research project and for being such a lovely person with me.

Thank you to the lunch-people: for all that talking, discussing, sharing and, most importantly, laughing, I thank Daniela, Erica, Erik, Giuseppe, Ina, Jing, John Gall Speed, Jose, Miquel, Mireia, Quentin, Romain, Yassine. Best-PhD-mates-ever. Gracias a todos por una de mis mejores fiestas de cumple! Dani, sei la mia wannabe italiana preferita! Erics, thank you for sharing so much with me. Not only lunchtimes, but also our home (spesso con tetris in cucina), the yoga classes, the trekking days, the ice-creams, the cooking and a few climbing sessions. Non dimenticherò mai i discorsi "motivatori", le arrabbiate condivise, i regalini e "la volta-che-mi-salvasti-dalla-furia-della-montagna-cantando", che tempra! Erik (i.e., Dr. Champsilvestre), carissimo, thank you for all the spare time we spent together, you taught me how to let hours pass without

a single serious action…with videos of whales exploding, pancakes and cartoons. Excellent party organizer and friend. Giuseppe (quello di Milano che però fa morire dal ridere), una new entry di qualità. And thank you for the daily phone call: "Hola, ¿donde estas?". E non ti dimenticare le chiavi. Jing, thank you for being so patient with us when we were talking Spanish at the beginning and por ser capaz de hacer que fuera una ventaja para tener el castellano espectacular que tienes ahora! I thank John Gall Speed for the good vibe! I still ask myself how twelve people can still find you entertaining, day after day. We must have something wrong, but we love you. Thank you Dr. Jose for always wearing your smile and looking like the only never-stressed PhD student I ever met! Miquel, you have a talent (or a problem): I cannot avoid laughing when you're nearby. Mir, per ser un solet, des de el primer dia. Tu penses que puc oblidar-me del somriure de la millor profe de swing? Impossible. I tu no t'oblidis de les classes d'angles, dels vinets/birres/tapes, dels discursos plorant i d'aquells rient molt. Quina sort que vas decidir fer un doctorat… ! M'has donat molta força i estic segura que continuaràs sent una referència. Quentino thank you for being a very good friend to talk to about anything and for being the first of the group in visiting me in Napoli without being scared. Ah, ¡gracias por la salchipapa y el aceite sabrosón también! Rom, boludo, gracie! Your company during the PhD was a blessing! I'll miss a lot your smiles, hugs and support (and the top of your head) in my next office! Yass, thank you for the time we shared, mainly out of the lab. The next Neapolitan dinner has to be in Napoli! Thank you Newsha, my craziest and brilliant friend, we needed very few time to become such good friends! Loved our cinema and chatting sessions!

Gracias también a Aldo y Milena, con quien pasé los buenos momentos de mi estancia en Glasgow. Me hicieron sentir enseguida en casa y eso no tiene precio cuando acabas de llegar a otro país. Todavía me rio pensando en nuestras noches por la ciudad escocesa!

Unas gracias enormes a mis xiquets Anna, David y Simon! Como siempre digo, mi pensamiento feliz. A pesar de no vernos, os tengo siempre en mi cabeza, haciéndome reír siempre que haga falta y pensar en muchos cafés (pasados y futuros)…

Grazie ad Antonio, un amico lontano ma vicinissimo in ogni momento di bisogno. Il tuo contributo in questi anni è stato veramente importante!

Grazie a Filippo, per aver sopportato ore di Skype, nervosismi e agitazioni e soprattutto per esserci sempre e comunque. Grazie per l'immensa cura che mi regali.

Grazie alle mie donne bellissime; abbiamo e continueremo a superare l'incredibile, non ho dubbi! Siate sempre così forti, perchè siete le colonne sulle quali crescono come edere gioie e serenità della mia vita.

Abstract

Despite being biocompatible and with optimum mechanical properties for application as a bone replacement material, titanium (Ti) lacks osteoinductive capacity, i.e. it supports new bone growth on its surface but does not foster its formation. This may lead to implant failure due to poor osseointegration. Together with infection, this is in fact the main cause of failure of orthopedic and dental implants. Therefore, this thesis explores the possibility to convert Ti surface into a bioactive substrate, which is actively capable of influencing cell fate *in vitro* and enhance implant osteointegration *in vivo*.

To install such bioactivity, surface chemical functionalization was chosen. Two families of extracellular matrix (ECM)-inspired integrin-binding biomolecules were tested. Integrins are the major cell surface receptor, thus addressing these receptors could be beneficial to tune cell response to the surface. One type of biomolecule tested is a double-branched peptidic ligand that allows for the simultaneous presentation of the cell-adhesive RGD (Arg-Gly-Asp) motif and the synergic PHSRN (Pro-His-Ser-Arg-Asn) motif, which synergizes the RGD-mediated binding to integrin $\alpha5\beta1$. Alternatively, non peptidic integrin-selective ligands were tested as surface coating molecules. These highly stable ligands were designed to be selective for either integrins $\alpha5\beta1$ or $\alpha v\beta3$. The role of both of these receptor subtypes in several bone biology events is currently matter of discussion in literature. Grafting of the ligands on Ti was either carried out via physisorption or chemical anchoring. Silanization was used to create a covalent bond between the synthetic molecules and the metallic oxide. Two cell types were used for the in vitro testing of the functionalization system: human osteoblast-like cells (SaOS-2) and mesenchymal stem cells. The testing of different combinations of biomolecule, grafting technique and cell type is the subject of the four full-papers reported in the thesis. Two of these papers also include the *in vivo* study of the effect of the chemical functionalization in an animal model.

The thesis also includes a work focused on the merging of two surface modification techniques, namely chemical functionalization and topographical modification, to create a multifunctional Ti substrate that simultaneously addresses the problem of infection and poor osseointegration.

Overall, the collection of works presented in the thesis offer a comprehensive view on how chemical functionalization with ECM-inspired ligands can act as a powerful tool to tune cell behavior and, ultimately, guide the biological response at the peri-implant site.

Preface

The present dissertation includes the research carried out by the author between December 2012 and September 2016, which was supervised by Dr. José Mª Manero Planella and Dr. Carlos Mas Moruno. The author was funded by the Generalitat de Catalunya (pre-doctoral grant FI-AGAUR) and by the UPC (pre-doctoral grant FPI-UPC). The experimental work was carried out at the Department of Materials Science and Metallurgical Engineering (UPC – Barcelona, Spain), at the Institute for Bioengineering of Catalonia (IBEC – Barcelona, Spain), and at the Centre for Cell Engineering (CCE) at the University of Glasgow (UoG – Glasgow, UK). The stay at the UoG was founded by the European Molecular Biology Organization (EMBO) through an EMBO Short Term Fellowship (ASTF No: 457-2015). The integrin-selective peptidomimetics used in the thesis were provided by the group of Prof. Kessler at the Technische Universität München (TUM – Munich, Germany).

The thesis is presented as a collection of papers. The Introduction presents an overview on bone replacement materials, focusing on metals and modifications of their surface. The three published works are reported in Chapters I and Chapter II. Though reported in the Annexes I, II, the last works follow a similar rationale as the previous ones and were also carried out within the thesis project, but are currently submitted or under revision in scientific journals. Finally, the overall results of the work are discussed and the main conclusions drawn.

List of publications

Fraioli R, Dashnyam K, Kim J-H, Perez R A, Kim H-W, Gil J, Ginebra M-P, Manero JM, Mas-Moruno C. Surface guidance of stem cell behavior: Chemically tailored co-presentation of integrin-binding peptides stimulates osteogenic differentiation *in vitro* and bone formation *in vivo*. *Acta Biomaterialia* 43:269-281 (**2016**).

Mas-Moruno C, **Fraioli R**, Rechenmacher F, Neubauer S, Kapp T, Kessler H. αvβ3- or α5β1-integrin selective peptidomimetics for surface coating. *Angewandte Chemie (International Edition in English)* 55 (25):7048-7067 (**2016**).

Fraioli R, Rechenmacher F, Neubauer S, Manero JM, Gil FJ, Kessler H, Mas-Moruno C. Mimicking bone extracellular matrix: Integrin-binding peptidomimetics enhance osteoblast-like cells adhesion, proliferation, and differentiation on titanium. *Colloids and Surfaces B: Biointerfaces* 128:191-200 (**2015**).

Mas-Moruno C, **Fraioli R**, Albericio F, Manero JM, Gil FJ. Novel Peptide-Based Platform for the Dual Presentation of Biologically Active Peptide Motifs on Biomaterials. *ACS Applied Materials & Interfaces* 6 (9):6525-36 (**2014**).

Conference contributions

Fraioli R, Dashnyam K, Kim J-H, Perez RA Kim H-W, Manero JM, Gil FJ, Mas-Moruno C. *European Chapter Meeting of the Tissue Engineering and Regenerative Medicine International Society 2016 (TERMIS-EU 2016)* 28th June-1st July 2016, Uppsala (Sweden) – Oral presentation.

Fraioli R, Neubauer S, Rechenmacher F, Manero JM, Kessler H, Mas-Moruno C. *XXIII Molecular Biology Meeting* 14th June 2016, Barcelona (Spain) – Poster presentation.

Fraioli R, Rechenmacher F, Neubauer S, Dashnyam K, Kim J-H, Perez RA Kim H-W, Manero JM, Gil FJ, Kessler H, Mas-Moruno C. *World Biomaterials Congress (WBC 2016)* 17th-22nd May 2016, Montreal (Canada) – Poster presentation.

Mas-Moruno C, **Fraioli R**, Hoyos-Nogués M, Manero J and Gil J. *World Biomaterials Congress (WBC 2016)* 17th-22nd May 2016, Montreal (Canada) – Oral presentation.

Fraioli R, Rechenmacher F, Neubauer S, Manero JM, Kessler H, Gil FJ, Mas-Moruno C. *Peptide Materials for Biomedicine and Nanotechnology (PepMat 2016)* 14th-16th March 2016, Barcelona (Spain) – Poster presentation.

Fraioli R, Rechenmacher F, Neubauer S, Manero JM, Kessler H, Gil FJ, Mas-Moruno C. *Nanopeptide 2015* 2nd – 4th March 2015, Glasgow (United Kingdom) – Poster presentation.

Fraioli R, Manero JM, Gil FJ, Mas-Moruno C. *27th Annual Conference of the European Society of Biomaterials (ESB 2015)* 30th August – 3rd September 2015, Krakow (Poland) - Poster presentation.

Fraioli R, Rechenmacher F, Neubauer S, Manero JM, Gil FJ, Kessler H, Mas-Moruno C. *XXXVII Congreso de la Sociedad Ibérica de Biomecánica y*

Biomateriales 28th – 29th November 2014, Madrid (Spain) – Oral presentation.

Fraioli R, Rechenmacher F, Neubauer S, Manero JM, Gil FJ, Kessler H, Mas-Moruno C. *7th IBEC Symposium. Bioengineering for Future Medicine* 29th September 2014, Barcelona (Spain) – Poster presentation.

Fraioli R, Rechenmacher F, Neubauer S, Manero JM, Gil FJ, Kessler H, Mas-Moruno C. *26th Annual Conference of the European Society of Biomaterials (ESB 2014)* 31st August – 3rd September 2014, Liverpool (United Kingdom) - Oral presentation.

Scholarships and awards

EMBO Short-Term Fellowship Award (ASTF No 457 – 2015) – *European Molecular Biology Organization (EMBO)*, January 2016.

Special mention for poster presentation - *Nanopeptide 2015* 2nd – 4th March 2015, Glasgow (United Kingdom).

Best oral presentation - *XXXVII Congreso de la Sociedad Ibérica de Biomecánica y Biomateriales* 28th – 29th November 2014, Madrid (Spain).

Pre-doctoral grant (FI-AGAUR) - Agència de Gestió d'Ajuts Universitaris i de Recerca (AGAUR), Generalitat de Catalunya. February 2013 – January 2016.

Pre-doctoral grant (FPI-UPC) – Universitat Politècnica de Catalunya (UPC, Barcelona). December 2012 – January 2013; February 2016 – November 2016.

Contents

Introduction **1**

1.1 Materials for hard tissue replacement devices 3

1.2 The concept of osseointegration 5

1.3 Ti-based materials for endosseous implants 10

1.3.1 Bulk properties: the stress-shielding effect 10

1.3.2 Surface properties: a bioinert substrate 12

1.4 Bioactivity 14

1.4.1Physical modifications 17

1.4.1 Chemical modifications 25

1.5 Surface biochemical functionalization 29

1.5.1 The communication machinery of cells: integrins 29

1.5.2 Ligands overview: from proteins to short peptidic sequences 35

1.5.3 Binding of ligands 37

1.6 References 41

Scope of the work **59**

Chapter I: Functionalizing with a peptide-based platform **63**

I.1 Paper I 69

I.2 Paper II 93

Chapter II: Functionalizing with peptidomimetics **111**

II.1 Review Paper 117

II.1 Paper III 139

Concluding remarks **157**

Annex I: Paper IV **161**

Annex II: Paper V **179**

Glossary of terms

ALP alkaline phosphatase

BM bone marrow

CAS cell-attachment site

CP commercially pure

ECM extracellular matrix

FA focal adhesion

FAK focal adhesion kinase

FN fibronectin

GF growth factor

HA hydroxyapatite

hMSC human mesenchymal stem cell

ITG integrin

MG63 rat osteoblast-like cell

MSC mesenchymal stem cell

OB osteoblast

PHSRN (Pro-His-Ser-Arg-Asn)

R_a arithmetical roughness

RGD (Arg-Gly-Asp)

SaOS-2 osteosarcoma-derived cell line ("sarcoma osteogenic")

TGF-β transforming growth factor beta

VN vitronectin

Introduction

Definition of biomaterial

Since its introduction in the late 60', the concept of biomaterials has expanded considerably, including an increasing number of devices and systems. The first definition of the Consensus Conference on Definitions in Biomaterials Science of the European Society for Biomaterials in 1987 as *non viable material used in a medical device, intended to interact with biological systems* has evidently become obsolete.[1] Nowadays, ranging from diseased or damaged tissue-replacement implants to drug delivery systems, **biomaterial** definition needs to embrace a much wider spectrum of systems: as recently proposed *a biomaterial is a substance that has been engineered to take a form which, alone or as part of a complex system, is used to direct, by control of interactions with components of living systems, the course of any therapeutic or diagnostic procedure, in human or veterinary medicine*.[1] Clearly, many branches of research have developed, each focusing on specific possibilities of innovation in a defined clinical scenario.

Implants

Among them, implantable materials, i.e. located partially or totally beneath the epithelial layer of the body, include hard tissue replacement implants, i.e. orthopedic and dental implants, whose actual demand is very high and

is expected to increase significantly over the next years. According to a projection study of primary and revision joint replacement surgeries from 2005 to 2030 in the United States, the demands for primary total hip arthroplasties and knee arthroplasties are expected to grow by 174% and 673%, respectively.[2] Despite both joint replacement and dental implants are generally successful, failure leading to revision still occurs. Given the huge volume of patients that need these procedures, the need to increase implant lifespan for an increasing older population, the economic burden of revisions, and the limited healthcare resources, implant performance improvement would be beneficial.

With an operative history of over 50 years, orthopedic and dental implants have already been the subjects of a plethora of modification, both in their shape design and material choice (bulk properties) as well as in their physicochemical properties (surface properties), aiming at increasing their lifespan and reducing failure rate. Focusing on implant materials, modifications of increasing complexity have been developed.

Biocompatibility, bioinertia and bioactivity

The starting point to define candidate materials is the requirement of **biocompatibility**, whose foundation has been identified in a *mutually acceptable and sustained co-existence of biomaterials and tissues*.[3] However, such concept is extremely dependent on the specific biological environment where the material will be implanted and on the knowledge and understanding we acquire on it. The time scale over which the material is in contact with the body is a crucial factor to consider when classifying a biomaterial as biocompatible or not: a specific material can be inert at short time scale but generate a toxic reaction if the exposition is prolonged. Consequently, biocompatibility is intrinsically a function of time and of the implantation site. In fact, biocompatibility definition has evolved hand in hand with our knowledge on the human body and its interactions with foreign materials. Traditionally, i.e. between 1940 and 1980, the concept of biocompatibility was linked to a series of negatives,

such as non-toxic, non-immunogenic, non-irritant, etc.[3] Nowadays, these features would rather be associated to a so-called **bioinert** material, i.e. not causing cell death, chronic inflammation, or any other impairment of cell/body functions. In other words, this category of materials has no active role in the healing process, neither hampering nor fostering the regeneration of damaged tissues. On the contrary, newer generations of implantable biomaterials aim at positively influencing the healing process, i.e. they aim at being **bioactive**. This feature means that a bioactive orthopedic implant, for instance, will foster bone formation at the material-tissue interface and discourage infection, by directly interacting with eukaryotic cells and bacteria.

The overall aim of this thesis was to design and test, both *in vitro* and *in vivo*, novel bioactive coatings for orthopedic and dental implantable materials. Our strategy and the numerous others documented in literature to install bioactivity on surfaces will be discussed in the following sections.

1.1 Materials for hard tissue replacement devices

Hard tissue replacement devices comprise mainly ceramics and metals, but also include some polymeric materials (Table 1.1). These materials have to be selected and customized to meet the requirements of the replaced tissue, both in their structural bulk properties and in their interaction with the body, mainly governed by surface properties. Apart from the biological requirements, materials have to be suited to be processed for the specific application. Issues such as sterilization and manufacturability are paramount for implantable devices, and have to be taken into account when selecting the material. Classification based on material category is done for the sake of simplicity, since most biomedical devices are composed of metallic, polymeric and/or ceramic parts.

Material	Application
Metals	
Cobalt-chromium alloys	Artificial heart valves, dental prosthesis, orthopedic fixation plates, artificial joint components, vascular stents
Stainless steel	Orthopedic fixation plates, vascular stents
Titanium and its alloys	Artificial heart valves, dental implants, artificial joint components, orthopedic screws, pacemaker cases
Gold or platinum	Dental fillings
Silver-tin-copper alloys	Dental amalgams
Ceramics	
Aluminium oxides	Orthopedic joint replacement, orthopedic load-bearing implants, implant coatings, dental implants
Zirconium oxides	Orthopedic joint replacement, dental implants
Calcium phosphates	Orthopedic and dental implant coatings, dental implant materials, bone graft substitute materials
Bioactive glasses	Orthopedic and dental implant coatings, dental implants, facial reconstruction components, bone graft substitute materials, bone cements
Synthetic polymers	
Polyethylene (UHMWPE)	Orthopedic joint implants (acetabular coating), syringes
Polymethylmethacrylate	Bone cements, intraocular contact lenses, dental implants

Table 1.1. Commonly used metals, ceramics and synthetic polymers in hard-tissue replacement applications. Adapted from [4].

1.2 The concept of osseointegration

When fracture or damage to the bone occurs, natural healing mechanisms are activated to regenerate the physiological function of the tissue.[5] However, in certain conditions synthetic materials are needed to support the body in the recovery of homeostasis. In such cases permanent endosseous implants are used to be continuously in contact with bone and help it withstand the load.

The definition by Brånemark and Albrektsson

The success of this kind of devices is based on an efficient **osseointegration**. As originally defined by Brånemark and Albrektsson at the end of the 70s, osseointegration refers to a stable anchorage of the implant to bone tissue:[6] they had observed that titanium (Ti) and bone could become practically fused and could not be separated without fracture. Since such direct bone apposition at the implant surface is considered a requisite for success, bone-implant contact (BIC), i.e. the percentage of the implant surface in contact with bone on a microscopic level, is often used as a parameter to assess the degree of osseointegration of a tested implant.

The osseointegration process

Rather than only indicating the fixation between the synthetic material and the tissue, the term osseointegration can also be used to indicate the whole process that generates this fused interface.[7] In fact, several steps lead to the formation of this interface.

I. **Contact with blood and formation of the fibrin clot.** Starting from the fracture, either caused by trauma or surgery, the first tissue that comes into contact with the implant is blood. Therefore, wound-healing mediators arrive to the site, including platelets. The inflammatory process starts at this point: platelets adsorb on the implant within seconds and activate (or degranulate), leading to the

release of growth factors (GFs), fibronectin (FN) and thrombin, which fosters the conversion of fibrinogen into fibrin. The tridimensional fibrin clot acts as a mechanical and biochemical substrate for cells: cell-adhesive proteins (FN, vitronectin (VN), von Willebrand factor, etc.) and GFs (transforming growth factor beta (TGF-β), vascular endothelial growth factor (VEGF), among others), which stimulate both angiogenesis and osteogenesis. **Angiogenesis**, i.e. the generation of new blood vessels replacing the damaged pre-existing vessels, is essential to support the formation of new bone, i.e. **osteogenesis**, with a proper vascularization.

II. **Acute inflammation.** Neutrophils are the first inflammatory cells to arrive to the implant site, typically within the first 24 h. By secreting inflammatory and chemotactic cytokines, these white blood cells recruit monocytes and macrophages. Clearance of necrotic tissues and provisional extracellular matrix (ECM) follows cell recruitment: macrophages phagocyte necrotic cells and the provisional fibrin matrix, while monocytes differentiate into osteoclasts, which resorb necrotic bone fragments. Degradation of the matrix is accompanied by liberation of GFs, which act as chemoattractants for fibroblasts and mesenchymal stem cells (MSCs). Macroscopically, acute inflammation is accompanied by warm and swelling of the tissues and pain.

III. **Granulation tissue.** Fibroblasts initiate the formation of granulation tissue. Abundant neovasculature and numerous proliferating MSCs characterize this connective tissue. The following steps depend on the blood supply and stability of the fracture site.

IV. **Ossification.** Two distinct scenarios are possible:

a. **High blood supply and good stabilization** (typically at short distance from the fracture site of large-gap fractures or in small fractures). Recruited MSCs differentiate into osteoblasts, which secrete alkaline phosphatase (ALP) and osteocalcin. Eventually, **woven bone** is formed via **intramembranous ossification**. Woven bone matrix is mainly constituted by type III collagen, with interfibrillar mineralization. The structure of this bone is completely unorganized and can easily bridge the implant surface and the host bone.

b. **Low blood supply and poor stabilization** (central areas of large-gap fractures). Hypoxic conditions, caused by the scarcity of vasculature, drive the differentiation of MSCs to chondrocytes, which produce cartilage, and chemoattract endothelial cells. These cells form tubular assemblies and start bridging the existing blood network. Recruited MSCs mainly come from the cambium layer of the periosteum and the endosteum. Together with cartilage, newly-formed fibrotic tissue forms the so-called **soft callus**, mainly composed by type II collagen, which is gradually invaded by new capillaries. This soft fibrocartilage acts as a scaffold for the formation of bone tissue via **endochondral ossification**: chondrocytes become hypertrophic and undergo apoptosis, secreting calcium. This process generates a calcified cartilage. Increasing stabilization and vascularization finally create the proper conditions for the deposition of woven bone on the fibrocatilage scaffold, i.e. the formation of the **hard callus**: when both ends of the fracture are bridged by the soft callus the formation of the new calcified tissue (woven bone) starts, proceeding from the periphery to the center of the fracture.

V. **Remodeling.** In the final stage of the fracture healing process conversion of woven bone into lamellar bone takes place. Osteoclasts resorb the unorganized tissue by attaching to the matrix and forming a tight seal area beneath them. Bone resorption liberates mineral ions and GFs that stimulate osteoblast-driven deposition of new bone. Thus, interplay between osteoblast and osteoclasts generate an organized tissue composed by multiple lamellae of type I collagen fibers with intrafibrillar mineralization. When osteoblasts become surrounded by the newly-formed ECM in a so-called *lacuna*, they become osteocytes, which no longer secrete bone matrix. This type of bone cells are sensitive to the loading vectors exerted on the bone. Signaling transduction of this information to osteoblasts allows the gradual deposition of load-oriented osteons during the continuous remodeling process that takes place in the implant-tissue area. When a load-oriented bone structure is formed in contact with the synthetic material, the external load is efficiently transferred from the implant to the surrounding bone. The formation of this functional interface is the essential requisite to obtain the aforementioned osseointegration of the endosseous device.

This process is summarized in figure 1.1.

As mentioned in the previous section, hard tissue replacement devices are modular in design, frequently constituted by several material categories. The following section will only concentrate on titanium-based metallic materials for joint-replacement or dental devices, given its crucial role in those clinical applications.

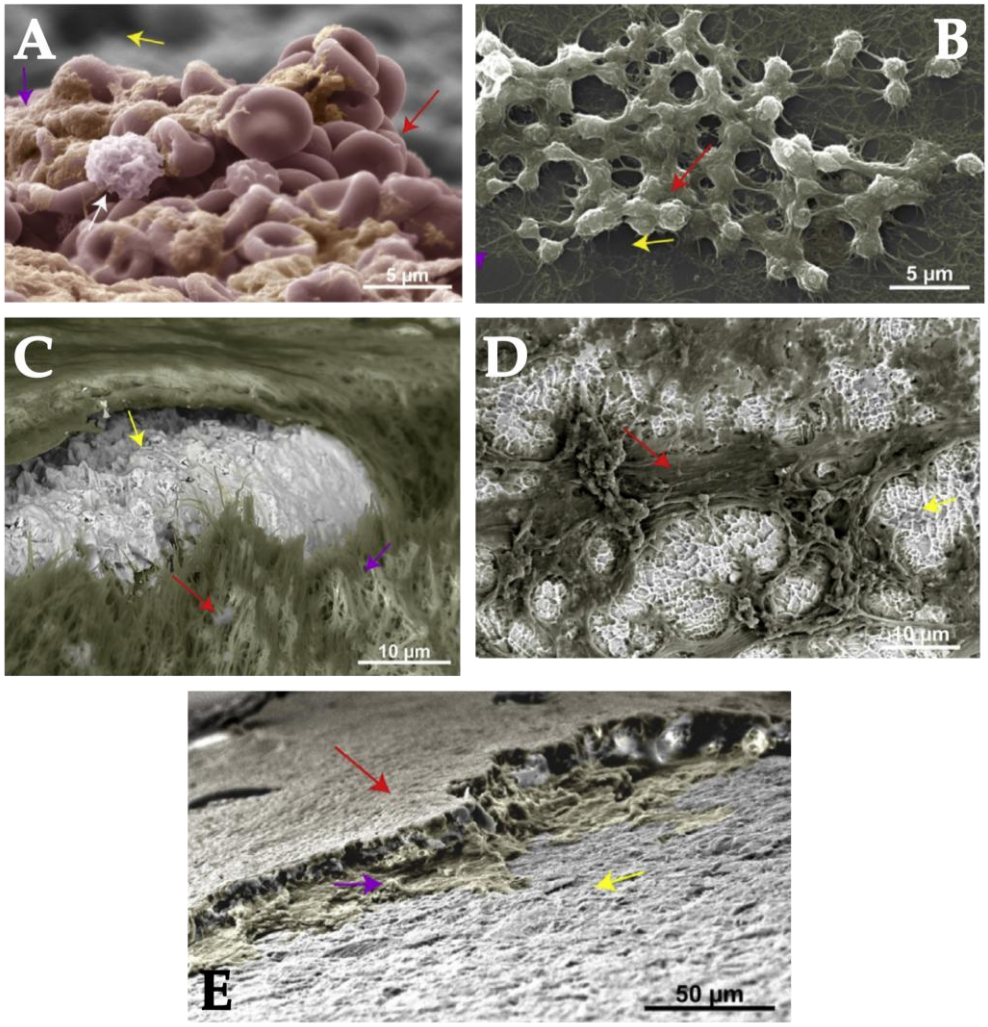

Figure 1.1. Steps of the osseointegration process around implants. (A) Erythrocytes (red arrow) accumulate at the implant surface (yellow arrow) contributing to the formation of the hemostatic plug, with platelet aggregates and fibrin (purple arrow). Within the first hours post implantation, leukocytes (white arrow) are responsible of the immune response. (B) The provisional matrix is composed by activated platelets (red arrow) that aggregate within the fibrin matrix (purple arrow) and adhere to the implant surface (yellow arrow). (C) The fibrin matrix (purple arrow) on an implant surface (yellow arrow) with embedded platelets (red arrow). (D) Differentiated osteoblasts (red arrow) spread on the implant surface (yellow arrow). (E) Image of an explanted implant. Implant osseointegration occurs when the implant surface (yellow arrow) is intimately fused with bone (red arrow). The purple arrow points at the interface, where a calcified layer with non-fibrillar organic material is observed. Adapted from [7].

1.3 Ti-based materials for endosseous implants

One of the most important criteria to select a material for permanent hard-tissue replacement is its mechanical properties: ideally the material should efficiently support the surrounding bone in bearing the external load for long periods of time. Due to their good mechanical properties, metallic materials are selected as the main load-bearing constituent of orthopedic and dental devices. Among them, Ti and its alloys are currently the most used metals for biomedical applications,[8] mainly due to their excellent biocompatibility. They are used in a plethora of applications, from dental implants to joint replacement prosthesis (hip, knee, elbow, shoulder, etc.) and artificial heart valves. In the following sections their bulk and surface properties will be described, focusing on the clinical implications of these properties in the context of bone replacement devices.

1.3.1 Bulk properties: the stress-shielding effect

Hardness, modulus, tensile and fatigue strength are essential bulk properties to guarantee the long-term success of the implant.

Elastic modulus

Among them, the elastic modulus of the implant material is a very critical parameter to tune: it should be as similar as possible to the one of bone, which varies between 4 and 30 GPa,[8] depending on the location of the bone and of the measuring direction. The elastic modulus of Ti alloys is, with few exceptions, one order of magnitude higher than the natural tissue modulus (Fig. 1.2), which causes important adverse effects: this biomechanical mismatch prevents the stress from being transferred from the implant to the bone, leading to the resorption of the bone in the peri-implant area. Such phenomenon, known as **stress shielding effect**, most probably causes failure due to implant loosening. Together with Ti, Ti6Al4V, the most used Ti alloy containing about 6 and 4 wt% of Al and V

respectively, has excellent corrosion resistance, but still much higher modulus than bone. Moreover, clinical concerns have been raised by the toxicity of V and its oxides, and the release of Al and V, which has been associated to with long-term health problems. Low-modulus Ti alloys have been developed to limit the stress shielding effect and avoid toxic ions. Nb, Ta, Mo, Hf,[9] among others, have been proposed as alloying elements to lower the elastic modulus and avoid problems related to ion release, since none of these ions has been demonstrated to be toxic so far.

In any case, the elastic modulus of CP Ti and its alloys varies from 110 GPa to 55 GPa, which is significantly lower compared to the other two most used categories of biomedical metals, i.e. stainless steel (316 L – 210 GPa) and CoCr alloys (240 GPa).[8]

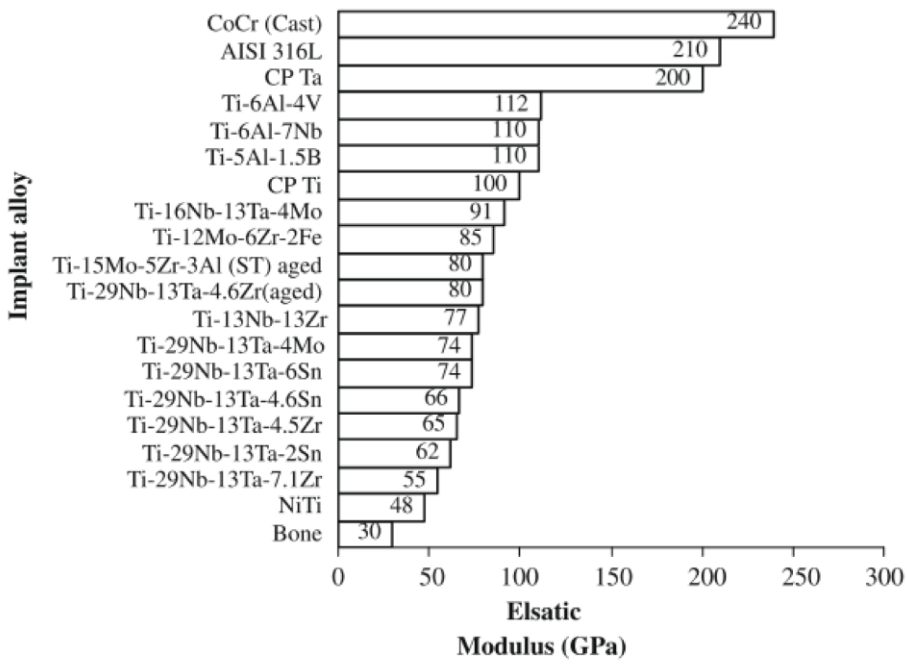

Figure 1.2. Elastic modulus of the most common metallic biomaterials. From [8].

1.3.2 Surface properties: a bioinert substrate

Despite bulk properties define the set of mechanical requisites to replace a structural tissue like bone, it is the surface of the implant that directly interacts with the host body and eventually determines its long-term success. In fact, surface properties of the synthetic material can be considered decisive on determining the success or failure of the implant, at the point that material biocompatibility ultimately depends on them.

Resistance to corrosion is particularly important in the implantation context, where the biological environment can be responsible of **biodegradation**. Consisting in an aqueous environment at 37 °C and an almost constant pH of 7.4, the extracellular fluid contains several anions (mainly Cl^-, HCO_3^-, and HPO_4^{2-}) and cations (mainly Na^+, Ca^{2+}, Mg^{2+}). The concentration of sodium chloride (112-120 mM), for instance, is approximately a third of that of sea water. Clearly, the chemical mechanisms of metal corrosion *in vivo* are the same as in a non-biological aqueous environment, i.e. oxidation of the metal to its salt and one or more cathodic reactions consuming the generated electrons.

Degradation in the body

Nonetheless, the biological scenario affects this process mainly in the following aspects:[10]

- **Consumption of the products of the anodic or cathodic reaction**. For instance, proteins binding metallic cations and transporting them away from the corrosion site or bacteria consumption of the generated hydrogen shift the equilibrium, allowing for further dissolution of the metal;
- **Change of pH**. Inflammation or bacteria can lower the pH locally, changing the stability of the oxide layer;
- **Availability of oxygen**. A local depletion of oxygen can cause the breakdown of the oxide layer.

Thus, metals that are subject of corrosion in the biologically environment release potentially toxic metallic ions into the body [11] and can be degraded to the point that load is no longer withstood by the prosthetic device. As a consequence, a limited range of metals are suitable metals for implantation into the harsh conditions of the body.

A protective oxide

The main reason for the success of Ti as implantable material is probably its excellent resistance to corrosion, which makes it an ideal bioinert material. The reason lies in the stability of its superficial oxide (mainly TiO_2): given the high solubility of oxygen in Ti, this passivation layer spontaneously forms on the metallic surface within seconds of exposition to air, and reaches from 1 to 5 nm in thickness.[12] Due to the very fast formation, this oxide film is highly amorphous. Since almost no grain boundary or other defects are frequent in amorphous oxide layers, Ti has a very high resistance to corrosion, which consequently gives it the capability of withstanding loads for long periods of time, despite the aggressive biological environment.

Though Ti intrinsic inertia makes it highly suitable for implantation, newer generations of biomaterials are often customized to have a certain degree of bioactivity to promote the healing process. In this quest, the surface is again the focus of attention, since it is the part of the biomaterial that directly comes into contact with the surrounding tissues. The following section will describe in detail the methods to install bioactivity on the surface of the biomaterial.

1.4 Bioactivity

The first official biomaterials meeting was held in Clemson University, South Carolina in 1969, defining biomaterials as synthetic or natural materials meant to replace structure and function of body parts. Since then, improvement and innovation of this class of materials has been gaining more and more importance. The range of natural tissues to be replaced has broadened enormously, creating the need for a deeper knowledge of the interaction of biomaterials with many different tissues. In fact, the actual biggest challenge is not only fitting the material to completely different environments and functions in the body, but also actively control tissues response, using the biomaterial as an information carrier, capable of instructing the body on how to heal in the fastest and more efficient way, i.e. creating a bioactive material.

Bioactive substrates

Thus, efforts are now focusing on how to deposit a specific message on the implant and evaluating how efficiently this message is forwarded to its surrounding tissues. Though originally referred to the osteoinductive capacity of some materials, bioactivity now covers a wide range of functions, such as growth factors delivery, stem cell recruitment or inflammation and infection control. With one or several of these targets in mind, it is evident that a multidisciplinary research must be carried out, integrating as much as possible biological, medical, and engineering tools.

This approach is followed also in the design of bone replacement materials, for which, as previously discussed, the process of osteointegration is crucial to guarantee the success. Implementation of bioactivity on the metallic material can focus on one or more critical steps of that process, with the aim of harnessing them towards a fast and efficient healing of the injury. To that end, a feasible solution is to apply **surface modifications** to the material: by doing so, bulk properties are retained, while the biological response at the implant-tissue interface can

be improved or tuned. This concept, also known as **functionalization** of the surface, includes any treatment which adds a biologically functional element to the external layer of the biomaterial. Thus, it can aim at controlling one or more aspects of the biological response to the implanted material, including inflammation, cell behavior and infection.

When aiming at tuning cell behavior, the rationale behind the surface functionalization approach relies on the machinery that cells possess to sense with their environment (the ECM). A bidirectional communication takes place between cells, which modulate the features of the matrix surrounding them, and ECM, which can in turn activate signaling pathways. This information exchange is also referred as **inside-out** and **outside-in signaling**, respectively. Numerous transmembrane receptors act as mediators of the signaling: integrins, which bind to ECM ligands, and GF receptors can work independently or synergically to transfer signals between cells and ECM (the reader is referred to section 1.5 for a complete view on this topic). Importantly, cells not only respond to ECM-derived biochemical signals: every property of the ECM influences cell response, including its biomechanical properties and its topography.

Signals from the ECM

The information carried by the ECM can be described to be mainly:

- **Biochemical**: the nature of ECM macromolecules is defined by their amino acid sequence, charge, hydrophilicity;
- **Physical**: the architecture of the environment, which determines its mechanical properties of the matrix.

Though being simplistic, this view sets the baseline for engineering ECM-mimicking biomaterials that emulate one or more of these aspects.

In the context of bone replacement implants, apart from guiding cell fate, bioactivity can be implemented also to reduce or avoid infection at the peri-implant site. Indeed, development of infection is a huge concern in the clinic. In the field of joint replacement devices, inflection is the first

leading cause of failure. According to a study aiming at understanding the main cause of failure and revision of total knee arthroplasties (TKA), infection is the main cause (25.2%) of revision procedures for TKA.[13]

Types of modifications

For the sake of simplicity, surface functionalization strategies can be classified into two main categories: modification of either the physical or the chemical properties, as represented in figure 1.3. Clearly, combined solutions are also reported in literature. Moreover, surface modifications rarely involve only changes in chemical or physical properties; in fact, chemical treatments usually affect physical properties, and vice versa, making classification and comparison between studies very complex.[14]

Finally, it is important to highlight that the following sections will focus only on the functionalization of metallic substrates and disregard the use of ceramics and polymers, which are also frequently object of bulk/surface modifications. An increasing number of fundamental studies on cell-substrate interactions in the literature are involving more compliant and realistic substrates such as hydrogel materials or 3D settings. Nevertheless, these studies are out of the topic of this thesis and will not be covered.

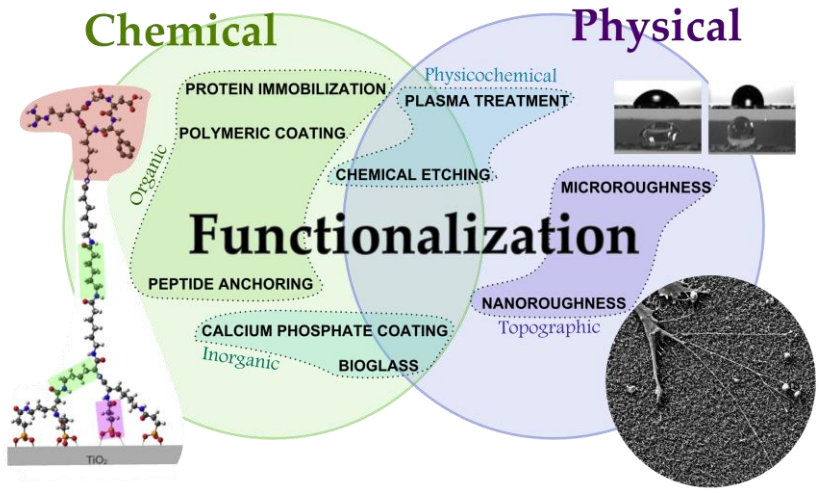

Figure 1.3. Schematic representation of the strategies to functionalize the surface of biomaterials.

1.4.1 Physical modifications

As previously introduced, cells are sensitive to their environment. From the mesoscale, to the microscale and the nanoscale, cells respond to the plethora of topographical features of their matrix. The ECM contains a milieu of topographical signals, such as the 500 μm villi of the intestinal mucosa or the 50-nm thick collagen fibers, which are interpreted by cells to guide numerous events, such as adhesion, migration, and differentiation.[15,16] Starting with modifications on the micro-scale and increasingly developing with nanometric features, topographical modifications of the substrate have been reported to be an effective tool to regulate cell fate *in vitro* and tissues responses *in vivo*. The following sections (1.4.1.1 and 1.4.1.2) will resume important contributions on this topic.

Another aspect of the matrix properties is its wettability. Section 1.4.1.3 will be focused on the effect of modulating this substrate property via physical modifications on cells and tissues response.

1.4.1.1 Microtopography

Pioneering studies in the 90's revealed the potential use of topographical superficial features to control the biological response.[17]

In vitro ***cellular response to micrometric topography***

Analysis of the cellular response to rough surfaces, frequently generated via smoothing, grit blasting and/or acid etching,[18] pointed out that cells are sensitive to depth, width and orientation of grooves. However, their reaction, from elongation in preferential directions to migration and differentiation, highly depends on cell type and correlating a clear effect of topography on cell behavior has remained elusive.[17] Work by Boyan and colleagues demonstrated that MG63 osteoblast-like cells response depended on both roughness and chemical composition of Ti and Ti6Al4V:

in brief, enhanced differentiation was observed on rough materials, where cells proliferated less, produced more ALP and OCN, compared to their smooth counterparts. Chemical composition of the surface also affected ALP production, which was fostered on rough Ti compared to rough Ti6Al4V.[19] Similarly, culturing chick embryonic calvarial osteoblasts on smooth, rough or porous Ti revealed enhanced differentiation on the non-smooth substrates.[20]

Numerous works by Anselme and co-workers extensively analyzed the effect of roughness amplitude and order on the attachment of human osteoblasts (hOBs) on Ti and Ti alloys, often using a modeling approach. Unlike previous studies, lower adhesion, proliferation and focal contact formation was observed on rough surfaces compared to smooth ones. Thus, a model for cell attachment and proliferation on the basis of surface topography was designed for quantitative analysis. Statistical analysis revealed that roughness organization parameters (i.e. the fractal dimension) affects cell response more than arithmetic roughness (R_a), which is used to describe surfaces in most studies. The main conclusion of the modeling study is that the more chaotic the surface (higher fractal dimension), the more the cell-substrate contact area decreases.[21] This study highlights the fact that only considering the average roughness of a surface might not be an accurate indicator to predict cell behavior. Instead, other roughness parameters, such as organization parameters, might provide more reliable information.

In vivo: ***micrometric roughness and osseointegration***

Parallel to investigations at the cellular level, extensive studies in animal models established that micrometric roughness positively affects osseointegration. A 1991 *in vivo* study by Buser and colleagues highlighted a positive correlation between surface roughness (around 20 μm) of the implant and osseointegration in a minipig model.[22] This study introduced an optimal surface treatment, produced using a large-grit (250-500 μm) sandblasting technique followed by a strong acid-etching with a

mixture of HCl/H_2SO_4 at elevated temperature, known as SLA (Sand-blasted, Large grit, Acid etched), which is still popular nowadays. Numerous studies followed and confirmed the crucial role of surface roughness.[23–26] According to a study by Daugaard et al., microtextured Ti implants fostered bone growth and reduced fibrous tissue formation at the implant surface, compared to smooth implants in a canine model.[24]

Models

Interestingly, the theory behind the effect of surface topography at the micron-scale on bone-implant contact is not established yet. At least three lines of thinking can be mentioned:[14] the biomechanical theory of Hansson and Norton,[27] the concept of contact osteogenesis,[28] and a cellular signaling-based theory.[29] The first theory, illustrated in figure 1.4 A, is based on the generation of a mechanical interlocking between

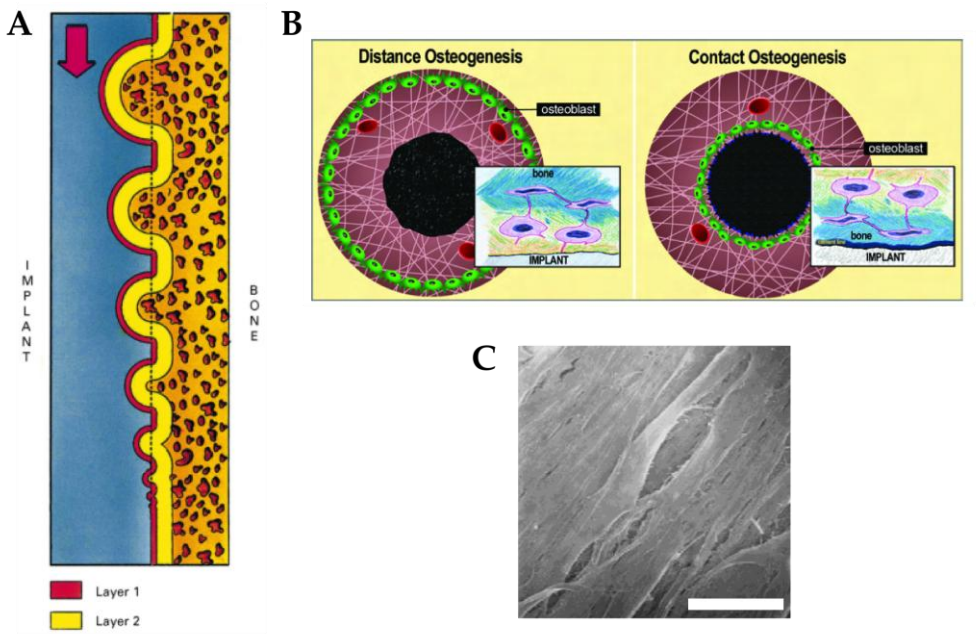

Figure 1.4. Three different interpretations of the effect of topography. Norton and Hansson describe a biomechanical theory (A), according to which only sufficiently big superficial pits can actually resist the interfacial shear by going through bone of full mechanical strength (orange with red spots), while smaller pits only go through tissues of much reduced strength (layer 1 - much reduced mechanical strength immediately adjacent to the implant surface; layer 2 - reduced strength). (B) Drawings to show the initiation of distance and contact osteogenesis where differentiating osteogenic cells line either the old bone or implant surface respectively. (C) Scanning electron microscopy observation of cells cultured on polished Ti6Al4V. Cell attachment, proliferation and differentiation are affected by topography. Adapted from [27], [28] and [21], respectively.

implant surface pits and bone. In order for pits to efficiently work as retention elements with regard to interfacial shear, pit shape and minimum dimension were defined via modeling.

The second line of thinking defines two types of osteogenesis (Fig. 1.4 B): distance osteogenesis, where bone growth proceeds from the old bone toward the implant, and contact osteogenesis, which implies that bone formation starts directly on the implant surface. Since osteoblast are secreting cells with no migrating ability (in synthesizing matrix they become trapped into it and become osteocytes), in order for contact osteogenesis to take place migration of osteogenic cells to the implant surface is required. The ability of the implant surface to retain a stable fibrin clot is essential for osteogenic cells to reach the implant surface and consequently form bone directly on it (fibrin clot formation has been described in section 1.2). This model points at microtopography as the key factor to promote such phenomenon, since it increases the available surface area for fibrin attachment and provides surface features with which fibrin could become entangled.

The third theory relies on the effect of surface features at the micron-scale on cellular behavior (Fig. 1.4 C), which has been mentioned at the beginning of this section; roughness is reported to act at the cellular level, stimulating differentiation into the osteoblastic phenotype and, therefore, bone formation. Nonetheless, the exact cellular mechanisms that underlie this effect are not established.

Recently, studies on surface features as small as cellular receptors are focusing on unrevealing them and are covered in the next section.

1.4.1.2 Nanotopography

With the increasing availability of cutting-edge techniques from nanotechnology and materials science, the shift from the micro-scale to the nano-scale has accelerated. While microtopography is used to influence cells in term of cellular and supra-cellular events (cell morphology, tissue organization, etc.), the rationale that pulls research towards smaller features is that nanotopography affects sub-cellular behavior, such as organization of the cell surfaces receptors (Fig. 1.5).[30–32] Numerous techniques have been used to generate nanotopographies that aim at fostering osseointegration.[14]

Randomly organized nanotopography

Among the physical methods, compaction of nanoparticles of Ti, Ti6Al4V and CoCrMo has been reported to enhance osteoblast adhesion.[33] Though generating randomly distibuted nanofeatures, chemical treatments are often chosen since they can be readily applied to large surfaces. They include acid etching, oxidation, anodization and alkali treatment. In a recent work, acid etching (H_2SO_4/HCl) was combined with sand blasting to obtain hierarchical Ti surfaces with micro and nano features (R_a between

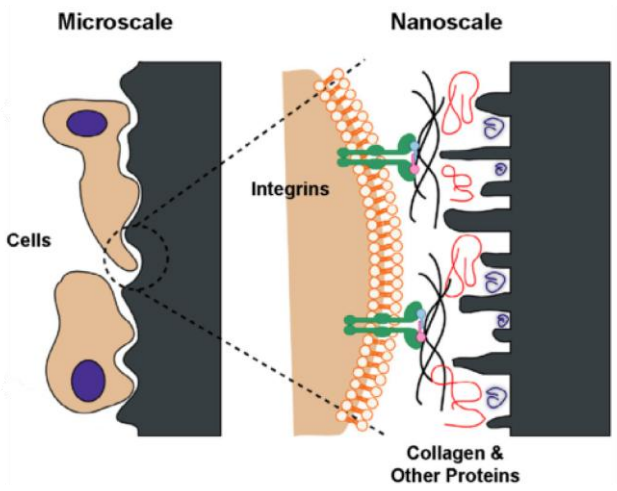

Figure 1.5. At the microscale, implant surface microtopography interacts with osteoblasts and mesenchymal stem cells at the cellular scale. At the nanoscale, cell membrane receptors, such as integrins, can recognize proteins adsorbed on the surface, which in turn are modulated by the nanostructures on the surface. Adapted from [32].

1.5 and 2.5 nm), which were demonstrated to be simultaneously antibacterial and osteogenic.[34] Surface roughness could be easily tuned by changing etching time and temperature. Oh et al. used anodization to generate TiO_2 nanotubes whose diameter (between 30 and 100 nm) could dictate cell fate.[35] Bigger nanotubes were associated to increased cell elongation and differentiation into the osteoblastic lineage. This led the authors to state that increased physical stress induces osteogenic differentiation, confirming analogous observations by other authors.[36,37]

Geometrical control

The surface modifications described so far generate features without any geometrical control. However, by coupling anodization to porous alumina mask [38] or block copolymer template [39], Dalby and co-workers could generate highly controlled patterns of TiO_2 dots on Ti surfaces, which were demonstrated to enhance osteogenesis compared to the flat metallic substrate. Clearly, lithographic techniques offer the possibility to generate highly controlled nanometric features.[14,40] Nonetheless, they are labor intensive and have been mainly tested *in vitro*, while further development is needed in order to readily apply them on implant surfaces. In fact, lithography has been mainly applied to model materials, such as polymers (polystyrene and polycaprolactone) and glass.[40–42]

Nanotopography kills bacteria

Notably, nanotopography has also been used as a novel bactericidal tool: biomimicry of insect wings (the Clanger cicada [43,44] and the dragonfly *Diplacodes bipunctata* [45]) led to the discovery of the bactericidal potential of high aspect ratio surface nanometric features: needle-like features kill bacteria by imposing high deformational stresses to their membrane, which leads to rupture or piercing.[43] Since such intrinsic bactericidal potential of the surface is devoid of most limitations of common antibacterial coatings, such as silver- or antibiotic-releasing coatings (i.e. the initial burst release, the difficulty to control the release profile, the risk of developing antibiotic resistance and the limited lifespan [46]), these

nanorough surfaces could be efficiently tested to reduce the incidence of infection at the peri-implant site.

1.4.1.3 Wettability

Water wettability is a surface property whose role in cell-material interactions has been investigated in the past twenty years. It has been reported to affect several important events in implant osseointegration, such as protein adsorption and blood coagulation and clot stability [47–49] (the reader is reported to section 1.2 for a complete view of the osseointegration process). Specifically, highly hydrophilic surfaces have been shown to support faster protein diffusion but less strength of surface-protein interaction than hydrophobic ones.[47] The fact that hydrophobic surfaces may promote higher protein adsorption can be explained thermodynamically. A hydrophobic surface in an aqueous solution is surrounded by a "shell" of water molecules that interact with each other more than with the surface. Such configuration is quite an ordered state, with a decreased level of entropy. Protein adsorption would cause the disruption of this ordered scenario and therefore be favored energetically due a concomitant increase in entropy.[50] On the contrary, on hydrophilic surfaces, which would readily generate hydrogen bonds with water molecules, a competition exists between proteins and water, making protein adsorption thermodynamically unfavorable. It should be noted that no unique trend of adsorption as a function of wettability can be identified, since this complex phenomenon has been demonstrated to be also dependent on substrate curvature and protein size and shape,[51] among other factors.

Nonetheless, blood quickly spreads on hydrophilic substrates, allowing an efficient activation of the coagulation cascade on the material,[48] which results in fibrin clot stabilization and higher VEGF local concentration.[49]

As previously mentioned, it is often difficult to split the effect of single properties, since modifying one of them usually causes concomitant alterations of other surface features. The effect of wettability has been frequently studied together with the one of topography.

The SLActive surface

Numerous recent works focused on chemical modifications to the SLA substrate (section 1.4.1.1) leading to increased hydrophilicity (SLActive surface).[52–56] Despite the high number of publications based on this specific surface, no unique conclusion can be drawn. *In vitro*, both human MSCs (hMSCs) and rat osteoblast-like cells (MG 63) were found to adhere and proliferate less on the most hydrophilic substrate, compared to the more hydrophobic one.[52,55,56] Cell differentiation into the osteoblastic lineage was found to be similar to the SLA surface, only moderately improved on the SLActive substrate,[52,55,56] indicating a preponderant role for topography, rather than wettability, on the enhancement of osteogenesis. Tested *in vivo* in human models, the SLActive implant was found to slightly improve osteogenesis and angiogenesis, compared to the SLA one, but to have similar bone resorptive and appositional events.[53,54]

Other methods

Apart from chemical modifications, other methods have been used to generate hydrophilic substrates. UV treatment on rough Ti and CoCr alloy was used to study the recovery from aging of metallic samples.[57,58] Though the treatment significantly increases wettability, the conclusion of both *in vitro* and *in vivo* testing was that the UV treatment mainly restored samples bioactivity due to carbon contaminants elimination rather than increased wettability.

1.4.2 Chemical modifications

Both organic and inorganic components form bone tissue and determine its properties. Often referred to as a mineralized collagen matrix, bone tissue is a hierarchical tissue whose primary building blocks are collagen type I fibers and plate-like hydroxyapatite (HA) crystals. Apart from collagen, a plethora of other organic molecules are also contained in bone matrix. In most cases, the strategies of inorganic and organic chemical modifications of implant surfaces can be seen as inspired by the mimesis of either the mineral or the organic phase of bone, respectively. However, many other organic and inorganic surface modifications exist that act via other mechanisms, rather than being directly bio-inspired from the matrix. The following sections briefly introduce the two paths of inorganic and organic modifications.

1.4.2.1 Inorganic modifications

The idea of coating metallic implants with HA crystals came from the observation of the bone bonding ability of calcium phosphate-based ceramics.[59] L.L. Hench first demonstrated that a glass with a specific composition, known as bioglass, showed direct bone apposition on its surface. Materials not promoting such intimate contact with the natural tissue would end up encapsulated by a fibrous tissue layer. Since the discovery of bioglasses, many other inorganic materials have shown bone-bonding ability, including HA. The first attempt to transfer this ability to the surface of metallic implants was to coat them with HA crystals. Plasma-coating was one of the techniques used to generate a superficial layer of inorganic material, on which newly deposited HA crystals served as a matrix for the bone-forming cells (OBs and MSCs).[60] However, such type of coating often suffered from very low stability, related to the weak bond created with the metal.[61]

Kokubo's method

To solve this issue, Kokubo and co-workers proposed an alternative method to directly generate an apatite layer in intimate contact with the metallic substrate.[62,63] By immersing the metal in NaOH solution and then applying a heat treatment, a stable layer of amorphous sodium titanate is formed (Fig. 1.7). Upon immersion in simulated body fluid (SBF, a solution with ion concentration similar to blood plasma), which is supersaturated with respect to apatite, ion exchange and electrostatic interactions lead to the formation of a calcium titanate and, finally, to the formation of a superficial layer of apatite. Unlike deposited coatings, the surface obtained with such methodology is highly stable. Moreover, apatite deposition was also observed to be efficiently stimulated by such treatment *in vivo*.[64] First demonstrated to be initiated by the NaOH treatment of the metal, the same outcome could later be obtained with acid solutions, which, instead of generating a negatively charged surface, create a positive charge on the surface that triggers an analogous formation of apatite.[63]

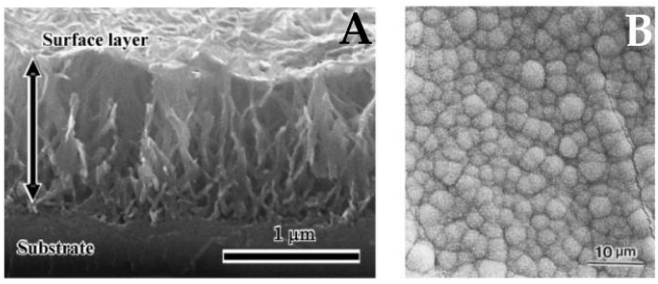

Figure 1.7. Scanning electron microscope image of the cross section of Ti after NaOH and heat treatment (A); the highlighted thickness is the amorphous sodium titanate layer. (B) Nucleation of apatite crystals after immersion in SBF for 4 weeks. Adapted from[62] and [63].

1.4.2.2 Organic modifications

Organic modifications consist in the incorporation of natural, such as proteins and peptides, and/or synthetic, i.e. polymers, organic molecules on the surface of the implant. In many cases, such modifications mimic cell ECM with the aim of creating an instructive microenvironment on the surface of the biomaterial. The ECM-inspired approach, based on the use of matrix proteins or peptidic sequences is fully covered in the next section.

Numerous alternative strategies that are not based on the biochemical interactions between cells and their matrix have also been described. Such modification can be obtained by diverse techniques, such as self-assembled monolayers (SAMs), and can be used for diverse purposes. Though not directing interacting with cell surface receptors, these modifications may exert an indirect biological effect mediated by changes in surface chemistry: alteration of the chemistry affects protein adsorption, which in turns influence cell behavior. A very well described example of this mechanism is offered by alkanethiol SAMs on gold surfaces. Gold-sulfur coordination generates closely packed alkyl chains that can be modified to present chemical groups of choice. With this approach SAMs presenting terminal $-CH_3$, -OH, -COOH, and $-NH_2$ functionalities were tested and demonstrated to modulate FN conformation and, as a consequence, cell response.[65]

Inhibition of bacterial colonization

Interestingly, organic coatings can be also used to inhibit bacterial colonization, a highly important target, given the burden of this complication in the premature failure of orthopedic and dental implants.[13] The antimicrobial action of surface coatings has been described to be via two modes: the bactericidal effect, i.e. the coating directly kills bacteria, or the bacteriostatic effect, i.e. hindering of microorganisms adhesion on the material.[66]

A direct bactericidal effect can be exerted by certain polymers such as chitosan, or by embedding antibacterial agents within the polymeric matrix (e.g. chlorhexidine, silver ions or antibiotics). Recently, the use of antimicrobial peptides (AMPs) to coat biomaterials has also emerged as a powerful strategy to overcome the disadvantages associated to the use of antibiotics. The bactericidal action of the coating is mediated by one or more of the following mechanisms: inhibition of the synthesis of bacterial cell wall (e.g. antibacterial agents such as penicillin or vancomycin), disruption of protein synthesis via interference in the mRNA translation process (e.g. the antibiotic gentamicin), permeabilization or disruption of cell membrane (e.g. chitosan and several AMPs), or inhibition of the transcription and replication of nucleic acids (silver ions are described to act via both this and the aforementioned mechanisms).

The indirect bacteriostatic effect is commonly obtained via

PEG poly(ethylene glycol) (PEG) (or similar polymeric molecules) immobilization on biomaterial surfaces. PEG coatings efficiently prevent unspecific protein adsorption on Ti [67] and also reduce bacterial adhesion and therefore infection occurrence in polymeric clinical devices [68]. Though being a promising antibacterial strategy, this hydrophilic coating concomitantly inhibits eukaryotic cell attachment, which may be detrimental in certain applications. To solve this, cell adhesive peptides (such as the peptidic sequence RGD (Arg-Gly-Asp)) are sometimes simultaneously anchored to the surface, to provide specific adhesive cues for the desired cell type.[69]

1.5 Surface biochemical functionalization

When the installation of bioactivity on the surface is meant to exert a biological effect through biochemical mechanisms, the chemical modification can be referred to as **biochemical functionalization** of the biomaterial. Such organic modifications mainly rely on the stimulation of specific signaling cascades known to promote the desired response. The rationale behind the design of such substrates is that cell response is dictated by a plethora of signals embedded in their ECM, which are not present in the biomaterial. In order to engineer a biomimetic surface that incorporates one or more biochemical cues from the matrix, the way cells sense and process the signals from the environment has to be analyzed. The following section (1.5.1) will describe the communication machinery of cells, deepening in the bone tissue microenvironment. The ligands that can interact with cell receptors and the methods to incorporate them on the material surface will then be reported in sections 1.5.2 and 1.5.3, respectively.

1.5.1 The communication machinery of cells: integrins

The ECM is a milieu of signaling components that regulate cell behavior under precise spatial and temporal control. Including both soluble, such as GFs and cytokines, and not soluble molecules, this highly complex microenvironment regulates cell recruitment, essential in the tissue regeneration process, and dictates proliferation, migration and differentiation of residing cells (Fig. 1.8).[70] Cell-ECM interactions are reciprocal, in the sense that cells receive a message from their matrix but also remodel it in response to intracellular signals (outside-in and inside-out signaling). Virtually all cells in the body are embedded in their tissue-specific matrix: fibroblasts in dermis, chondrocytes in cartilage and

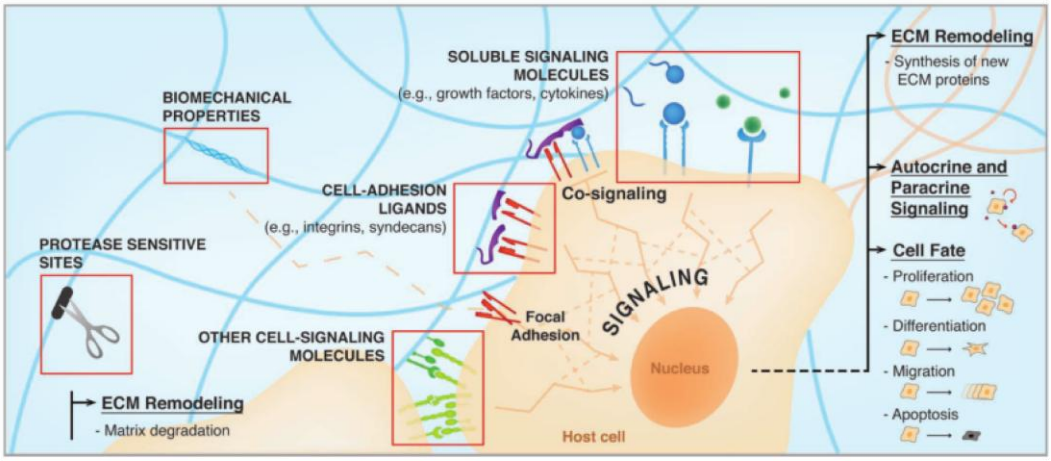

Figure 1.8. Soluble and non soluble components are integrated in the ECM of cells and regulate their fate. Adapted from [70].

osteocytes in bone are completely surrounded by it, while blood cells reside in a dynamic environment but are still exposed to ECM proteins, such as FN.

Integrin family

The way cells adhere to the ECM and exchange biochemical signals is through cell membrane receptors. The major class of these proteins is **integrins**, a family of 24 heterodimeric transmembrane receptors composed by non-covalently bound α and β subunits (Fig. 1.9 A). So far, 18 α and 8 β subunits have been identified; each of these subunits consists of a large

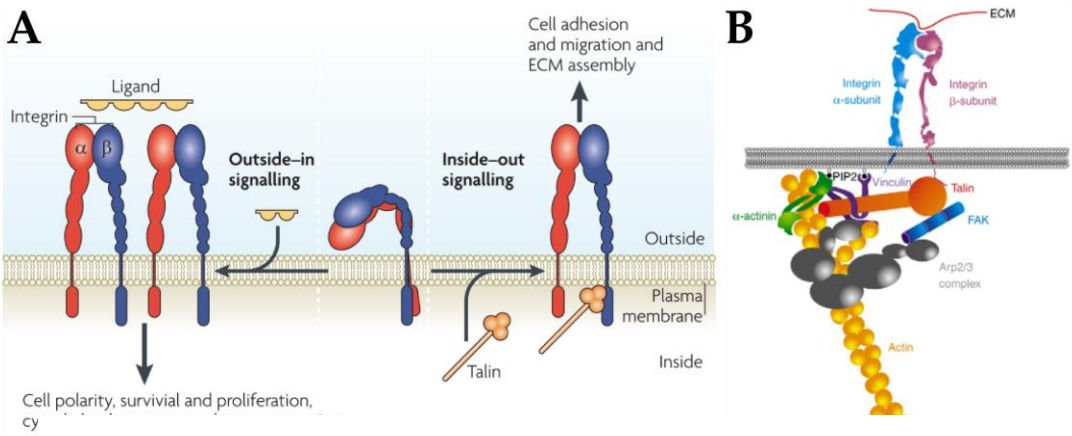

Figure 1.9. (A) Outside-in and inside-out signaling regulate integrin conformational changes from the resting bent form to the activated form. (B) The focal adhesion is composed by several mediators that bridge the transmembrane receptor with the actin cytoskeleton. Adapted from [72] and [73].

ectodomain and a typically short noncatalytic cytoplasmic domain, linked by a single transmembrane domain. These transmembrane receptors exist in two states: a **resting state**, in which the two subunits are in a bent form and do not interact with the matrix, and an **activated state**, in which α and β transmembrane domains are dissociated and binding to ECM proteins is favored.[71,72] Upon integrin binding to the ligand, intracellular protein aggregates form, known as **focal adhesions** (FAs). The FA is formed by proteins such as talin, vinculin, and α-actinin (Fig. 1.9 B).[73] The first two belong to the family of the actin-binding proteins, whose function is essentially to connect the dimeric receptor to the actin fiber, mediating mechanical coupling and, thus, force transmission across the FA; α-actinin is an actin filament cross-linking protein that also transduce intracellular forces across the membrane.[74]

Though integrin-binding proteins are promiscuous, i.e. one protein can bind several integrin receptors (Fig. 1.10),[75] it is still matter of discussion whether their individual roles are overlapping or not. As reported in a commentary paper by one of the pioneers of integrin research, Richard Hynes, in 2002 "there is no evidence for overlapping functions or

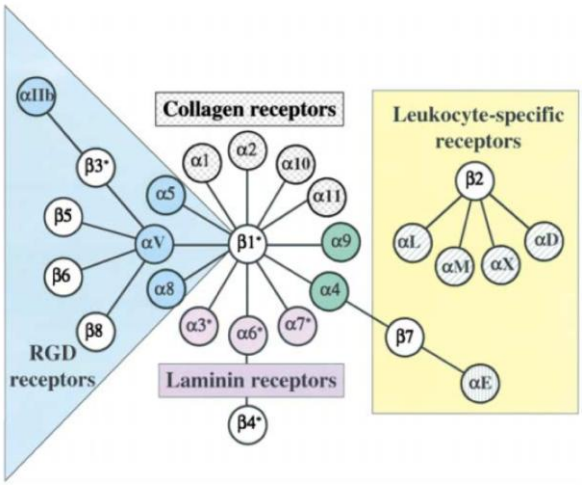

Figure 1.10. The integrin receptor family in mammals. $\alpha\beta$ associations are organized in subfamilies, according to the ligand specificity. Coloring of α subunits reflects the division into evolutionary subfamilies, which is not relevant for the present discussion. From [75].

compensation among integrins, but the possibility of some unknown form of compensation cannot be eliminated".[76] In fact, integrin role is often investigated via integrin blocking antibodies or genetic modifications leading to integrin null organisms, which do not provide any control over the possibility of other integrins taking up the role of the blocked or absent ones (Hynes even suggests the possibility that antibodies that are antagonists of the interaction with a solid substrate might be agonists of the signaling cascade activated by the bound receptor). Nevertheless, a more recent work already demonstrated that overlapping and compensation of functions of integrins α5 and αv do exist in the context of remodeling of vasculature during development,[77] testifying that the discussion is still open.

Since integrins act as one of the most important messengers between the environment and cells, strategies targeting these receptors have been developed to guide the biological response on biomaterials. Surface functionalization techniques that rely on this communication system consist of the tethering of integrin-binding molecules on the external layer of the biomaterial. Importantly, integrin receptors are tissue-specific, meaning that only a subset of the 24 heterodimers is highly expressed and biologically relevant in the context of a specific tissue. The following section focuses on the most biologically important integrins in bone biology.

1.5.1.1 The integrin system in bone regeneration scenarios: focus on osteoblasts and stem cells

As described in section 1.2, OB and MSC action is crucial in the osseointegration process. The most highly expressed receptors in OBs are the β1 subfamily.[78] Moreover, expression of integrins β3 and β5 has also been observed.[78–80] Similarly, hMSCs also highly express the β1 subfamily (more than 80% of cells), along with other integrin subtypes.[81,82] A schematic summary of the most expressed subtypes and their roles are reported in figure 1.11 and in table 1.2, respectively.

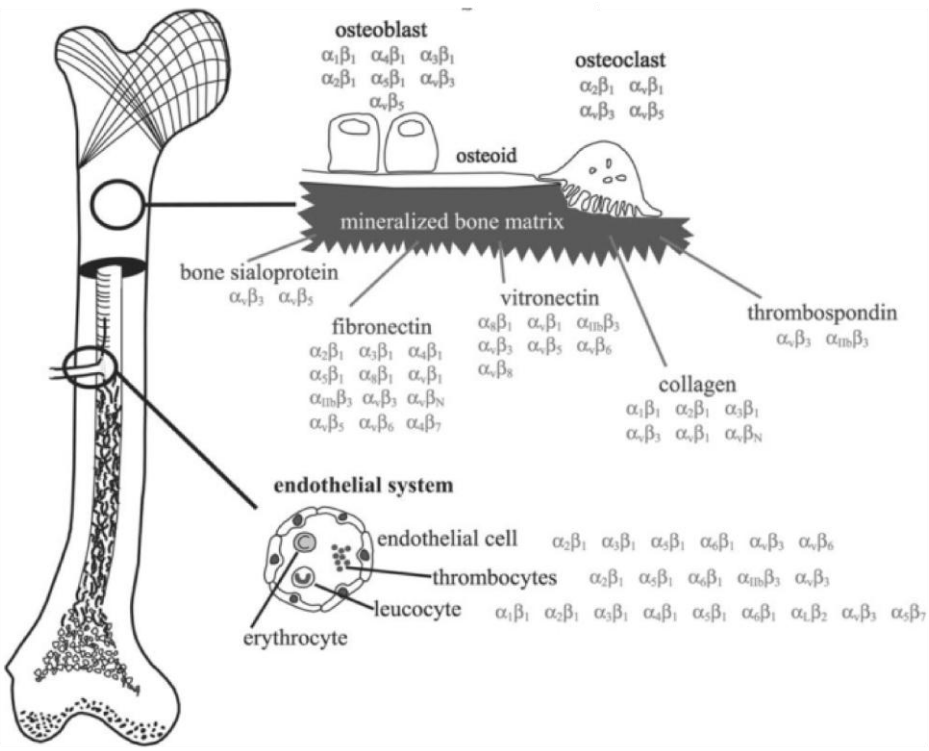

Figure 1.11. Schematic drawing of bone and endothelial system structure and tissue-specific integrin systems. From [79].

Integrin subtype	OB and OB-like cells	hMSCs	Reported roles
$\alpha 1\beta 1$	[78,79]	[81]	Pro-osteogenic pathways, primary adhesion receptor to collagen, activation Runx2/Cbfa1, phosphorylation of focal adhesion kinase (FAK) [78].
$\alpha v\beta 3$	[78,79]	[81]	Vitronectin attachment [81], negative effect on proliferation and differentiation [83,84], increased proliferation rates [85], major integrin receptor expressed by osteoclasts [86], present in nascent focal complexes [87], broad lamellipodia and low RhoA activity [88], initiation of mechanotransduction [89].
$\alpha 5\beta 1$	[78,79]	[81]	Fibronectin attachment,[78] expressed during several stages of osteogenesis and related to ALP expression [83], present in mature FAs [87], associated to well-defined stress fibers and high RhoA activity [88], support of high matrix forces [89,90].
$\alpha v\beta 5$	[78]	[81]	Mediate bone resorption [81].
$\alpha 3\beta 1$	[78,79]		Partially mediates adhesion to FN [78].

Table 1.2. The main integrin subtypes expressed by OBs, OB-like cells and hMSCs. The second and third columns of the table contain the works in which the integrin subtype was reported to be expressed by the cell type. The list of reported roles is limited to the context of bone biology.

Apart from the integrins reported in table 1.2, subtypes $\alpha 2\beta 1$ is also reported to be expressed in OB and hMSC cultures,[78,81] $\alpha 4\beta 1$ in OBs cultures,[79] and $\alpha 6\beta 1$ in hMSC cultures.[81]

It is worth noting that the roles of single subtype are often contrasting. Especially on integrins $\alpha 5\beta 1$ and $\alpha v\beta 3$, which are recognized as important in bone biology, there seems to be no clear agreement in literature: the group of García and co-workers and others authors produced several studies attesting the positive role of $\alpha 5\beta 1$ and the detrimental one of $\alpha v\beta 3$ in osteogenesis induction;[83,91–93] nonetheless other authors reported a positive role for the $\alpha v\beta 3$ in the progression of undifferentiated cells into the osteoblastic lineage.[94–96]

1.5.2 Ligands overview: from proteins to short peptidic sequences

Full-length proteins

90% of bone ECM is composed by collagenous proteins (97% collagen type I) and several non-collagenous proteins, as osteocalcin, osteonectin, bone sialoproteins, FN and VN.[97] These macromolecules can offer a plethora of signals to cells, such as several cell attachment sites via different integrins, non-integrin binding domains (such as heparin-binding domains), or GF-binding domains. Clearly, their high complexity makes them good candidates to coat implant materials and stimulate a positive biological response on their surface. Nonetheless, complexity also means a lack of tight control over the specific biochemical signal presented to cells: the simultaneous presentation of the numerous bioactive domains of the full-length molecule hinders the individuation of the main cause of the experimental outcome. Along with this, the use of proteins as coating molecules bears other drawbacks, such as risk of infection and immune response, related to their production in living organisms, low stability to degradation (both via enzyme, temperature or pH changes), and complexity of manipulation and of production in large amounts. Moreover, no control over the exact presentation of motifs is easily achievable, due to the sensitivity of protein conformation to surface physicochemical properties.[98]

Protein fragments

A lower level of macromolecule complexity and a higher level of control can be obtained by engineering **protein fragments** that only encompass the domain of interest. A clear example is offered by FN: this ECM protein contains a cell attachment site (CAS) in its type III repeat domain ($FNIII_{7-10}$), where the adhesive sequence **RGD** (10th III domain) and the synergic sequence **PHSRN** (9th III domain) are found, as shown in figure 1.12. The role of the synergy site is to increase the affinity of the RGD, which is known to bind several integrin subtypes, for integrin $\alpha5\beta1$.

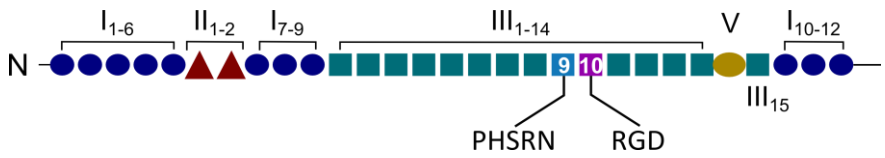

Figure 1.12. FN subunit containing the CAS, where the RGD and PHSRN sequences are located.

To test the role of this subtype in bone biology, García and co-workers produced fragments of FN encompassing this region to coat metallic implants with the aim of promoting osteogenic differentiation *in vitro* and osseointegration *in vivo*.[93,99]

Linear peptides

An even less complex alternative to the use of proteins is the selection of the bioactive sequence of amino acids of interest. In other words, **linear peptides** can be synthesized to recapitulate only a very specific cue of the full-length protein. The RGD peptide, contained in FN and several other proteins, is probably the most well-known sequence used to stimulate cell adhesion and influence cell proliferation and differentiation on biomaterial surface.[98] Such class of ligands has many advantages, including the ease of production via peptide synthesis techniques, in large amounts and low cost, the absence of infection and immune reaction, the high stability to pH and temperature changes, and the possibility to be anchored to the material in a controlled way and at high densities. Importantly though, these very simple molecules often lack stability *in vivo*, due to enzymatic degradation, and show a modest stimulation of cell response compared to proteins. In some cases, this might be related to the fact that presentation of the amino acid sequence may not be optimal to interact with cell receptor due to the lack of a secondary structure, or the absence of synergic motifs. Moreover, in the case of the RGD sequence, no specificity towards a defined integrin subtype or cell type is achievable, since this sequence is known to be highly promiscuous.

Other approaches to enhance the biological performance of linear peptides have been reported:

- **Peptide mixtures**: the immobilization of more than one peptide is a straightforward and very simple way to provide more than one cue on the material surface. The main drawback of this approach is that the exact disposition of the peptides on the surface cannot be controlled;[100,101]
- **Peptide rational design**: multiple peptide sequences can also be presented in a chemically-controlled fashion via design of a peptidic structure that contains more than one peptide. To do so, linear sequences of peptides and branched structures have been used and proved effective both *in vitro* and *in vivo*;[102]
- **Cyclic peptides**: restriction of the conformational freedom of peptides is useful to increase stability to enzymatic degradation, bioactivity and selectivity;[103,104]
- **Peptidomimetics**: these non-peptidic ligands overcome many limitations of peptides, such as stability in serum and lack of selectivity. They can be designed to reach very high affinity and selectivity for one integrin receptor, thus offering the possibility of generating integrin-selective surfaces. However, as for cyclic molecules, their design is not trivial.[105,106]

1.5.3 Binding of ligands

1.5.3.1 Physisorption of integrin ligands

The simplest method to deposit these integrin-binding components on the surface of the implantable device is **physisorption**. This method relies on non-covalent interactions between the biomolecule and the synthetic material (hydrophobic and electrostatic interactions, van der

Waal forces and hydrogen bonds), which makes it very simple and fast (simple impregnation of the material in the molecule solution is often enough), with no need for excessive chemical treatments of the surface (Fig. 1.13 A).[107] Nonetheless, it evidently lacks stability and control of the deposition process. Conformation, orientation, density and arrangement of the ligands adsorbed on the surfaces are very difficult to control.[65] For instance, this method could lead to adsorption of the biomolecule in a conformation that hinders the bioactive motif(s) and therefore reduces the efficacy of the coating. Such limitations can deeply affect the biological activity of the ligand, leading to modest improvements in terms of cellular response.

1.5.3.2 Covalent grafting of integrin ligands

An alternative method to physisorption is **covalent immobilization**. In this case covalent bonds are formed between the biomolecule and the surface, which makes the anchoring much more stable under physiological conditions and chemically controlled. Specifically, the orientation of the ligand is in this case strictly controlled, since the molecule only binds the surface at defined "anchoring" sites. In case the ligand is synthetically prepared, the anchor units can be inserted at precise locations to guarantee the correct presentation of bioactive sequence to cells. As a drawback, however, these techniques are more complex than physisorption and require several chemical steps to be carried out.

A plethora of techniques to covalently graft ligands to synthetic substrates exist, making this method easily adaptable to any substrate. In order to get a successful covalent immobilization, the following aspects should be taken into account:[7]

General guidelines

- the attachment site and chemistry must not interfere with the functional structure or the active site of the biomolecule;

- the distance of the bioactive species from the surface substrate should be large enough to allow for the flexible movement and self-adjusting that is required for the biomolecules to fulfill the desired biological response;
- the attached biomolecule must not be denatured or inactivated at the surface during or following its attachment;
- the surface density of the immobilized species cannot be too high, since over-loading results in overcrowding and reduced activity, nor too low, since the deficient loading cannot motivate cell response.

In the case of metallic implants, the superficial layer where molecules should be anchored is in most cases a metallic negatively charged oxide. The most common methods to create a covalent bond with metallic oxide are the chemical binding of the hydroxyl groups of the surface to silanes or phosphonates.

Silanization

Figure 1.13 B shows a classical modification by **silanization** with (3-aminopropyl)triethoxysilane (APTES), which reacts with the OH groups of the surface and polymerizes to forms polysiloxane groups, followed by the coupling of the heterobifunctional crosslinker (N-succimidyl- 3-maleimidopropionate, SMP). Such crosslinker can react with thiol anchor groups present in the biomolecule to provide chemically specific binding. Such strategy has been used to immobilize cyclic RGD or AMPs to Ti.[108–110]

Chemisorption

Alternatively, **phosphonates** also provide binding to metallic oxides (Fig. 1.13 C), which is reported to be more stable to hydrolysis than silanol groups. The immobilization of bioactive molecules via phosphonic acids has been proved efficient on Ti oxide and other metallic oxides.[111,112]

Recently, a novel chemisorption technique has emerged from the mimesis of mussels, which are promiscuously fouling to a wide range of surfaces. Analysis of the composition of the adhesive plaque of these animals revealed the presence of 3,4-dihydroxy-L-phenylalanine (DOPA) , which was found to be a key agent in the formation on covalent and non-covalent bonds to inorganic and organic materials.[113] This property was recently exploited to bind cyclic RGD and an heparin-binding domain [114] or polymer nanoparticles for drug release [115] to titanium.

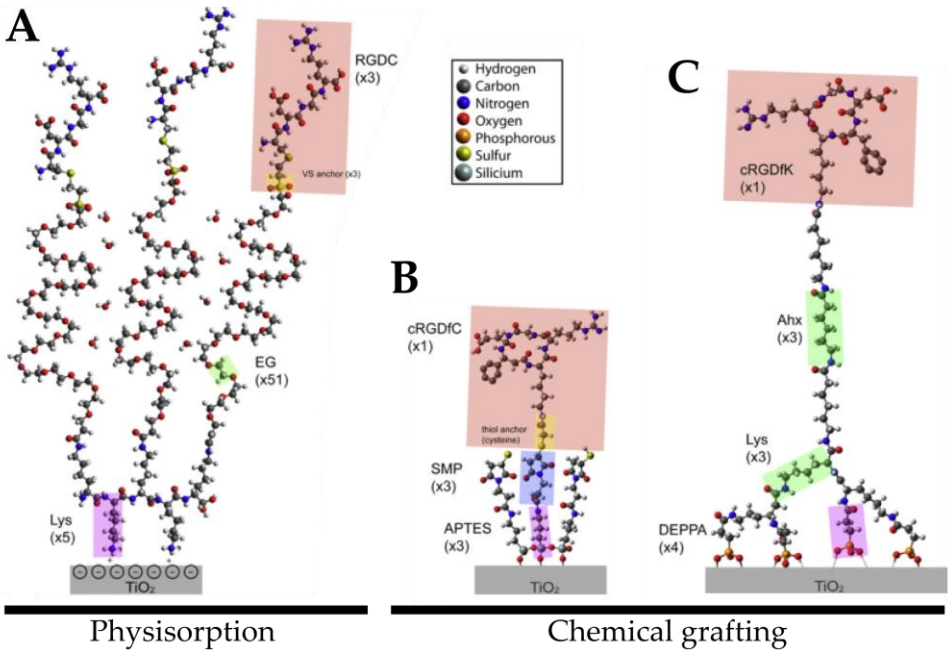

Figure 1.13. Chemical structures of three immobilization strategies on Ti. (A) Poly-L-lysine-g-poly(ethylene glycol) (EG) layer adsorbed electrostatically onto a titania surface. The positively charged amino termini of the polylysine backbone interact with the negatively charged Ti oxide. The water molecules between the polymer chains are indicative of the hydration of the brush. Vinylsulfone and one free cysteine (C) of the peptide allow establishing a double thiol specific binding between the polymeric brush and the bioadhesive RGDC peptide. (B) Silanization of the Ti oxide surface by APTES and covalent attachment of a heterobifunctional maleimide crosslinker (N-succinimidyl-3-maleimidopropionate) (SMP) followed by specific thiol tethering of the cysteine residue of a cyclic RGDfC peptide. (C) Self-assembly of four 3-(dietohoxy-phosphoryl)propionic acid (DEPPA) on Ti oxide linked together by three branching lysine residues. A spacer consisting in three aminohexanoic acids (Ahx) binds to the terminal amino of a free lysine of a cyclic RGDfK peptide. Adapted from [7].

1.6 References

[1] D.F. Williams, On the nature of biomaterials, Biomaterials. 30 (2009) 5897–5909. doi:10.1016/j.biomaterials.2009.07.027.

[2] S. Kurtz, K. Ong, E. Lau, F. Mowat, M. Halpern, Projections of primary and revision hip and knee arthroplasty in the United States from 2005 to 2030, J. Bone Joint Surg. Am. 89 (2007) 780–5. doi:10.2106/JBJS.F.00222.

[3] D.F. Williams, On the mechanisms of biocompatibility, Biomaterials. 29 (2008) 2941–53. doi:10.1016/j.biomaterials.2008.04.023.

[4] S. Bauer, P. Schmuki, K. von der Mark, J. Park, Engineering biocompatible implant surfaces. Part I: Materials and surfaces, Prog. Mater. Sci. 58 (2013) 261–326. doi:10.1016/j.pmatsci.2012.09.001.

[5] F. Loi, L.A. Córdova, J. Pajarinen, T. Lin, Z. Yao, S.B. Goodman, Inflammation, fracture and bone repair, Bone. 86 (2016) 119–130. doi:10.1016/j.bone.2016.02.020.

[6] R. Brånemark, P.I. Brånemark, B. Rydevik, R.R. Myers, Osseointegration in skeletal reconstruction and rehabilitation: a review, J. Rehabil. Res. Dev. 38 (2001) 175–81. http://www.ncbi.nlm.nih.gov/pubmed/11392650.

[7] R. Tejero, E. Anitua, G. Orive, Toward the biomimetic implant surface: Biopolymers on titanium-based implants for bone regeneration, Prog. Polym. Sci. 39 (2014) 1406–1447. doi:10.1016/j.progpolymsci.2014.01.001.

[8] M. Geetha, A.K. Singh, R. Asokamani, A.K. Gogia, Ti based biomaterials, the ultimate choice for orthopaedic implants – A review, Prog. Mater. Sci. 54 (2009) 397–425. doi:10.1016/j.pmatsci.2008.06.004.

[9] M. González, J. Peña, J.M. Manero, M. Arciniegas, F.J. Gil, Design and characterization of new Ti-Nb-Hf alloys, J. Mater. Eng. Perform. 18 (2009) 490–495. doi:10.1007/s11665-009-9381-2.

[10] B.D. Ratner, A.S. Hoffman, F.J. Schoen, J.E. Lemons, Biomaterials Science, Second Edi, Elsevier Academic Press, 2004.

[11] H. Matusiewicz, Potential release of in vivo trace metals from metallic medical implants in the human body: From ions to nanoparticles - A systematic analytical review, Acta Biomater. 10 (2014) 2379–2403. doi:10.1016/j.actbio.2014.02.027.

[12] T. Hanawa, A comprehensive review of techniques for biofunctionalization of titanium, J. Periodontal Implant Sci. 41 (2011) 263–72. doi:10.5051/jpis.2011.41.6.263.

[13] K.J. Bozic, S.M. Kurtz, E. Lau, K. Ong, V. Chiu, T.P. Vail, et al., The epidemiology of revision total knee arthroplasty in the united states, Clin. Orthop. Relat. Res. 468 (2010) 45–51. doi:10.1007/s11999-009-0945-0.

[14] G. Mendonça, D.B.S. Mendonça, F.J.L. Aragão, L.F. Cooper, Advancing dental implant surface technology – From micron- to nanotopography, Biomaterials. 29 (2008) 3822–3835. doi:10.1016/j.biomaterials.2008.05.012.

[15] M. Nikkhah, F. Edalat, S. Manoucheri, A. Khademhosseini, Engineering microscale topographies to control the cell-substrate interface, Biomaterials. 33 (2012) 5230–46. doi:10.1016/j.biomaterials.2012.03.079.

[16] C.C. DuFort, M.J. Paszek, V.M. Weaver, Balancing forces: architectural control of mechanotransduction, Nat. Rev. Mol. Cell Biol. 12 (2011) 308–19. doi:10.1038/nrm3112.

[17] A. Curtis, C. Wilkinson, Topographical control of cells, Biomaterials.

18 (1997) 1573–1583. doi:10.1016/S0142-9612(97)00144-0.

[18] A. Bagno, C. Di Bello, Surface treatments and roughness properties of Ti-based biomaterials, J. Mater. Sci. Mater. Med. 15 (2004) 935–949. doi:10.1023/B:JMSM.0000042679.28493.7f.

[19] J. Lincks, B.D. Boyan, C.R. Blanchard, C.H. Lohmann, Y. Liu, D.L. Cochran, et al., Response of MG63 osteoblast-like cells to titanium and titanium alloy is dependent on surface roughness and composition, Biomaterials. 19 (1998) 2219–32. http://www.ncbi.nlm.nih.gov/pubmed/9884063.

[20] B. Groessner-Schreiber, R.S. Tuan, Enhanced extracellular matrix production and mineralization by osteoblasts cultured on titanium surfaces in vitro, J. Cell Sci. 101 (1992) 209–217.

[21] K. Anselme, M. Bigerelle, B. Noel, E. Dufresne, D. Judas, A. Iost, et al., Qualitative and quantitative study of human osteoblast adhesion on materials with various surface roughnesses, J. Biomed. Mater. Res. 49 (2000) 155–66. http://www.ncbi.nlm.nih.gov/pubmed/10571901.

[22] D. Buser, R.K. Schenk, S. Steinemann, J.P. Fiorellini, C.H. Fox, H. Stich, Influence of surface characteristics on bone integration of titanium implants. A histomorphometric study in miniature pigs, J. Biomed. Mater. Res. 25 (1991) 889–902. doi:10.1002/jbm.820250708.

[23] D.L. Cochran, R.K. Schenk, A. Lussi, F.L. Higginbottom, D. Buser, Bone response to unloaded and loaded titanium implants with a sandblasted and acid-etched surface: A histometric study in the canine mandible, J. Biomed. Mater. Res. 40 (1998) 1–11. doi:10.1002/(SICI)1097-4636(199804)40:1<1::AID-JBM1>3.0.CO;2-Q.

[24] H. Daugaard, B. Elmengaard, J.E. Bechtold, K. Soballe, Bone growth enhancement in vivo on press-fit titanium alloy implants with acid

etched microtexture, J. Biomed. Mater. Res. A. 87 (2008) 434–40. doi:10.1002/jbm.a.31748.

[25] G. Giavaresi, M. Fini, a Cigada, R. Chiesa, G. Rondelli, L. Rimondini, et al., Histomorphometric and microhardness assessments of sheep cortical bone surrounding titanium implants with different surface treatments., J. Biomed. Mater. Res. A. 67 (2003) 112–120. doi:10.1002/jbm.a.10044.

[26] H.J. Rønold, S.P. Lyngstadaas, J.E. Ellingsen, Analysing the optimal value for titanium implant roughness in bone attachment using a tensile test, Biomaterials. 24 (2003) 4559–4564. doi:10.1016/S0142-9612(03)00256-4.

[27] S. Hansson, M. Norton, The relation between surface roughness and interfacial shear strength for bone-anhcored implants. A mathematical model, J. Biomech. 32 (1999) 829–836.

[28] J.E. Davies, Understanding peri-implant endosseous healing, J. Dent. Educ. 67 (2003) 932–49. http://www.ncbi.nlm.nih.gov/pubmed/12959168.

[29] D.A. Puleo, A. Nanci, Understanding and controlling the bone-implant interface, Biomaterials. 20 (1999) 2311–21. http://www.ncbi.nlm.nih.gov/pubmed/10614937.

[30] M.J. Dalby, N. Gadegaard, R.O.C. Oreffo, Harnessing nanotopography and integrin-matrix interactions to influence stem cell fate, Nat. Mater. 13 (2014) 558–69. doi:10.1038/nmat3980.

[31] F. Guilak, D.M. Cohen, B.T. Estes, J.M. Gimble, W. Liedtke, C.S. Chen, Control of stem cell fate by physical interactions with the extracellular matrix, Cell Stem Cell. 5 (2009) 17–26. doi:10.1016/j.stem.2009.06.016.

[32] R.A. Gittens, R. Olivares-Navarrete, Z. Schwartz, B.D. Boyan,

Implant osseointegration and the role of microroughness and nanostructures: Lessons for spine implants, Acta Biomater. 10 (2014) 3363–3371. doi:10.1016/j.actbio.2014.03.037.

[33] T.J. Webster, J.U. Ejiofor, Increased osteoblast adhesion on nanophase metals: Ti, Ti6Al4V, and CoCrMo, Biomaterials. 25 (2004) 4731–4739. doi:10.1016/j.biomaterials.2003.12.002.

[34] Y. Huang, G. Zha, Q. Luo, J. Zhang, F. Zhang, X. Li, et al., The construction of hierarchical structure on Ti substrate with superior osteogenic activity and intrinsic antibacterial capability., Sci. Rep. 4 (2014) 6172. doi:10.1038/srep06172.

[35] S. Oh, K.S. Brammer, Y.S.J. Li, D. Teng, A.J. Engler, S. Chien, et al., Stem cell fate dictated solely by altered nanotube dimension, Proc. Natl. Acad. Sci. U. S. A. 106 (2009) 2130–5. doi:10.1073/pnas.0813200106.

[36] R. McBeath, D.M. Pirone, C.M. Nelson, K. Bhadriraju, C.S. Chen, Cell shape, cytoskeletal tension, and RhoA regulate stem cell lineage commitment, Dev. Cell. 6 (2004) 483–95. doi:10.1016/S1534-5807(04)00075-9.

[37] K.A. Kilian, B. Bugarija, B.T. Lahn, M. Mrksich, Geometric cues for directing the differentiation of mesenchymal stem cells, Proc. Natl. Acad. Sci. U. S. A. 107 (2010) 4872–7. doi:10.1073/pnas.0903269107.

[38] T. Sjöström, M.J. Dalby, A. Hart, R. Tare, R.O.C. Oreffo, B. Su, Fabrication of pillar-like titania nanostructures on titanium and their interactions with human skeletal stem cells., Acta Biomater. 5 (2009) 1433–41. doi:10.1016/j.actbio.2009.01.007.

[39] T. Sjöström, L.E. McNamara, L. Yang, M.J. Dalby, B. Su, Novel anodization technique using a block copolymer template for nanopatterning of titanium implant surfaces, ACS Appl. Mater.

Interfaces. 4 (2012) 6354–6361. doi:10.1021/am301987e.

[40] M. Ventre, F. Causa, P.A. Netti, Determinants of cell-material crosstalk at the interface: towards engineering of cell instructive materials, J. R. Soc. Interface. 9 (2012) 2017–2032. doi:10.1098/rsif.2012.0308.

[41] M. Schvartzman, M. Palma, J. Sable, J. Abramson, X. Hu, M.P. Sheetz, et al., Nanolithographic control of the spatial organization of cellular adhesion receptors at the single-molecule level, Nano Lett. 11 (2011) 1306–12. doi:10.1021/nl104378f.

[42] R.J. McMurray, N. Gadegaard, P.M. Tsimbouri, K. V Burgess, L.E. McNamara, R. Tare, et al., Nanoscale surfaces for the long-term maintenance of mesenchymal stem cell phenotype and multipotency, Nat. Mater. 10 (2011) 637–44. doi:10.1038/nmat3058.

[43] E.P. Ivanova, J. Hasan, H.K. Webb, V.K. Truong, G.S. Watson, J.A. Watson, et al., Natural bactericidal surfaces: Mechanical rupture of pseudomonas aeruginosa cells by cicada wings, Small. 8 (2012) 2489–2494. doi:10.1002/smll.201200528.

[44] J. Hasan, H.K. Webb, V.K. Truong, S. Pogodin, V.A. Baulin, G.S. Watson, et al., Selective bactericidal activity of nanopatterned superhydrophobic cicada Psaltoda claripennis wing surfaces, Appl. Microbiol. Biotechnol. 97 (2013) 9257–9262. doi:10.1007/s00253-012-4628-5.

[45] E.P. Ivanova, J. Hasan, H.K. Webb, G. Gervinskas, S. Juodkazis, V.K. Truong, et al., Bactericidal activity of black silicon, Nat. Commun. 4 (2013) 2838–2844. doi:10.1038/ncomms3838.

[46] J. Raphel, M. Holodniy, S.B. Goodman, S.C. Heilshorn, Multifunctional Coatings to Simultaneously Promote Osseointegration and Prevent Infection of Orthopaedic Implants,

Biomaterials. 84 (2016). doi:10.1016/j.biomaterials.2016.01.016.

[47] E.P. Vieira, S. Rocha, M. Carmo Pereira, H. Möhwald, M. a N. Coelho, Adsorption and diffusion of plasma proteins on hydrophilic and hydrophobic surfaces: effect of trifluoroethanol on protein structure., Langmuir. 25 (2009) 9879–9886. doi:10.1021/la9009948.

[48] E. a Vogler, Structure and reactivity of water at biomaterial surfaces, Adv. Colloid Interface Sci. 74 (1998) 69–117. doi:10.1016/S0001-8686(97)00040-7.

[49] A.L. Raines, R. Olivares-Navarrete, M. Wieland, D.L. Cochran, Z. Schwartz, B.D. Boyan, Regulation of angiogenesis during osseointegration by titanium surface microstructure and energy, Biomaterials. 31 (2010) 4909–4917. doi:10.1016/j.biomaterials.2010.02.071.

[50] D.A. Puleo, R. Bizios, Overview of Material Surface Properties Relevant to Protein Adsorption, in: Biol. Interact. Mater. Surfaces Underst. Control. Protein, Cell, Tissue Responses, n.d.

[51] P. Roach, D. Farrar, C.C. Perry, Surface tailoring for controlled protein adsorption: Effect of topography at the nanometer scale and chemistry, J. Am. Chem. Soc. 128 (2006) 3939–3945. doi:10.1021/ja056278e.

[52] I. Wall, N. Donos, K. Carlqvist, F. Jones, P. Brett, Modified titanium surfaces promote accelerated osteogenic differentiation of mesenchymal stromal cells in vitro., Bone. 45 (2009) 17–26. doi:10.1016/j.bone.2009.03.662.

[53] N. Donos, S. Hamlet, N.P. Lang, G.E. Salvi, G. Huynh-Ba, D.D. Bosshardt, et al., Gene expression profile of osseointegration of a hydrophilic compared with a hydrophobic microrough implant surface, Clin. Oral Implants Res. 22 (2011) 365–372.

doi:10.1111/j.1600-0501.2010.02113.x.

[54] N.P. Lang, G.E. Salvi, G. Huynh-Ba, S. Ivanovski, N. Donos, D.D. Bosshardt, Early osseointegration to hydrophilic and hydrophobic implant surfaces in humans, Clin. Oral Implants Res. 22 (2011) 349–356. doi:10.1111/j.1600-0501.2011.02172.x.

[55] A.A. Mamalis, S.S. Silvestros, Analysis of osteoblastic gene expression in the early human mesenchymal cell response to a chemically modified implant surface: An in vitro study, Clin. Oral Implants Res. 22 (2011) 530–537. doi:10.1111/j.1600-0501.2010.02049.x.

[56] J. Hwa, C.E. Wasilewski, N. Almodovar, R. Olivares-navarrete, B.D. Boyan, R. Tannenbaum, et al., The responses to surface wettability gradients induced by chitosan nano films on microtextured titanium mediated by specific integrin receptors, Biomaterials. 33 (2012) 7386–7393. doi:10.1016/j.biomaterials.2012.06.066.

[57] W. Att, N. Hori, F. Iwasa, M. Yamada, T. Ueno, T. Ogawa, The effect of UV-photofunctionalization on the time-related bioactivity of titanium and chromium-cobalt alloys, Biomaterials. 30 (2009) 4268–4276. doi:10.1016/j.biomaterials.2009.04.048.

[58] T. Ueno, M. Yamada, T. Suzuki, H. Minamikawa, N. Sato, N. Hori, et al., Enhancement of bone-titanium integration profile with UV-photofunctionalized titanium in a gap healing model, Biomaterials. 31 (2010) 1546–1557. doi:10.1016/j.biomaterials.2009.11.018.

[59] H. Ohgushi, A.I. Caplan, Stem cell technology and bioceramics: From cell to gene engineering, J. Biomed. Mater. Res. 48 (1999) 913–927. doi:10.1002/(SICI)1097-4636(1999)48:6<913::AID-JBM22>3.0.CO;2-0.

[60] R.G.T. Geesink, K. De Groot, C.P.A.T. Klein, Chemical Implant Fixation Using Hydroxyl-Apatite Coatings: The Development of a

Human Total Hip Prosthesis for Chemical Fixation to Bone Using Hydroxyl-Apatite Coatings on Titanium Substrates, Clin. Orthop. Relat. Res. (1987) 147–170.

[61] J.J. Lee, L. Rouhfar, O.R. Beirne, Survival of hydroxyapatite-coated implants: A meta-analytic review, J. Oral Maxillofac. Surg. 58 (2000) 1372–1379. doi:10.1053/joms.2000.18269.

[62] H. Kim, F. Miyaji, T. Kokubo, T. Nakamura, Preparation of bioactive Ti and its alloys via simple chemical surface treatment, J. Biomed. Mater. Res. 32 (1996) 409–417. doi:10.1002/(SICI)1097-4636(199611)32:3<409::AID-JBM14>3.0.CO;2-B.

[63] T. Kokubo, S. Yamaguchi, Bioactive Ti metal and its alloys prepared by chemical treatments: State-of-the-art and future trends, Adv. Eng. Mater. 12 (2010) 579–591. doi:10.1002/adem.201080087.

[64] M. Neo, T. Nakamura, C. Ohtsuki, T. Kokubo, T. Yamamuro, Apatite formation on three kinds of bioactive material at an early stage in vivo: a comparative study by transmission electron microscopy., J. Biomed. Mater. Res. 27 (1993) 999–1006. doi:10.1002/jbm.820270805.

[65] B.G. Keselowsky, D.M. Collard, A.J. García, Surface chemistry modulates fibronectin conformation and directs integrin binding and specificity to control cell adhesion, J. Biomed. Mater. Res. A. 66 (2003) 247–59. doi:10.1002/jbm.a.10537.

[66] L. Zhang, C. Ning, T. Zhou, X. Liu, K.W.K. Yeung, T. Zhang, et al., Polymeric nanoarchitectures on Ti-based implants for antibacterial applications, ACS Appl. Mater. Interfaces. 6 (2014) 17323–17345. doi:10.1021/am5045604.

[67] Y. Ito, H. Hasuda, M. Sakuragi, S. Tsuzuki, Surface modification of plastic, glass and titanium by photoimmobilization of polyethylene glycol for antibiofouling, Acta Biomater. 3 (2007) 1024–1032.

doi:10.1016/j.actbio.2007.05.010.

[68] X. Ding, C. Yang, T. Lim, L. Hsu, A. Engler, Antibacterial and antifouling catheter coatings using surface grafted PEG- b-cationic polycarbonate diblock copolymers, Biomaterials. 33 (2012). doi:10.1016/j.biomaterials.2012.06.001.

[69] K.G. Neoh, X. Hu, D. Zheng, E.T. Kang, Balancing osteoblast functions and bacterial adhesion on functionalized titanium surfaces, Biomaterials. 33 (2012) 2813–2822. doi:10.1016/j.biomaterials.2012.01.018.

[70] J.J. Rice, M.M. Martino, L. De Laporte, F. Tortelli, P.S. Briquez, J. A. Hubbell, Engineering the regenerative microenvironment with biomaterials, Adv. Healthc. Mater. 2 (2013) 57–71. doi:10.1002/adhm.201200197.

[71] C. Mas-Moruno, R. Fraioli, F. Rechenmacher, S. Neubauer, T.G. Kapp, H. Kessler, αvβ3- or α5β1-Integrin-Selective Peptidomimetics for Surface Coating, Angew. Chemie Int. Ed. (2016) 7048–7067. doi:10.1002/anie.201509782.

[72] S.J. Shattil, C. Kim, M.H. Ginsberg, The final steps of integrin activation: the end game, Nat. Rev. Mol. Cell Biol. 11 (2010) 288–300. doi:10.1038/nrm2871.

[73] M. Vicente-Manzanares, C.K. Choi, A.R. Horwitz, Integrins in cell migration--the actin connection, J. Cell Sci. 122 (2009) 199–206. doi:10.1242/jcs.018564.

[74] C. Ciobanasu, B. Faivre, C. Le Clainche, Integrating actin dynamics, mechanotransduction and integrin activation: The multiple functions of actin binding proteins in focal adhesions, Eur. J. Cell Biol. 92 (2013) 339–348. doi:10.1016/j.ejcb.2013.10.009.

[75] R.O. Hynes, Integrins: bidirectional, allosteric signaling machines,

Cell. 110 (2002) 673–87. http://www.ncbi.nlm.nih.gov/pubmed/12297042.

[76] R.O. Hynes, A reevaluation of integrins as regulators of angiogenesis, Nat. Med. 8 (2002) 918–21. doi:10.1038/nm0902-918.

[77] A. van der Flier, K. Badu-Nkansah, C. a Whittaker, D. Crowley, R.T. Bronson, A. Lacy-Hulbert, et al., Endothelial alpha5 and alphav integrins cooperate in remodeling of the vasculature during development, Development. 137 (2010) 2439–2449. doi:10.1242/dev.049551.

[78] S. Gronthos, K. Stewart, Integrin Expression and Function on Human Osteoblast-like Cells, J. Bone Miner. Res. 12 (1997) 1190–1197. doi:10.1359/jbmr.1997.12.8.1189.

[79] P. Schaffner, M.M. Dard, Structure and function of RGD peptides involved in bone biology, Cell. Mol. Life Sci. 60 (2003) 119–132. doi:10.1007/s000180300008.

[80] M.C. Siebers, P.J. ter Brugge, X.F. Walboomers, J.A. Jansen, Integrins as linker proteins between osteoblasts and bone replacing materials. A critical review, Biomaterials. 26 (2005) 137–146. doi:10.1016/j.biomaterials.2004.02.021.

[81] S. Gronthos, P.J. Simmons, S.E. Graves, P.G. Robey, Integrin-mediated interactions between human bone marrow stromal precursor cells and the extracellular matrix, Bone. 28 (2001) 174–81. http://www.ncbi.nlm.nih.gov/pubmed/11182375.

[82] J.E. Frith, R.J. Mills, J.E. Hudson, J.J. Cooper-White, Tailored integrin-extracellular matrix interactions to direct human mesenchymal stem cell differentiation, Stem Cells Dev. 21 (2012) 2442–56. doi:10.1089/scd.2011.0615.

[83] M.M. Martino, M. Mochizuki, D.A. Rothenfluh, S.A. Rempel, J.A.

Hubbell, T.H. Barker, Controlling integrin specificity and stem cell differentiation in 2D and 3D environments through regulation of fibronectin domain stability, Biomaterials. 30 (2009) 1089–97. doi:10.1016/j.biomaterials.2008.10.047.

[84] A. Shekaran, A.J. García, Extracellular matrix-mimetic adhesive biomaterials for bone repair, J. Biomed. Mater. Res. A. 96 (2011) 261–72. doi:10.1002/jbm.a.32979.

[85] S.L. Cheng, C.F. Lai, S.D. Blystone, L. V Avioli, Bone mineralization and osteoblast differentiation are negatively modulated by integrin alpha(v)beta3, J. Bone Miner. Res. 16 (2001) 277–288. doi:10.1359/jbmr.2001.16.2.277.

[86] S. Nesbitts, A. Nesbit, M. Helfrich, M. Horton, Biochemical Characterization of Human Osteoclast Integrins, 268 (1993) 16737–16745.

[87] R. Zaidel-Bar, C. Ballestrem, Z. Kam, B. Geiger, Early molecular events in the assembly of matrix adhesions at the leading edge of migrating cells, J. Cell Sci. 116 (2003) 4605–4613. doi:10.1242/jcs.00792.

[88] M.R. Morgan, A. Byron, M.J. Humphries, M.D. Bass, Giving off mixed signals--distinct functions of alpha5beta1 and alphavbeta3 integrins in regulating cell behaviour, IUBMB Life. 61 (2009) 731–8. doi:10.1002/iub.200.

[89] P. Roca-Cusachs, N.C. Gauthier, A. Del Rio, M.P. Sheetz, Clustering of alpha(5)beta(1) integrins determines adhesion strength whereas alpha(v)beta(3) and talin enable mechanotransduction., Proc. Natl. Acad. Sci. U. S. A. 106 (2009) 16245–16250. doi:10.1073/pnas.0902818106.

[90] S. Rahmouni, A. Lindner, F. Rechenmacher, S. Neubauer, T.R.A.

Sobahi, H. Kessler, et al., Hydrogel micropillars with integrin selective peptidomimetic functionalized nanopatterned tops: a new tool for the measurement of cell traction forces transmitted through αvβ3- or α5β1-integrins, Adv. Mater. 25 (2013) 5869–74. doi:10.1002/adma.201301338.

[91] Z. Hamidouche, O. Fromigué, J. Ringe, T. Häupl, P. Vaudin, J.-C. Pagès, et al., Priming integrin alpha5 promotes human mesenchymal stromal cell osteoblast differentiation and osteogenesis, Proc. Natl. Acad. Sci. U. S. A. 106 (2009) 18587–91. doi:10.1073/pnas.0812334106.

[92] T.A. Petrie, J.E. Raynor, C.D. Reyes, K.L. Burns, D.M. Collard, A.J. García, The effect of integrin-specific bioactive coatings on tissue healing and implant osseointegration, Biomaterials. 29 (2008) 2849–57. doi:10.1016/j.biomaterials.2008.03.036.

[93] R. Agarwal, C. González-García, B. Torstrick, R.E. Guldberg, M. Salmerón-Sánchez, A.J. García, Simple coating with fibronectin fragment enhances stainless steel screw osseointegration in healthy and osteoporotic rats, Biomaterials. 63 (2015) 137–145. doi:10.1016/j.biomaterials.2015.06.025.

[94] G.B. Schneider, R. Zaharias, C. Stanford, Osteoblast integrin adhesion and signaling regulate mineralization, J. Dent. Res. 80 (2001) 1540–1544. doi:10.1177/00220345010800061201.

[95] C.-F. Lai, S.-L. Cheng, Alphavbeta integrins play an essential role in BMP-2 induction of osteoblast differentiation, J. Bone Miner. Res. 20 (2005) 330–40. doi:10.1359/JBMR.041013.

[96] K.A. Kilian, M. Mrksich, Directing stem cell fate by controlling the affinity and density of ligand-receptor interactions at the biomaterials interface, Angew. Chemie - Int. Ed. 124 (2012) 4975–4979. doi:10.1002/anie.201108746.

[97] K. Anselme, Osteoblast adhesion on biomaterials, Biomaterials. 21 (2000) 667–81. http://www.ncbi.nlm.nih.gov/pubmed/10711964.

[98] U. Hersel, C. Dahmen, H. Kessler, RGD modified polymers: biomaterials for stimulated cell adhesion and beyond, Biomaterials. 24 (2003) 4385–4415. doi:10.1016/S0142-9612(03)00343-0.

[99] S. Cutler, A.J. García, Engineering cell adhesive surfaces that direct integrin $\alpha 5\beta 1$ binding using a recombinant fragment of fibronectin, Biomaterials. 24 (2003) 1759–1770. doi:10.1016/S0142-9612(02)00570-7.

[100] N. Broggini, S. Tosatti, S.J. Ferguson, M. Schuler, M. Textor, M.M. Bornstein, et al., Evaluation of chemically modified SLA implants (modSLA) biofunctionalized with integrin (RGD)- and heparin (KRSR)-binding peptides, J. Biomed. Mater. Res. - Part A. 100 A (2012) 703–711. doi:10.1002/jbm.a.34004.

[101] D.S.W. Benoit, K.S. Anseth, The effect on osteoblast function of colocalized RGD and PHSRN epitopes on PEG surfaces., Biomaterials. 26 (2005) 5209–20. doi:10.1016/j.biomaterials.2005.01.045.

[102] M. Dettin, M. Conconi, R. Gambaretto, A. Pasquato, M. Folin, C. Di Bello, et al., Novel osteoblast-adhesive peptides for dental/orthopedic biomaterials, J. Biomed. Mater. Res. 60 (2002) 466–471. doi:10.1002/jbm.10066.

[103] C. Mas-Moruno, P.M. Dorfner, F. Manzenrieder, S. Neubauer, U. Reuning, R. Burgkart, et al., Behavior of primary human osteoblasts on trimmed and sandblasted Ti6Al4V surfaces functionalized with integrin $\alpha v\beta 3$-selective cyclic RGD peptides, J. Biomed. Mater. Res. A. 101 (2013) 87–97. doi:10.1002/jbm.a.34303.

[104] J. Auernheimer, D. Zukowski, C. Dahmen, M. Kantlehner, A. Enderle, S.L. Goodman, et al., Titanium implant materials with

improved biocompatibility through coating with phosphonate-anchored cyclic RGD peptides, Chembiochem. 6 (2005) 2034–40. doi:10.1002/cbic.200500031.

[105] C. Dahmen, J. Auernheimer, A. Meyer, A. Enderle, S.L. Goodman, H. Kessler, Improving implant materials by coating with nonpeptidic, highly specific integrin ligands, Angew. Chem. Int. Ed. Engl. 43 (2004) 6649–52. doi:10.1002/anie.200460770.

[106] F. Rechenmacher, S. Neubauer, J. Polleux, C. Mas-Moruno, M. De Simone, E.A. Cavalcanti-Adam, et al., Functionalizing $\alpha v\beta 3$- or $\alpha 5\beta 1$-selective integrin antagonists for surface coating: a method to discriminate integrin subtypes in vitro, Angew. Chem. Int. Ed. Engl. 52 (2013) 1572–5. doi:10.1002/anie.201206370.

[107] Y. Hirano, D.J. Mooney, Peptide and Protein Presenting Materials for Tissue Engineering, Adv. Mater. 16 (2004) 17–25. doi:10.1002/adma.200300383.

[108] S.-J. Xiao, M. Textor, N.D. Spencer, Covalent Attachment of Cell-Adhesive, (Arg-Gly-Asp) -Containing Peptides to Titanium Surfaces, Langmuir. 14 (1998) 5507–5516.

[109] S.J. Xiao, M. Textor, N.D. Spencer, M. Wieland, B. Keller, H. Sigrist, Immobilization of the cell-adhesive peptide Arg-Gly-Asp-Cys (RGDC) on titanium surfaces by covalent chemical attachment, J. Mater. Sci. Mater. Med. 8 (1997) 867–872. http://www.ncbi.nlm.nih.gov/pubmed/15348806.

[110] M. Godoy-Gallardo, C. Mas-Moruno, M.C. Fernández-Calderón, C. Pérez-Giraldo, J.M. Manero, F. Albericio, et al., Covalent immobilization of hLf1-11 peptide on a titanium surface reduces bacterial adhesion and biofilm formation., Acta Biomater. 10 (2014) 3522–3534. doi:10.1016/j.actbio.2014.03.026.

[111] J. Guasch, B. Conings, S. Neubauer, F. Rechenmacher, K. Ende, C.G. Rolli, et al., Segregation Versus Colocalization: Orthogonally Functionalized Binary Micropatterned Substrates Regulate the Molecular Distribution in Focal Adhesions, Adv. Mater. (2015) n/a-n/a. doi:10.1002/adma.201500900.

[112] M. López-Garcia, H. Kessler, Stimulation of Bone Growth on Implants by Integrin Ligands, in: M. Epple, E. Bäuerlein (Eds.), Handb. Miner., Wiley-VCH, Weinheim, Germany, 2007: pp. 109–126.

[113] H. Lee, S.M. Dellatore, W.M. Miller, P.B. Messersmith, Mussel-Inspired Surface Chemistry for Multifunctional Coatings, Science (80-.). 318 (2007) 426–430.

[114] M. Pagel, R. Hassert, T. John, K. Braun, M. Wießler, B. Abel, et al., Multifunctional Coating Improves Cell Adhesion on Titanium by using Cooperatively Acting Peptides, Angew. Chemie Int. Ed. (2016) n/a-n/a. doi:10.1002/anie.201511781.

[115] J.L. Hong, N.K. Ahn, W.L. Suk, H.L. Myung, C.L. Sang, Catechol-functionalized adhesive polymer nanoparticles for controlled local release of bone morphogenetic protein-2 from titanium surface, J. Control. Release. 170 (2013) 198–208. doi:10.1016/j.jconrel.2013.05.017.

[116] D.J. Leahy, I. Aukhil, H.P. Erickson, 2.0 A crystal structure of a four-domain segment of human fibronectin encompassing the RGD loop and synergy region., Cell. 84 (1996) 155–64. http://www.ncbi.nlm.nih.gov/pubmed/8548820.

[117] S. Aota, M. Nomizu, K.M. Yamada, The short amino acid sequence Pro-His-Ser-Arg-Asn in human fibronectin enhances cell-adhesive function., J. Biol. Chem. 269 (1994) 24756–61. http://www.ncbi.nlm.nih.gov/pubmed/7929152.

Index

A

angiogenesis 6

B

bioactive 3
bioactivity 14
biochemical functionalization 29
biocompatibility 2
biodegradation 12
bioinert 3, 13
biomaterials 1
bone-implant contact (BIC) 5
bulk properties 10

Ch

chemisorption 39

C

covalent grafting 38

D

dopamine 40

E

ECM 15, 29
endochondral ossification 7

F

focal adhesion 31
functionalization 15

G

granulation tissue 6

H

hard callus 7

I

inflammation 6
inside-out signaling 15
integrins 30
intramembraneous ossification 7
ion release 13

L

linear peptide 36

M

metals 10
microtopography 17

N

nanotopography 21

O

osseointegration 5
osteogenesis 6
outside-in signaling 15

P

peptide (cyclic) 37
peptide (mixtures) 37
peptide (rational design) 37
peptidomimetics 37
phosphonates 39
PHSRN 35
physisorption of integrin ligands 37
poly(ethylene glycol) (PEG) 28
protein fragment 35

R

remodeling 8
RGD 35

S

silanization 39
soft callus 7
stress shielding effect 10
surface modification 14
surface modification (chemical) 25
surface modification (inorganic) 25
surface modification (organic) 27
surface modification (physical) 17
surface properties 12

W

wettability 23
woven bone 7

Scope of the work

The present thesis was developed in the context of metals for hard tissue replacement implants, with a special focus on superficial modifications of Ti that can be applied to support a faster and more efficient osseointegration. As discussed previously, there is a growing interest in converting biocompatible materials into "smart" information carriers, which can deliver specific messages to the surrounding tissues and actively guide the healing process. This can be easily done by directly modifying the surface, which is responsible for the interactions between the synthetic material and the body. Among the methods described in the Introduction, the grafting of integrin-binding cues on the surface stands out as a straightforward solution to confer such bioactivity.

General objective

Therefore, the overall aim of the thesis is to ***convert titanium surface into a bioactive substrate via chemical functionalization with integrin-binding biomolecules, and test the effects of the receptor-selective cues in*** in vitro ***cell cultures and in an*** in vivo ***model.***

This general goal is further divided into the following specific objectives:

Sub goals

Objective 1: Anchor to Ti a **double** branched peptidic platform that mimics the integrin-binding site of FN to trigger specific cell response *in vitro* and enhance osseointegration *in vivo*. This topic is covered in Chapter I, which includes the studies of the response of OB-like cells (Paper I) and of hMSCs (Paper II) and the study in a small animal model (Paper II).

Objective 2: Anchor to Ti two **integrin-selective peptidomimetics**, each of which binds with high affinity one specific integrin subtype to trigger integrin-specific cell response *in vitro* and enhance osseointegration *in vivo*. Chapter II is focused on this objective by first introducing the design and biological potential of these biomolecules in a review paper (Review Article) and then describing their application as coating molecules. The *in vitro* response of OB-like cells and hMSCs is reported in Paper III and Annex I, respectively, while the *in vivo* response in a small animal models in Annex I.

Objective 3: The third objective derives from the combination of two surface modification strategies, namely a biochemical- and a topographical-based one. Nanorough bactericidal Ti surfaces were functionalized with the biomolecules described in Objectives 1 and 2 and the response of hMSCs and the bacteria strain *P. aeruginosa* were studied. This objective, which describes the simple merging of two classical modification strategies to generate a multifunctional coating, is described in Annex II.

The different works described so far are schematically resumed in figure 2.1.

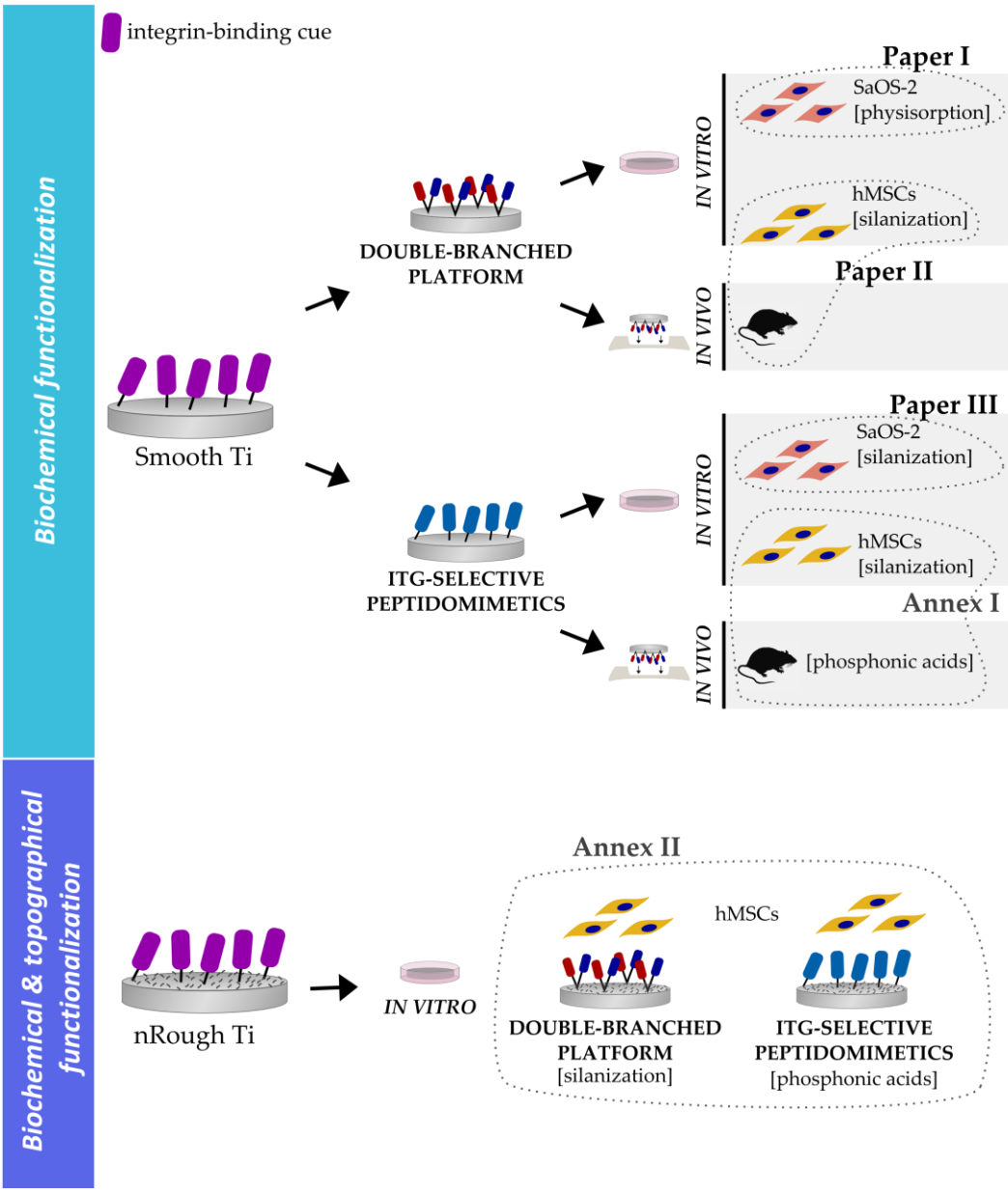

Figure 2.1. Schematic representation of the experimental systems studied and the *in vitro* and *in vivo* assays planned. For each study the surface modification technique is indicated in square brackets.

Chapter I: Functionalizing with a peptide-based platform

The biomolecule

The **peptide-based platform** consists in a double-branched structure that allows for the simultaneous immobilization of two bioactive peptidic sequences, as illustrated in figure I.1.

This molecular design offers a straightforward solution to the limitation of linear peptides, which, as discussed in section 1.5.2, are inherently lacking multifunctionality and often, as in the case of the RGD sequence, selectivity toward a specific cell line or integrin subtype. The possibility to include two sequences in the double-branched design brings several advantages: notably, by grafting two different sequences ligand multifunctionality is readily obtained, the two motifs are always presented at a 1:1 ratio, and the distance between the motifs is controlled by the molecule's spacer length. Moreover, these advantages come with a high degree of versatility, since the choice of the sequences, their geometrical presentation and the anchor can be customized for any application and the platform synthesized *ad hoc*.

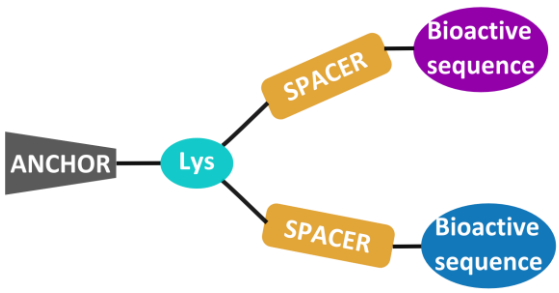

Figure I.1. General structure of the double-branched biomolecule.

Mimicking FN

This structure is particularly adequate to mimic the CAS of FN, which presents the two bioactive motifs RGD and PHSRN at about 35 Å of distance,[116] as represented in figure I.2 A. The presence of the synergic motif PHSRN makes this attachment site highly affine for integrin subtype $\alpha 5\beta 1$,[117] which was reported to be relevant in several events in bone

biology.[91] The double branched structure can easily recapitulate this feature in a low molecular weight ligand, by offering the possibility of immobilizing both motifs in the same ligand at a controlled distance. To mimic the spacing between ligands of FN, four units of aminohexanoic acid were chosen for the spacer arms of the molecule (Fig. I.2 B). The synthesis of the ligand was carried out using solid-phase peptide chemistry by Dr. C. Mas-Moruno at the Department of Materials Science and Metallurgical Engineering of the UPC.

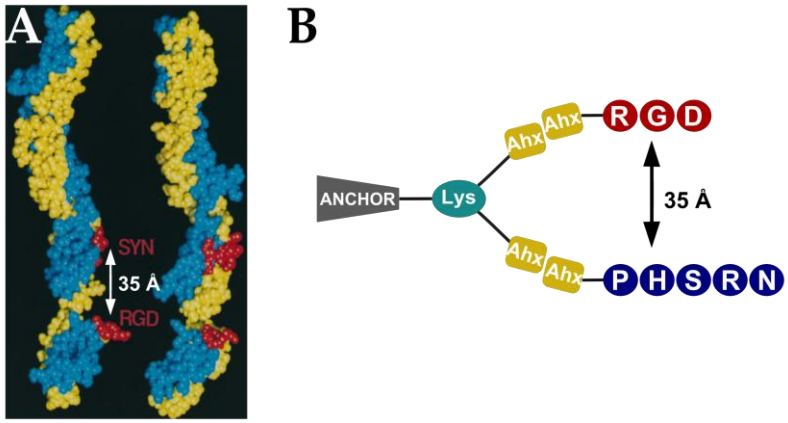

Figure I.2. (A) A space-filling model of the FNIII$_{7\text{-}10}$ domain, showing in red the two bioactive sequences: the adhesive RGD and the synergic motif PHSRN (SYN). Adapted from [116]. (B) The mimetic double branched structure presenting RGD and PHSRN.

The first publication of this chapter is centered on the synthesis of the novel ligand and the *in vitro* testing of the efficacy of the strategy in promoting SaOS-2 OB-like cell adhesion, proliferation and differentiation into the osteoblastic lineage on Ti. In this proof of concept work, physisorption was used to deposit the biomolecule on the metal. ***Paper I***

In the second publication of this chapter a covalent binding technique (silanization) was used to anchor the ligand to Ti. The *in vitro* studies were ***Paper II***

carried out with hMSCs, given their importance in the osseointegration process (discussed in section 1.2). Moreover, an *in vivo* study in a rat model is performed to assess the ability of the novel ligand to induce new bone growth in an animal model.

Annex II

The double branched platform molecule was also used to add cell-instructive properties to antibacterial nanotopographies that do not support efficient cell adhesion. This study, which merges a topography-based and a chemical-based strategy to generate a multifunctional Ti surface, is reported in Annex II.

References

[1] D.J. Leahy, I. Aukhil, H.P. Erickson, 2.0 A crystal structure of a four-domain segment of human fibronectin encompassing the RGD loop and synergy region., Cell. 84 (1996) 155–64. http://www.ncbi.nlm.nih.gov/pubmed/8548820.

[2] S. Aota, M. Nomizu, K.M. Yamada, The short amino acid sequence Pro-His-Ser-Arg-Asn in human fibronectin enhances cell-adhesive function., J. Biol. Chem. 269 (1994) 24756–61. http://www.ncbi.nlm.nih.gov/pubmed/7929152.

[3] Z. Hamidouche, O. Fromigué, J. Ringe, T. Häupl, P. Vaudin, J.-C. Pagès, et al., Priming integrin alpha5 promotes human mesenchymal stromal cell osteoblast differentiation and osteogenesis, Proc. Natl. Acad. Sci. U. S. A. 106 (2009) 18587–91. doi:10.1073/pnas.0812334106.

I.1 Paper I

Novel peptide-based platform for the dual presentation of biologically active peptide motifs on biomaterials

Author's contribution:

Performance of surface characterization and *in vitro* assays. Data analysis and contribution to manuscript preparation.

ATTENTION ¡
Pages 70 to 82 of the thesis are available at the editor's web
http://pubs.acs.org/doi/abs/10.1021/am5001213

SUPPORTING INFORMATION

A novel peptide-based platform for the dual presentation of biologically-active peptide motifs on biomaterials

Carlos Mas-Moruno, Roberta Fraioli, Fernando Albericio, José María Manero, and F. Javier Gil*

* To whom correspondence should be addressed. E-mail: carles.mas.moruno@upc.edu

Figure S1

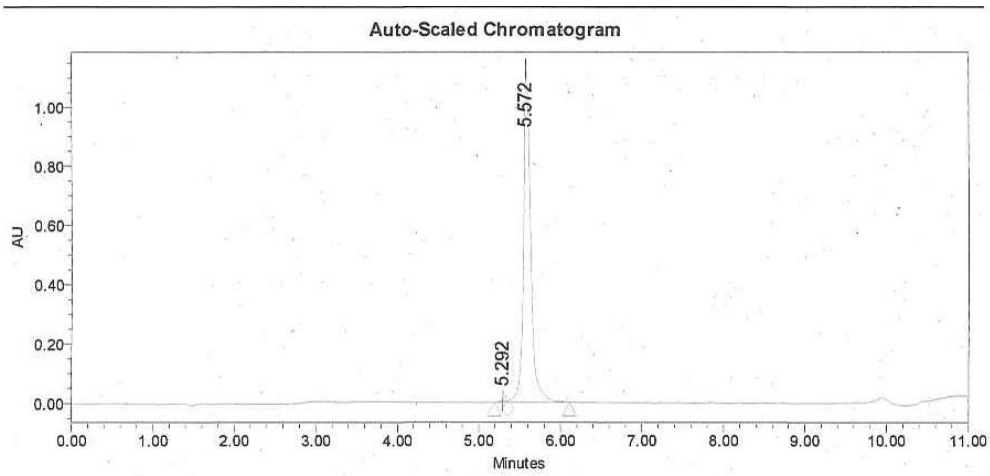

Peak Results

	RT	Area	Height	Total Area	% Area
1	5.292	30142	5855	6973850	0.43
2	5.572	6943708	1125681	6973850	99.57

Figure S1. HPLC chromatogram of the peptide-based platform. The analysis was performed using a Waters Alliance 2695 chromatography system (Waters), a reversed-phase XBridge BEH130 C-18 column (4.6 mm x 100 mm, 3.5 μm) and a photodiode array detector (Waters 2998). The system was run at a flow rate of 1.0 mL/min over 8 min at room temperature using water (0.045 % TFA, v/v) and ACN (0.036 % TFA, v/v) as solvents (linear gradient from 0 to 40 % of ACN). The platform was eluted at t_R = 5.572 min, and showed a purity > 99 %.

Figure S2

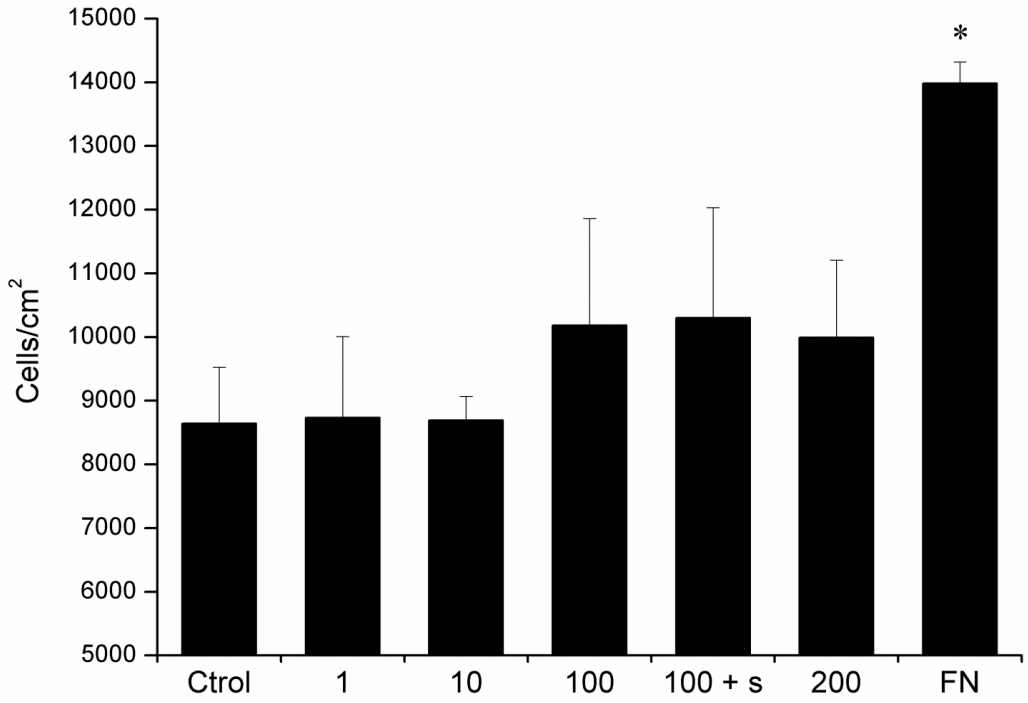

Figure S2. Adhesion of Saos-2 cells on biofunctionalized surfaces after 4h of incubation. Ti samples were functionalized with increasing concentrations of the platform (*1*, *10*, *100* and *200* μM). The number of cells attached (cells/cm^2) was analyzed by means of an LDH assay. Prior to the cell adhesion assays, a set of samples were subjected to 3 x 5 min treatments of ultrasonication in distilled water (*100 + s*). Fibronectin (*FN*) was used as positive control. The complete experimental details are described in the Materials and Methods section. (*) $p < 0.1$ vs. other conditions. Values are expressed as mean ± standard deviation.

Thickness of the peptide layer (platform) attached on the Ti surface

The thickness of the peptide layer physically adsorbed on Ti samples was calculated from the attenuation of the Ti 2p3/2 signal in the XPS spectra according to equations (1) and (2):

$$I = I_0 \exp [-d / (\lambda \sin\theta)] \qquad (1)$$

$$\lambda = B(KE)^{1/2} \qquad (2)$$

Where *I* is the intensity of the Ti 2p 3/2 signal in the presence of the platform, I_0 the intensity of the same signal for control non-coated Ti, *d* the layer thickness, λ the inelastic mean free path, θ the take-off angle (θ = 90), B has a value of 0.087 nm $(eV)^{-1/2}$ for organic materials, and KE is the kinetic energy of the photoemitted electrons of Ti 2p 3/2 [Ref: 1,2].

The measured layer thickness obtained for the platform on Ti was of d = 0.50 nm.

References:

[1] Dettin, M.; Bagno, A.; Gambaretto, R.; Iucci, G.; Conconi, M. T.; Tuccitto, N.; et al. Covalent surface modification of titanium oxide with different adhesive peptides: Surface characterization and osteoblast-like cell adhesion. *J. Biomed. Mater. Res., Part A* **2009**, *90*, 35-45.

[2] Briggs, D.; Seah, M. P. Practical Surface Analysis, Vol. 1: Auger and X-ray Photoelectron Spectroscopy. Wiley: Chichester, **1990**; pp 183.

Figure S3

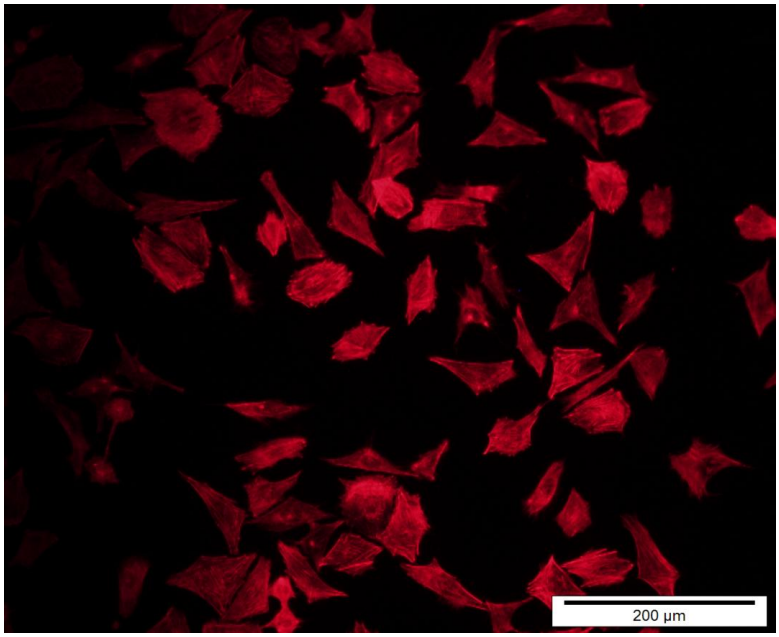

Figure S3. Spreading of Saos-2 cells on surfaces biofunctionalized with fibronectin (FN) after 4h of incubation. Images were acquired by fluorescence microscopy and show only staining of actin filaments with phalloidin-rodhamine.

Functionalization of Ti with the platform via silanization

Ti samples were passivated by immersion in a 32.5 % (v/v) solution of HNO_3 for 1 h at room temperature. After extensive washes with distilled water, ethanol and acetone, the samples were dried with nitrogen gas and silanized with (3-aminopropyl)triethoxysilane (APTES) (2 %, v/v) (Sigma-Aldrich). The reaction was performed in anhydrous toluene for 1 h at 70 ºC under nitrogen atmosphere. After this time, Ti disks were subjected to sonication for 10 min to remove non-covalently-bound silanes, and washed with toluene, isopropanol, distilled water, ethanol and acetone, and dried with nitrogen. Aminosilanized samples were then further modified by reaction with 2 mg/mL of the bifunctional crosslinker 3-maleimidopropionic acid N-hydroxysuccinimide ester (SMP) (Alfa Aesar) in DMF for 1 h at room temperature. Samples were finally washed with DMF, distilled water, ethanol and acetone, and dried with nitrogen. Finally, the platform was dissolved in PBS at pH 6.5 at a 100 μM concentration, and deposited onto Ti samples (100 μL/disk) overnight at room temperature. After peptide incubation, samples were gently washed with PBS and dried with nitrogen.

Figure S4

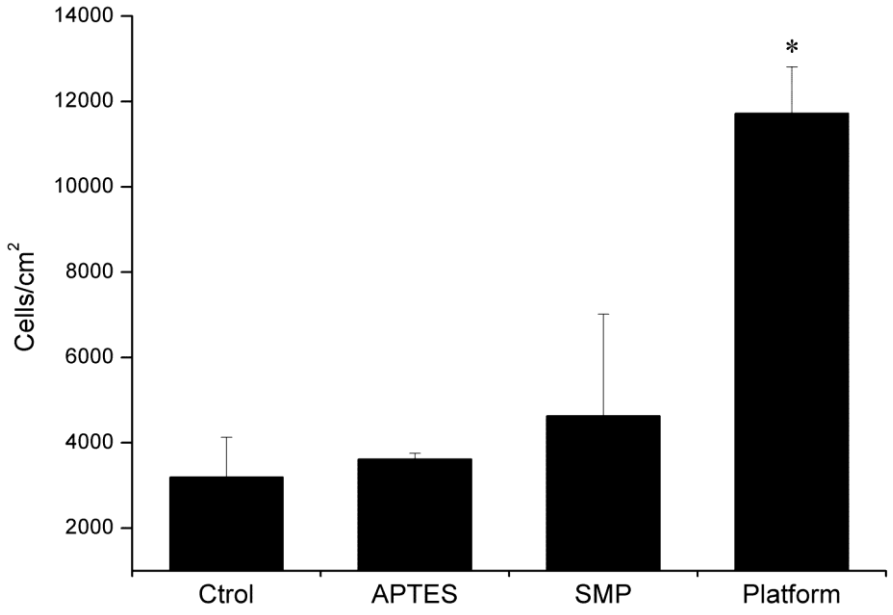

Figure S4. Adhesion of Saos-2 cells on biofunctionalized surfaces after 4h of incubation. The platform was covalently attached to Ti surfaces via silanization. The cell adhesive capacity of the platform was compared with control samples: non-coated Ti samples (Ctrol), Ti samples silanized (APTES), Ti samples silanized and treated with the crosslinker (SMP). The number of cells attached (cells/cm^2) was analyzed by means of an LDH assay. The complete experimental details are described in the Materials and Methods section. (*) $p < 0.05$ vs. other conditions. Values are expressed as mean ± standard deviation.

I.2 Paper II

Surface guidance of stem cell behavior: chemically tailored co-presentation of integrin-binding peptides stimulates osteogenic differentiation in vitro and bone formation in vivo

Author's contribution:

Design and performance of the surface characterization and *in vitro* experimental research. Design of the *in vivo* experiment. Data analysis and manuscript preparation.

ATTENTION ¡

Pages 92 to 105 of the thesis are available at the editor's web
http://www.sciencedirect.com/science/article/pii/S1742706116303841

SUPPORTING INFORMATION

Surface guidance of stem cell behavior: chemically tailored co-presentation of integrin-binding peptides stimulates osteogenic differentiation *in vitro* and bone formation *in vivo*

Roberta Fraioli[1,2], Khandmaa Dashnyam[3,4], Joong-Hyun Kim[3,4], Roman A Perez[3,4], Hae-Won Kim[3,4,5], Javier Gil[1,2], Maria-Pau Ginebra[1,2,6], José María Manero[1,2*], and Carlos Mas-Moruno[1,2*]

Table of contents

Table S1	Page 2
Figure S1	Page 3
Figure S2	Page 3
Figure S3	Page 4
Figure S4	Page 4

Table S1. Deconvolutions of XPS spectra, reporting the assignments and percentage of the peaks.

Modification step	Signal	BE (eV) / %	Assignment (main contributions)
P	O 1s	530.0 / 50.7%	TiO_2
		531.7 / 49.3%	TiOH, physisorbed H_2O, organic contaminants
	C 1s	284.7 / 59.4%	$-CH_2-CH_2-$
		285.9 / 28.6%	$-CH_2-OH$
		288.7 / 12.0%	carbonyl groups (C=O)
HNO_3	O 1s	530.0 / 64.1%	TiO_2
		531.7 / 35.9%	TiOH, physisorbed H_2O, organic contaminants
	C 1s	284.7 / 63.9%	$-CH_2-CH_2-$
		285.9 / 29.4%	$-CH_2-OH$
		288.7 / 6.7%	carbonyl groups (C=O)
APTES	O 1s	529.6 / 57.1%	TiO_2
		532.0 / 42.9%	-Si-O-, TiOH
	C 1s	284.7 / 58.6	$-CH_2-CH_2-$
		285.8 / 35.7%	-C-N, $-CH_2-OH$
		287.9 / 5.7%	carbonyl groups (C=O)
SMP	O 1s	530.0 / 49.4%	TiO_2
		532.0 / 50.6%	-C=O, -Si-O-
	C 1s	284.7 / 54.7%	$-CH_2-CH_2-$
		285.9 / 32.3%	-C-N, $-CH_2-OH$
		288.0 / 13.0%	amide (-NH-C=O), imide (O=C-N-C=O)
PTF	O 1s	530.0 / 34.3%	TiO_2
		532.0 / 65.7%	-C=O, -OH
	C 1s	284.7 / 55.0%	$-CH_2-CH_2-$
		285.9 / 32.7%	-C-N, $-CH_2-OH$
		288.0 / 12.3%	amide (-NH-C=O)
	N 1s	399.7 / 84.7%	amide (-NH-C=O)
		400.7 / 15.3%	$-NH_3^+$
PTF (S)	O 1s	530.0 / 32.9%	TiO_2
		532.0 / 67.1%	-C=O, -OH
	C 1s	284.7 / 55.0%	$-CH_2-CH_2-$
		285.9 / 30.5%	-C-N, $-CH_2-OH$
		288.0 / 14.5%	amide (-NH-C=O)
	N 1s	399.7 / 81.8%	amide (-NH-C=O)
		400.7 / 18.2%	$-NH_3^+$

Figure S1. (A) Chemical structure of the functionalization system with single (left) or branched peptide (PTF, right) (Ahx: aminohexanoic acid; MPA: 3-mercaptopropionic acid). (B) Chemical structure of the coating molecules at each modification step: silanization (yellow), addition of the crosslinker (blue) and coupling of the biomolecule (purple).

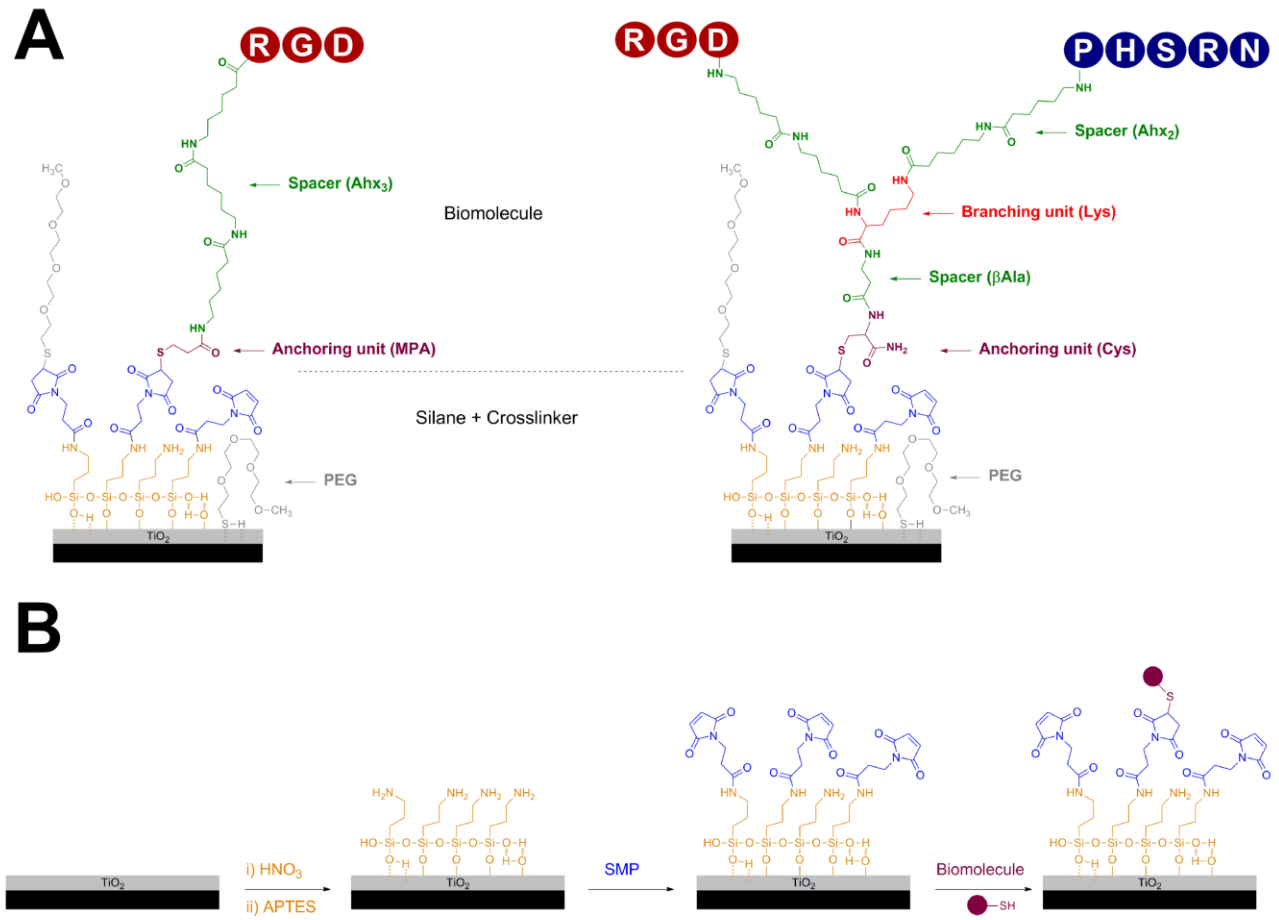

Figure S2. Surgical procedure. (A) Press-fit stabilization of the custom-made guide-plate on the rat calvaria and initial insertion of the screws. (B) Bone bed preparation for the cylindrical Ti rod implantation by LS-reamer. (C) Flat-bottomed bone bed. (D) Stabilization of the custom-made polymer cap device by fitting the retention screws.

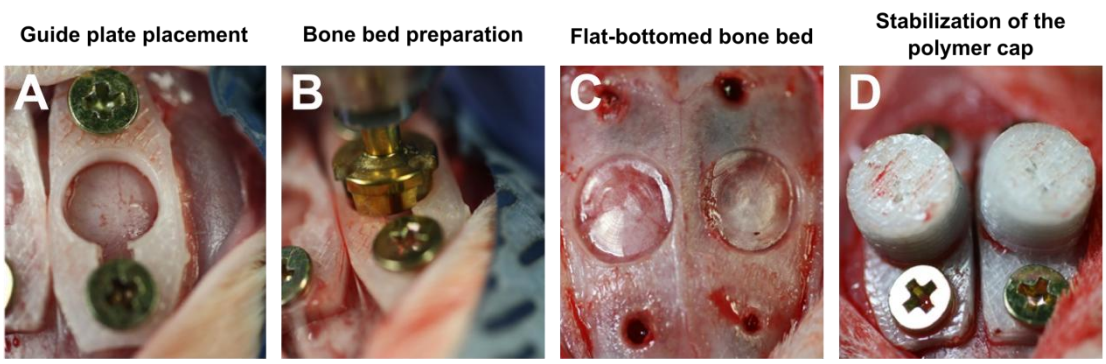

Figure S3. BSA adsorption on the uncoated polished Ti (P) is significantly higher compared to the PEGylated Ti (CTRL), the RGD-coated Ti (RGD) and the PTF-coated Ti (PTF), as visible by quantifying the fluorescence intensity of the adsorbed FITC-BSA (A). PTF and RGD are also PEGylated after coating with the biomolecule. Fluorescence microscopy images of the FITC-BSA on Ti are reported in B. * indicates statistical difference ($p<0.05$) vs. P.

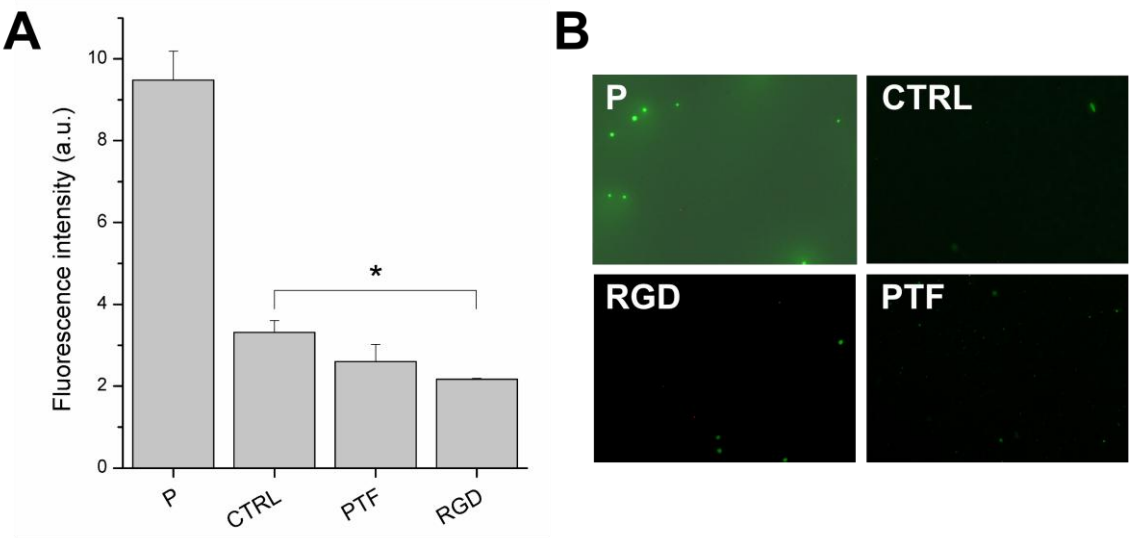

Figure S4. Alizarin Red-positive areas on the functionalized surfaces. Significantly higher mineralization is observed on the MIX, PTF and FN in basal medium, while only PTF and FN have significantly more deposits compared to the uncoated control (CTRL). * indicates statistical difference ($p<0.05$) vs. CTRL.

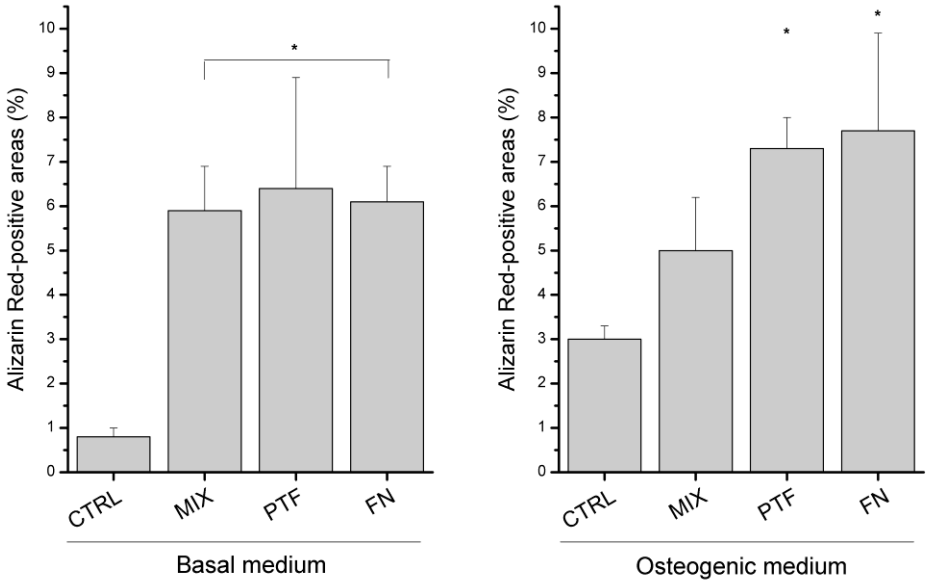

Chapter II: Functionalizing with peptidomimetics

An interesting alternative to go beyond the use of peptides and proteins as coating molecules is given by **peptidomimetics**. These synthetic molecules are generated by *mimicking the essential elements of natural peptides or proteins in 3D space, retaining the ability to interact with the biological target and produce the same biological effect*.[1] Such mimicking process is performed by re-assembling the critical elements of the natural peptide/protein (i.e. the pharmacophore) in a modified scaffold that optimizes the interactions with the cell receptor of interest (such as integrins), resulting in enhanced biological activity and receptor selectivity.[2] Another direct consequence of the introduction of non-peptide variants in the resulting molecule is high stability against proteolysis, which makes these molecules particularly interesting for *in vivo* applications.

Peptidomimetic definition

In the field of integrin-binding ligands, such rationale allows for the development of ligands that are specific for only one integrin heterodimer. Interestingly, such approach can be used to explore the biological role of a specific receptor and to create integrin-specific substrates.

αvβ3- or α5β1-selective mimetics

In this Chapter the use of two peptidomimetics as Ti coating molecules is reported. These ligands illustrate the aforementioned mimesis process: derived from the promiscuous RGD sequence, of which they replicate the main functional moieties, they are designed to selectively bind either αvβ3 or α5β1 heterodimers. Design and synthesis of these ligands was performed by Dr S. Neubauer and Dr F. Rechenmacher at the group of Prof H. Kessler at Technische Universität München (Munich, Germany). Optimization of their structure has been performed by carrying out docking studies into the crystal structure of the receptor (or a homology model of it) and competitive solid-phase integrin binding assays.[3,4] Their chemical structures, together with the RGD sequence, are illustrated in

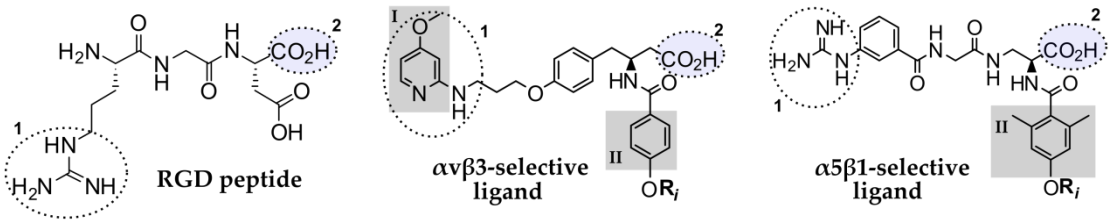

Figure II.1. Chemical structure of the RGD peptide and the two peptidomimetics. The chemical groups of the mimetics which resemble the ones found in RGD are circled (**1** and **2**). As an example, two moieties that give selectivity among the two integrin heterodimers are highlighted in gray rectangles (**I** and **II**).

figure II.1, where the similarities in terms of pharmacophoric groups between the natural peptide and its mimetics are highlighted. For instance, the 2-amino-4-methoxypyridine group **1** in the αvβ3-selective ligand acts as a surrogate of the guanidine of the arginine in RGD. The α5β1-selective ligand directly presents a guanidine at the N-terminal of the molecule. The carboxyl group **2** is present in all molecules and coordinates a divalent metallic cation at the metal-ion-dependent adhesion site (MIDAS) of the integrin. In the RGD sequence, the Gly residue ensures an appropriate spacing between the basic and acidic moieties, which is crucial to preserve the integrin-binding affinity of the molecules. A Gly unit is also present in the α5β1-selective peptidomimetic, whereas in the αvβ3-selective peptidomimetic this distance is maintained by the β-homotyrosine group. The OR*i* group present at the C-terminal aromatic residue of both integrin-selective ligands points out of their respective integrin-binding pockets and thus represents an ideal position for further derivatization of the ligands for surface coating without affecting their biological activity.[4]

Moreover, the difference among the two mimetics, which determine the selectivity among integrins αvβ3 and α5β1, are also highlighted in the structures. One of them is the aminopyridine ring in the αvβ3-selective ligand in which a methoxy group is introduced in the para-position (**I** in fig. II.1): Such moiety favors the recognition by the RGD-binding region of

the αv-subunits, which is bigger and more acidic than the α5 binding pocket. Another modification highlighted in the structure in figure II.1 is the presence of the mesitylene group in the α5β1-selective ligand (**II** in fig. II.1), which cannot fit into the narrower αvβ3 pocket due to steric clash.

Review Paper

The first publication of this Chapter is a Review Paper, which describes the development of the aforementioned and others αvβ3- or α5β1-selective molecules. Given the high similarity between these two integrins (αv:α5, 53% identity; β3:β1, 55% identity in the integrin headgroup),[5] the design of the ligands is not trivial. The reason behind the choice of focusing on these two specific integrin subtypes is also discussed in the paper.

Paper III

The use of these two mimetics as surface coating molecules on Ti is reported in the second paper of this Chapter. In this work, the selective ligands are anchored covalently to the metallic substrate via organosilane chemistry and the response of SaOS-2 OB-like cells is studied.

Annex I

One of the advantages of working with synthetic ligands is the versatility of their structure. Specifically, the anchor moiety of the biomolecule can be customized and adapted to the chosen substrate and immobilization technique. In the work reported in Annex I two immobilization techniques are tested: organosilane chemistry is used for the anchoring mimetics with thiol anchor on the surfaces to be tested *in vitro*, while ligands with phosphonic acids as anchors are immobilized via chemisorptions for the *in vivo* study. Attachment, spreading, shape, proliferation, and osteogenic differentiation of hMSCs on the functionalized Ti substrate are analyzed. The *in vivo* testing is performed in a rat calvarial defect model.

The two peptidomimetics ligands, together with the peptidic platform, are also used to coat bactericidal nanotopographies that do not support efficient cell adhesion. This study, which merges a topography-based and a chemical-based strategy to generate a multifunctional Ti surface, is reported in Annex II.

References

[1] J. Vagner, H. Qu, V.J. Hruby, Peptidomimetics, a synthetic tool of drug discovery, Curr. Opin. Chem. Biol. 12 (2008) 292–296.

[2] S. Neubauer, F. Rechenmacher, R. Brimioulle, F.S. Di Leva, A. Bochen, T.R. Sobahi, et al., Pharmacophoric Modifications Lead to Superpotent αvβ3 Integrin Ligands with Suppressed α5β1 Activity, J. Med. Chem. 57 (2014) 3410–3417. doi:10.1021/jm500092w.

[3] F. Rechenmacher, S. Neubauer, C. Mas-Moruno, P.M. Dorfner, J. Polleux, J. Guasch, et al., A molecular toolkit for the functionalization of titanium-based biomaterials that selectively control integrin-mediated cell adhesion, Chem. - A Eur. J. 19 (2013) 9218–23. doi:10.1002/chem.201301478.

[4] F. Rechenmacher, S. Neubauer, J. Polleux, C. Mas-Moruno, M. De Simone, E.A. Cavalcanti-Adam, et al., Functionalizing αvβ3- or α5β1-selective integrin antagonists for surface coating: a method to discriminate integrin subtypes in vitro, Angew. Chem. Int. Ed. Engl. 52 (2013) 1572–5. doi:10.1002/anie.201206370.

[5] L. Marinelli, A. Meyer, D. Heckmann, A. Lavecchia, E. Novellino, H. Kessler, Ligand binding analysis for human alpha5beta1 integrin: strategies for designing new alpha5beta1 integrin antagonists, J. Med. Chem. 48 (2005) 4204–4207. doi:10.1021/jm040224i.

II.1 Review Paper

αvβ3- or α5β1-integrin-selective peptidomimetics for surface coating

Author's contribution:

Preparation of the section *Biological Role of Integrin Subtypes αvβ3 and α5β1*.

Bibliographic search, manuscript revision and figures preparation.

ATTENTION ¡

Pages 118 to 138 of the thesis are available at the editor's web

http://onlinelibrary.wiley.com/doi/10.1002/anie.201509782/abstract

II.2 Paper III

Mimicking bone extracellular matrix: Integrin- binding peptidomimetics enhance osteoblast-like cells adhesion, proliferation, and differentiation on titanium

Author's contribution:

Design and performance of the surface characterization and *in vitro* experimental research. Data analysis and manuscript preparation.

ATTENTION ¡

Pages 140 to 150 of the thesis are available at the editor's web

http://www.sciencedirect.com/science/article/pii/S0927776515000168

Supporting Information

Mimicking Bone Extracellular Matrix: Integrin-Binding Peptidomimetics Enhance Osteoblast-like Cells Adhesion, Proliferation, and Differentiation on Titanium

Roberta Fraioli, Florian Rechenmacher, Stefanie Neubauer, José M. Manero, Javier Gil, Horst Kessler, Carlos Mas-Moruno

Table of contents

Table S1	Page 2
Table S2	Page 3
Fig. S1	Page 4
Fig. S2	Page 5

Table S1. Arithmetic roughness (R_a) of Ti disk surfaces before and after polishing treatment, and through the process of functionalization. Values are reported as mean ± standard deviation.

	R_a (nm)
Ti (not polished)	491.4 ± 75.3
Ti (polished)	14.8 ± 1.7
HNO_3	14.3 ± 2.2

Table S2. Binding energy and relative intensity of the deconvolution peaks of the XPS spectra of Ti surfaces throughout each step of the functionalization process.

Sample	Element	BE (eV)	Relative Intensity (%)
Ti	C 1s	284.4	75.00
		286.0	17.69
		288.2	7.30
	O 1s	531.05	57.8
		532.56	42.2
APTES	C 1s	284.7	64.59
		285.9	27.92
		288.0	7.48
	O 1s	531.1	49.20
		533.5	50.80
	N 1s	400.7	66.82
		402.7	33.18
Compound 1	C 1s	284.5	47.36
		285.8	34.54
		288.1	18.10
	O 1s	531.2	40.23
		533.3	59.77
	N 1s	400.7	22.26
		402.0	77.74
Compound 2	C 1s	284.6	51.94
		285.9	27.90
		288.1	20.16
	O 1s	531.1	39.67
		533.3	60.33
	N 1s	401.1	46.91
		402.0	53.09

Figure S1.

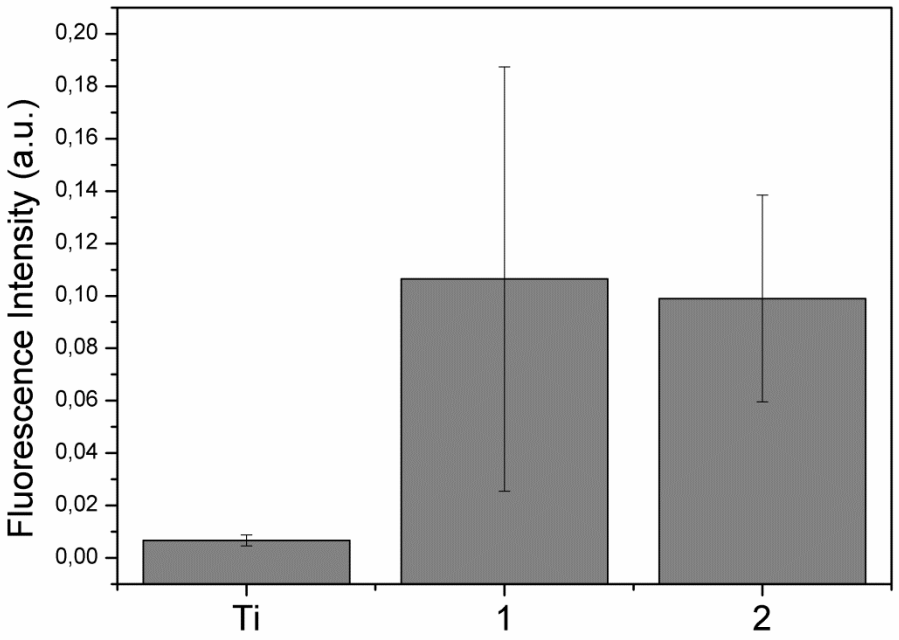

Fig. S1. Fluorescent labeling of peptidomimetics bound to Ti surfaces. Fluorescence microscopy images were acquired with a Nikon E600 fluorescence microscope and quantification of fluorescence intensity was done using Fiji/Image-J software.

Figure S2.

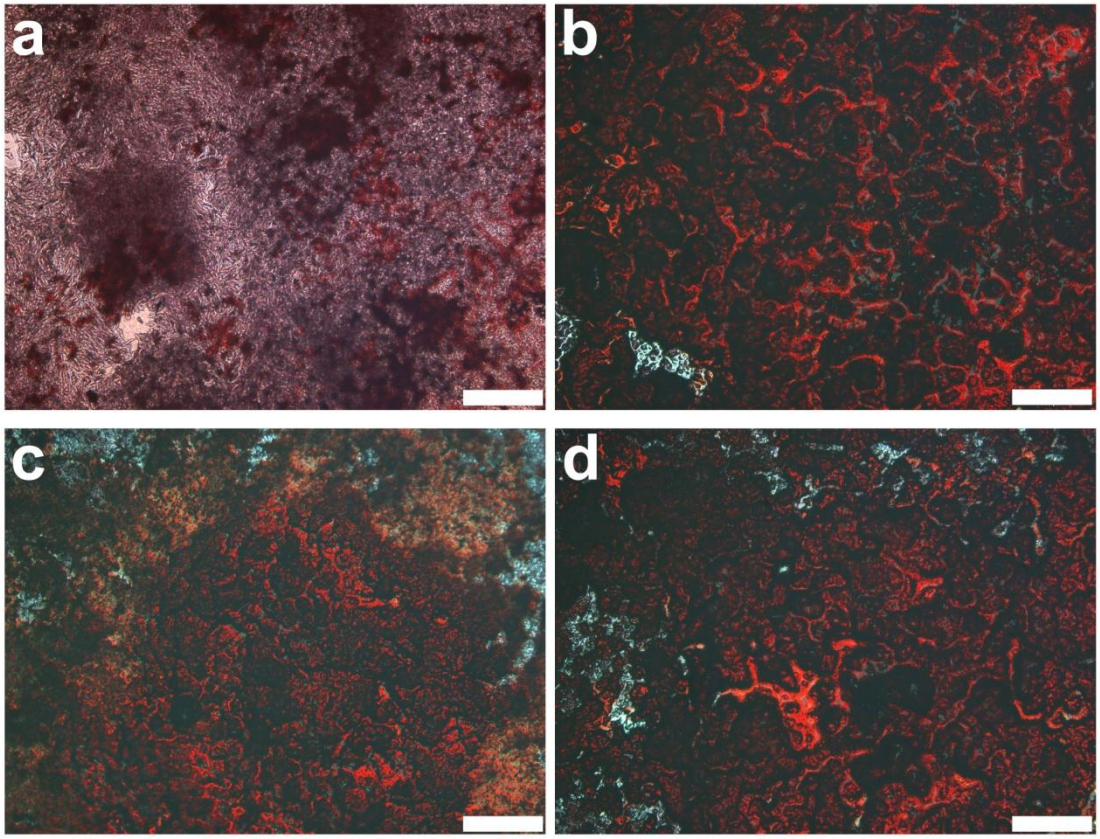

Figure S2. Calcification of the ECM visualized by Alizarin Red S staining of calcium after 21 days of incubation in osteogenic medium on the (a) uncoated; (b) VN-coated; (c) compound **1**-coated; and (d) compound **2**-coated Ti surfaces. Scale bar: 500 μm.

Concluding remarks

The economic and social burden of the premature failure of joint-replacement and dental implants is enormous. Given the high number of devices implanted every year and the projections of highly increasing need in the population, the cost of revision surgeries for the public health system and the patients is very high and is expected to increase. Especially considering the progressive aging of the population, solutions to ensure optimal and lasting osseointegration of the bone-replacement materials urge.

One of the most recent strategies to improve the performance of implantable devices is to convert biocompatible inert materials into smart ones, which not only act as "witnesses" of the healing process, but also take an active part into it, by supporting and accelerating the reestablishment of homeostasis. To this end, we aimed at mimicking the extracellular matrix, since it is a milieu of signals that drive cell fate *in toto*, mainly through integrin receptors. The immobilization of integrin-binding

ligands on the surface of the material would readily give its surface the capability of guiding cell fate and, in the case of bone replacing implants, enhance osseointegration *in vivo*. Several functionalization systems of titanium, based on two families of integrin-binding ligands, were studied throughout the thesis and tested both *in vitro* and *in vivo*. In both cases, the starting point for the design of the ligands was the biomimicry of matrix proteins. However, all biomolecules were engineered in different ways to obtain customized properties.

RGD-PHSRN platform

Chapter I was focused on the double branched peptidic platform containing the RGD and PHSRN sequences from the integrin-binding site of FN. Comparing the linear RGD, the random mix of the motifs and the platform, no significant effect was observed on the attachment of both OB-like cells and hMSCs on Ti, in terms of cell number. These results suggest that at short time and in absence of serum, the number of attached cells, though significantly higher compared to the uncoated titanium, is not affected by the specific ligand immobilized. Nonetheless, the controlled presentation of the sequences within the platform did foster cell spreading at short time, compared to RGD alone and the randomly distributed sequences, both in the case of SaOS-2 and stem cells. Interestingly, an aspect that was found to be deeply influenced by the structure of the ligand was cell differentiation into the osteoblastic lineage: mineralization, of both cell types, and gene expression of MSCs were boosted by the presence of the double-branched ligand, which also induces *de novo* bone formation in the *in vivo* model.

Peptido-mimetics

The coating of the metallic substrate with $\alpha v\beta 3$- or $\alpha 5\beta 1$-selective peptidomimetics was explored in the second Chapter and in Annex I. Again, as observed with the platform, both OB-like cells and hMSCs are

more prone to adhere on functionalized Ti, but do not discern among the specific ligand presented. Nevertheless, MSC shape and differentiation potential were sensitive to the integrin-specific substrate. The $\alpha v\beta 3$-selective surfaces promoted a star-like shape of cells, while cells elongated more on the $\alpha 5\beta 1$-selective Ti. Importantly, the $\alpha v\beta 3$-selective ligand was found to promote osteogenic differentiation of stem cells *in vitro* and increased bone growth *in vivo*, supporting a positive role of this receptor in the progression into the osteoblastic lineage.

Overall, the results of this thesis prove that biochemical functionalization of implant surfaces is a potent tool to harness cell behavior. Though not explored in this thesis, such substrate-mediated control of cell fate would be beneficial in several different contexts, from the basic research aiming at elucidating the effects of environmental signals, such as receptor-activated signaling cascades, to the *in vitro* induction of a specific lineage for tissue engineering applications.

In the field of bone replacement implants, the use of biochemical functionalization is sometimes looked at with skepticism. Most biomolecules, such as full length proteins, linear peptides and protein fragments, would likely suffer from enzymatic degradation into the body, which could hamper their efficacy. On the other hand, more stable alternatives, namely cyclic peptides and peptidomimetics, require a complex molecular design, which necessitates specific expertise and might be highly time-consuming. Stable and controlled immobilization on the biomaterial can be another important concern: chemoselective strategies minimizing the uncertainty on reaction yield are desirable for robust application of the coating. Notwithstanding that, the results obtained in this thesis demonstrate that such subtle modification of the implantable

device with synthetic ligands, which only affects the chemistry of the surface and has no effect on the design or bulk properties of the implant, has a high potential of guiding cell fate and can be effective in the *in vivo* scenario, despite the aforementioned concerns. Moreover, synthetic ligands have important advantages that would facilitate their translation in clinical applications: peptidic coating solutions can be used for multiple coatings since about 0.3-1.3% of the total amount of peptide in the coating solution binds to the surface and coated surfaces have been demonstrated to be resistant to several sterilization methods. Though the exact chronology of events happening *in vivo* at the implant surface is not elucidated yet, the positive results obtained in this work encourage the further development of this versatile and potent strategy, aiming at creating bioactive interfaces with increasing control of the surrounding microenvironment. The study reported in Annex II offers an example of this versatility: by grafting the receptor-binding ligands to Ti nanostructures, eukaryotic cell response is readily tailored, while antibacterial properties of the substrate remain unaffected.

The spectrum of application of chemical functionalization is potentially huge: functionalization can be static (via surface immobilization) or dynamic (e.g. stimuli-responsive release), it can involve numerous categories of biomolecules, from adhesive or antimicrobial peptides, to growth factors or chemoattractants, and it can be applied to many substrates only by tailoring the chemistry of immobilization. All these features give biochemical functionalization a degree of specificity (to cell-type, tissue or application) that would be difficult to obtain with other surface-focused modifications.

Annex I

Paper IV

Integrin-selective peptidomimetic coating of titanium drives stem cell response *in vitro* and enhances bone growth *in vivo*

Considered their high activity, selectivity and stability, non-peptidic integrin antagonists stand out as promising molecules for surface coating applications. Nonetheless, this category of ligands has been seldom used for this purpose. Especially *in vivo* characterization of peptidomimetic-coated implants is missing. In this work we use two different strategies to chemically anchor $\alpha v\beta 3$ or $\alpha 5\beta 1$ integrin-selective RGD mimetics to titanium, either via terminal thiol or phosphonic acid moieties, and report for the first time that surfaces functionalized with integrin-binding peptidomimetics tune both *in vitro* and *in vivo* biological response. Both integrin-specific surfaces promote mesenchymal stem cell adhesion and spreading to the same extent as full-length proteins. Moreover, on the $\alpha 5\beta 1$-selective surface cells adopted more elongated morphologies and increased cell growth rates were observed, while on the $\alpha v\beta 3$-selective surfaces cells developed a star-like shape and displayed commitment into the osteoblastic lineage. *In vivo*, bone growth in rat calvarial defects was increased on implants coated with the $\alpha v\beta 3$-selective peptidomimetic compared to uncoated and $\alpha 5\beta 1$-functionalized implants. These results demonstrate that this molecular chemistry-derived approach could be successful to engineer instructive coatings for orthopedic applications.

Authors: R. Fraioli, S. Neubauer, F. Rechenmacher, K. Dashnyam, J-H Kim, R. A. Perez, H-W Kim, F. J. Gil, M. P. Ginebra, J. M. Manero, H. Kessler and C. Mas-Moruno.

Format: communication

Graphical abstract

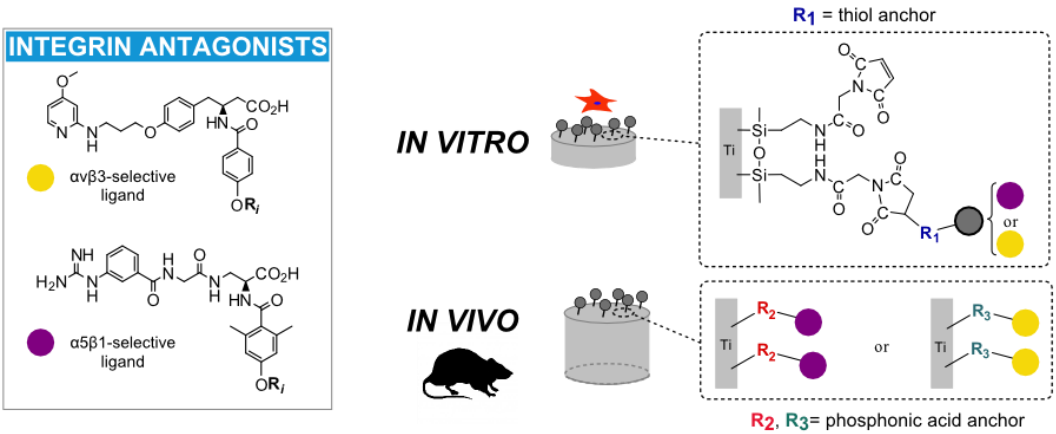

Surface chemical modification of implant materials is a viable strategy to address unmet needs of orthopedic and dental implants. Indeed, interactions between biomaterials and tissues at the surface level are responsible for the most important causes of failure of these devices, such as aseptic loosening, infection and fibrous encapsulation.[1] To deal with these issues, cell-instructive coatings have been proposed as a solution to promote osseointegration by stimulating direct bone deposition on the implant.[1–4] Ligands from the extracellular matrix (ECM) of bone have been used as a source of inspiration to design numerous peptidic ligands[5–8] and protein fragments[2,9] to coat metallic substrates. Many examples exist of RGD-containing peptides or fibronectin (FN) fragments encompassing the integrin-binding site of the protein tethered to

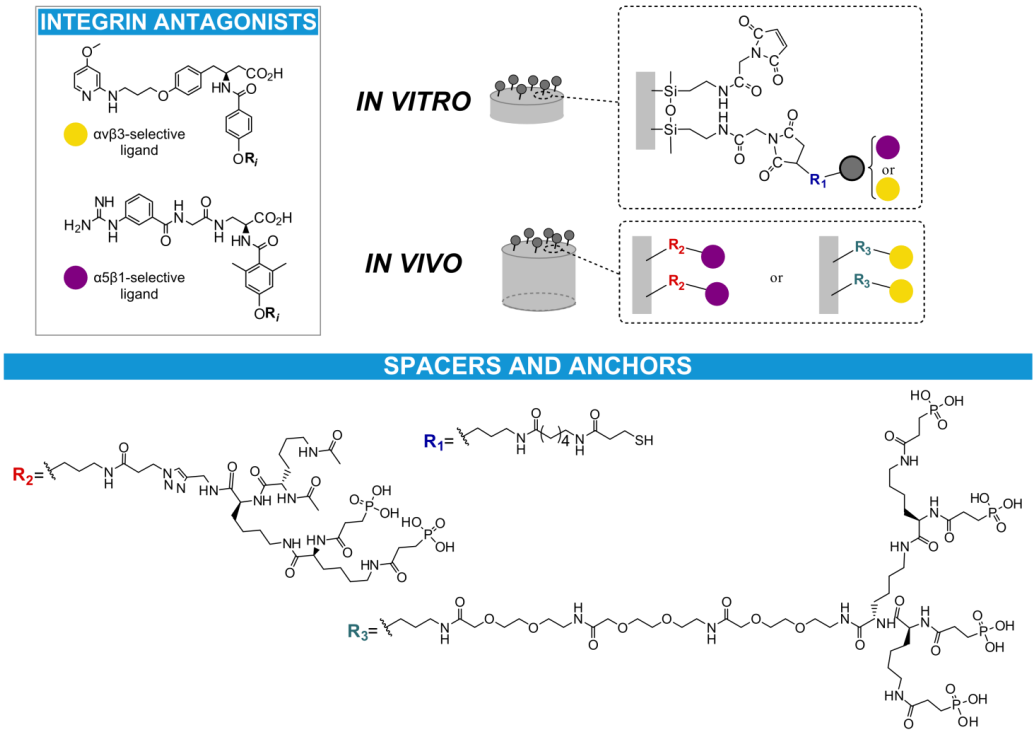

Fig 1. Chemical structure of the integrin antagonists, spacers and anchor groups, and schematic representation of the functionalization strategy. Peptidomimetics were anchored via thiol group for the in vitro assays (R1 spacer and anchor), and directly tethered via phosphonic acid for the in vivo study (either R2 or R3 spacers and anchors).

biomaterials and tested in vitro.[10–12] Several in vivo studies are also reported.[2,3,13,14] On the contrary, non-peptidic integrin antagonists have been rarely used for this purpose. Highly active, subtype selective, and with good pharmacokinetic profiles, these ligands hold high potential for implementation as surface-coating molecules.[15] While few examples of *in vitro* studies are available in literature,[16–18] *in vivo* characterization of peptidomimetic-coated implants has never been reported.

Recently, our group proposed the application of peptidomimetic ligands as surface-coating molecules to generate either $\alpha v\beta 3$ or $\alpha 5\beta 1$ integrin-selective surfaces.[19,20] Among the integrin family, $\alpha v\beta 3$ and $\alpha 5\beta 1$ subtypes have been identified as important receptors in the adhesion, proliferation and differentiation of osteoblasts and mesenchymal stem cells (MSCs).[21,22,12] Based on this, addressing these receptors could be beneficial to enhance the osseointegration of bone-replacing implants. Thus, in this study we explored the chemical anchoring of $\alpha v\beta 3$- or $\alpha 5\beta 1$-selective RGD mimetics onto titanium (Ti), the most relevant metallic material for orthopedic and maxillofacial applications,[23] and evaluated the biological effect of these molecules both *in vitro* and *in vivo*. On the basis of the biological application, two distinct immobilization methods were investigated (Figure 1): i) for the *in vitro* studies, the two mimetics were designed with a mercaptopropionic acid as terminal group and linked to the metal via the thiol functionality, through a Michael addition on the maleimido-functionalized silane layer; ii) for the *in vivo* tests, a direct binding of the molecules to the superficial layer of Ti dioxide was preferred, and therefore the use of phosphonic acids via chemisorption was exploited. This method reduces the number of steps and manipulation of implant materials and would be more appropriate than silanization in a clinical setting. Moreover, the capacity to fine tune the chemical grafting of

the peptidomimetics by simply changing the anchoring moiety of the synthetic ligands highlights the versatility of our coating strategy.

Thus, to conduct *in vitro* cellular studies Ti surfaces were functionalized with the peptidomimetics via silanization. This protocol was optimized by us in a previous study and characterized by means of contact angle measurements, fluorescent labeling and X-ray photoelectron spectroscopy (XPS).[20] In *vitro* studies were focused on the response of human MSCs (hMSCs). This choice is due to the crucial role of these multipotent cells in the healing process:[24] evidence exists of cell homing to the injured tissue, active participation in the reparative events via differentiation into bone-forming cells, and contribution to the creation of the regenerative microenvironment, by secreting bioactive factors.[25]

By functionalizing Ti with the $\alpha v\beta 3$- or $\alpha 5\beta 1$-selective peptidomimetics ($\alpha v\beta 3$-s or $\alpha 5\beta 1$-s surfaces, respectively) adhesion of hMSCs on the substrate was highly increased after 6 h of incubation in serum-free conditions (Figure 2a), to the same extent as the full-length glycoproteins vitronectin (VN) and FN. No difference was observed between the number of cells adhering to the proteins and to the $\alpha 5\beta 1$-selective and the $\alpha v\beta 3$-selective compounds. Following the same behavior as the number of attached cells, hMSCs spread more on all integrin-binding substrates, compared to the uncoated metal (Figure 2b). Nevertheless, cell shape was found to be ligand-dependent (Figures 2c, 2d, 2e). When no functionalization was done, cells remained small and rounded. On VN cells were highly rounded and almost no cytoskeletal elongation was observed; the distribution of actin fibers was either parallel to the cell boundary or centrifugal, i.e. from the nucleus to cell edges.

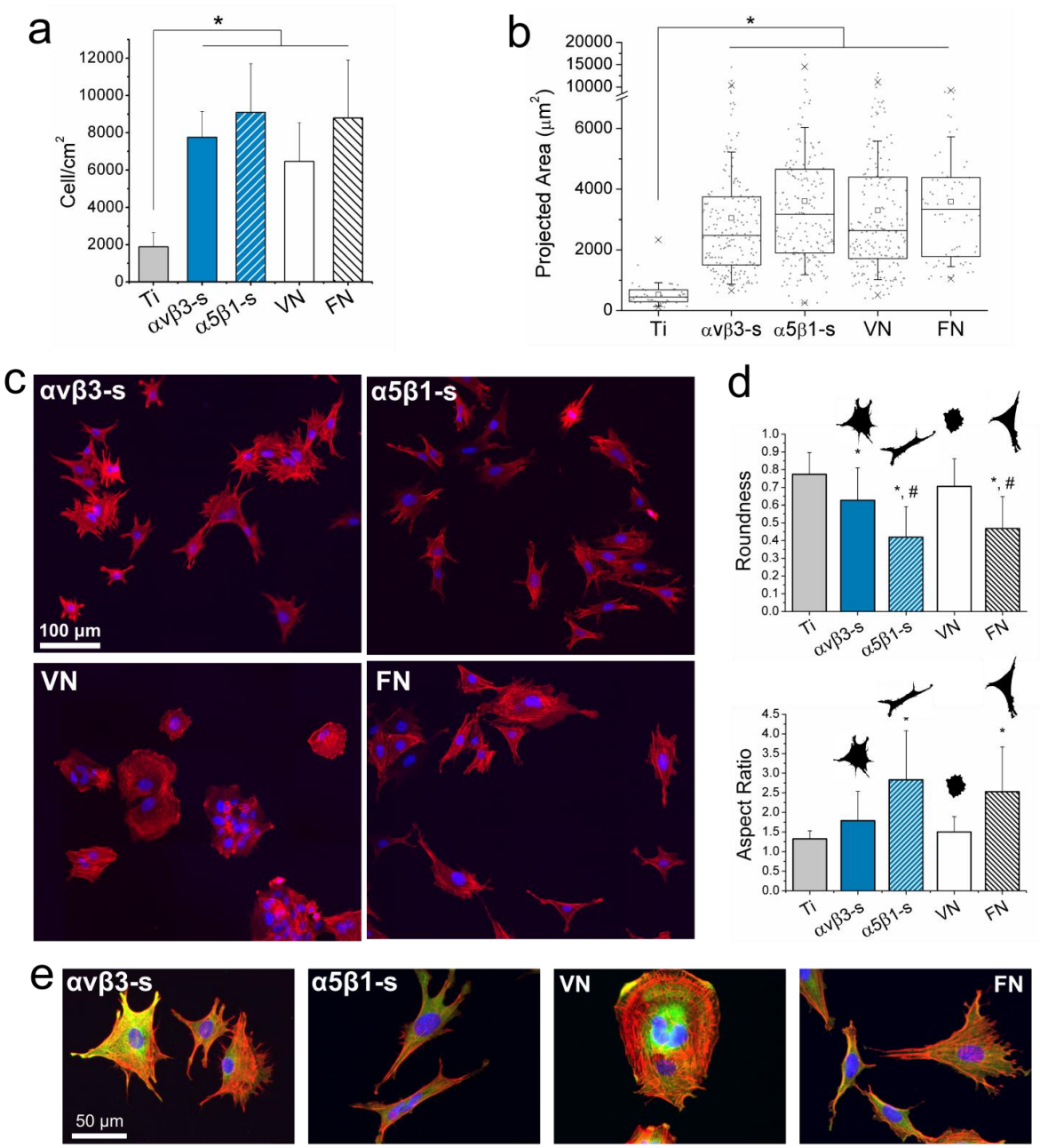

Fig 2. (a) Cell attachment in serum-free conditions is significantly increased on coated Ti, irrespectively of the specific ligand presented. * means p<0.01. (b) Cell projected area after 6 hours of incubation in serum-free medium is increased by all ligands. Dots represent individual cells, the boxes represent the 25th and 75th percentile, the middle line is the median, the whiskers are one standard deviation, □ is the average, × correspond to the 99% and 1% of the values. * means p<0.01. (c) Immunostaining of actin fibers and nuclei after 6 hours of incubation in serum-free medium. Cell shape, number and direction of cytoskeletal elongations depends on the ligand anchored to Ti. (d) Values of mean roundness and aspect ratio of cells seeded on the functionalized substrates. * means p<0.05 vs. Ti, # means p<0.05 vs. αvβ3-s. (e) Immunostaining of actin fibers, vinculin and nuclei after 6 hours of incubation in serum-free medium.

On the contrary, many cytoskeletal elongations were observed on FN, where cells also reached a less rounded morphology; actin fibers in this case distributed mostly parallel to cell edges. On both mimetics, hMSCs developed elongations. However, these were more numerous on the $\alpha v\beta 3$-selective mimetic, with no preferential direction, giving a star-like shape. On the $\alpha 5\beta 1$-selective ligand cells attained a much more elongated shape, with few elongations per cell distributed in one preferential direction. Overall, these observations translated in statistically lower values of roundness and higher values of aspect ratio on FN and $\alpha 5\beta 1$-s, compared to all other conditions ($p<0.05$). Cell shape has been demonstrated to be a regulator of the commitment of MSCs into different lineages;[26–28] therefore, the observed differences might reflect in different differentiation behavior.

Response at long term was also ligand-dependent: the number of metabolically active cells was higher on all functionalized surfaces, compared to uncoated Ti ($p<0.01$), with FN-coated Ti being the surface promoting the highest proliferation among all conditions ($p<0.01$) (Figure 3a). The $\alpha 5\beta 1$-selective ligand supported the same proliferation as the full length VN at all time points. Proliferation was lower at 3 and 6 days of incubation on the $\alpha v\beta 3$-selective mimetic, compared to all other coated surfaces ($p<0.01$). To qualitatively observe cell growth on the metallic substrate, actin cytoskeleton and nuclei were immunostained after 2 and 4 days of incubation (Figure 3b). In terms of number of attached cells, microscopic observations were coherent with the trend of cell growth observed via the proliferation assay (Ti<$\alpha b\beta 3$-s<$\alpha 5\beta 1$-s~VN<FN).

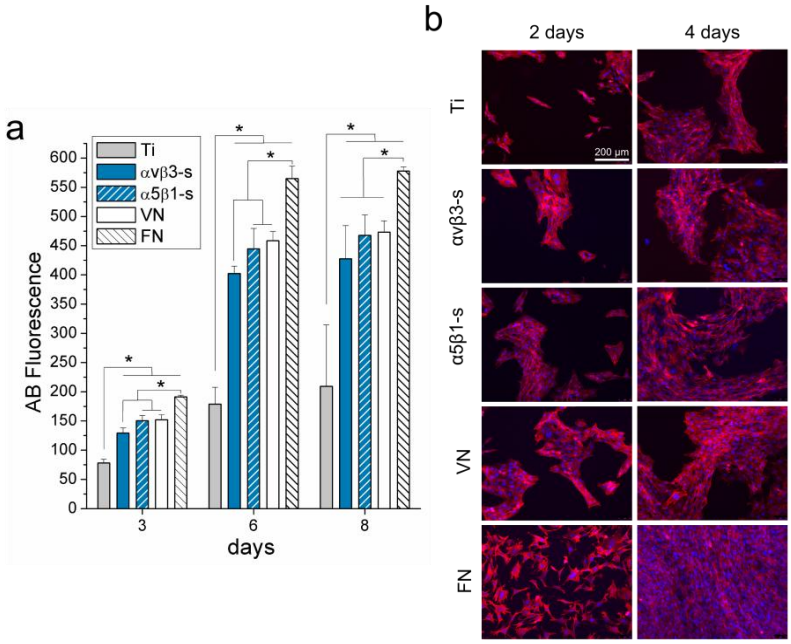

Fig 3. (a) Alamar blue assay of cell proliferation indicates that cell growth follows this trend: FN>VN~α5β1-s>αvβ3-s>Ti, therefore indicating that FN (among proteins) and the α5β1-selective mimetic (among peptidomimetics) foster the highest value of proliferation. * means $p<0.01$. (b) Immunostaining of actin fibers and nuclei after 2 and 4 days of incubation on the substrates; cell growth follows the same trend observed in (a).

However, the spatial distribution of cells after 2 days of incubation was strongly affected by the surface-bound ligand: hMSCs formed isolated cell clusters on αvβ3-s, α5β1-s and VN, while they distributed homogeneously on FN. After 4 days of incubation, this behavior was maintained, and a multilayer of cells covering the entire surface was observed on FN-coated samples, in accordance with a faster cell growth on these surfaces. Having observed higher cell number on the α5β1-selective ligand, than on the αvβ3-selective one, these results support a positive role for α5β1 in proliferation. We could observe a similar behavior with human osteoblast-like cells in a previous work.[20] However, hMSCs proliferate significantly more on FN at all time points, also in comparison with the α5β1-slective surface. This behavior could stem from the promiscuity of the full length glycoprotein, which, apart from having high affinity for integrin α5β1, has

multiple domains that interact with other cell receptors and growth factors, as observed in previous works.[29,30]

Since different proliferation trends and cytoskeletal organization were observed on the mimetics, differentiation was expected to vary depending on the receptor-selective coating. As previously introduced, Kilian et al. characterized the relationship between shape and lineage commitment, demonstrating that shapes that fostered increased cell contractility promote osteogenesis.[27] Despite their study used FN islands to confine cell shape, star-like shape was associated to osteogenesis due to increased myosin contractility. In our work no constraint is applied to cells, however hMSCs acquired different shapes depending on the integrin antagonist anchored to the surface. To investigate the commitment of cells to the osteoblastic lineage RT-PCR was used, evaluating gene expression of two markers of osteogenic differentiation (Figure 4a). After 7 days of incubation in basal medium, the expression of both RUNX2 and OCN is increased on the $\alpha v\beta 3$-selective mimetic, compared to uncoated Ti. Moreover, expression of RUNX2 is the highest among all other functionalized substrates. Enhanced levels of RUNX2 were also reported for MSCs seeded on self-assembled monolayers encompassing a cyclic RGD peptide with high affinity for $\alpha v\beta 3$.[12] Overall results suggest a more osteoinductive effect of the $\alpha v\beta 3$-selective surface, compared to the $\alpha 5\beta 1$-selective one, which more efficiently supports proliferation.

To verify this trend in the in vivo scenario, we tested the osteoinductive capacity of mimetic-coated Ti implants in a partial thickness calvaria defect of rat. For this study direct binding of phosphonic acid groups to Ti oxide was used. This is a simple one-step process; however, coupling of these types of anchor groups to the bioactive sequence is synthetically more demanding than the incorporation of one

terminal thiol group.[31,32] We used XPS to study phosphonate-anchor mimetic binding to the metal (Figure 5). Four coating concentrations were tested, from 1 μM to 200 μM. Phosphorous (P 2p), only present in traces on the uncoated Ti surface, was detected after binding the two mimetics, and its atomic percentage increased proportionally to concentration, until reaching a plateau at 100 μM, which was chosen as the coating concentration. This signal corresponds to the Ti-O-P bond, as reported in other studies.[32,33] Moreover, the coating was proved to be stable, since neither atomic percentages of Ti and P, nor P 2 p spectrum were affected by the ultrasonication treatment. For the implantation in rats, custom-made mimetic-functionalized cylindrical implants (5.5 mm diameter, 5 mm long) were inserted in the 5.5 mm defect and covered with rigid polymer caps (Figure 4b). After 2 or 4 weeks of implantations, animals were euthanized, and tissues were harvested and stained for histological observation with hematoxylin and eosin (H&E) stain. Confirming in vitro observations, the substrate with high affinity for integrin $\alpha v\beta 3$ was more osseoinductive, promoting increased new bone growth at the defect site (Figure 4c). Newly formed bone showing woven features was visible in contact to the $\alpha v\beta 3$-s surface, with osteoblasts aligning on the surface of the bone, while more fibrous tissue formed at the interface between the $\alpha 5\beta 1$-s implant and the calvaria. Bone formation was also observed in some $\alpha 5\beta 1$-s samples after 2 weeks of implantation; however results were more modest in this case and not reproducible through all samples. These effects could stem from the different biological roles described for these membrane receptors.[17,34,35] Previous in vivo studies evaluating Ti or Ti alloy implants coated with cyclic RGD, known to have high affinity for integrin $\alpha v\beta 3$,[36] also reported significant increase in bone formation,[37] less fibrous tissue formation surrounding the implant and, therefore, increased implant fixation[14,38] in presence of the peptidic coating. Accelerated bone repair

adjacent to the αvβ3-s implants was evident at early time points (2 weeks); this result is of relevance because early bone fixation is critical to guarantee orthopedic and dental implant success.[39,40] Stimulation of α5β1 has been shown to promote bone formation in other studies using FN mimics,[2] however a remarkable effect was not observed in our in vivo model.

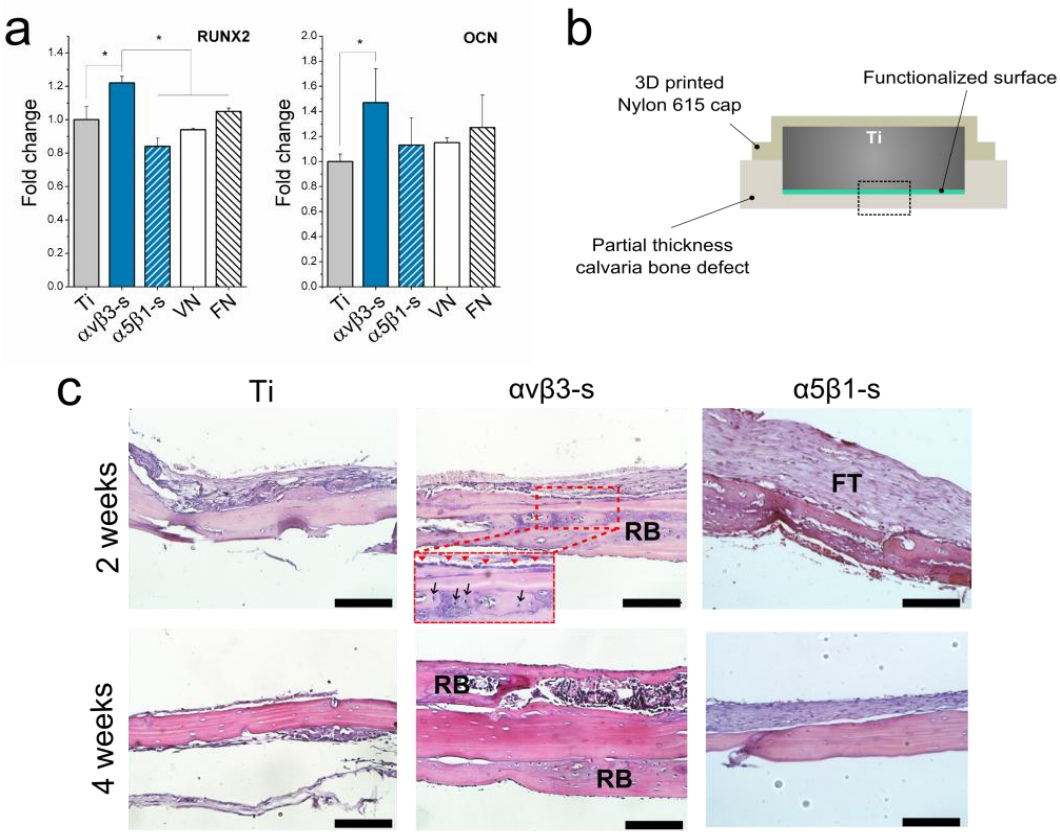

Fig 4. (a) Expression of osteogenic markers on the functionalized substrates. Increased expression is observed on the αvβ3-selective mimetic for both genes, compared to Ti. * means $p<0.05$. (b) Implantation scheme: the dashed area represents the area shown in the histologies in (c). (c) Representative H&E staining histological images. Scale bar = 150 μm. The bottom part of the images is the dural side of the calvaria. Increased new bone growth (regenerated bone, RB) is observed in presence of the αvβ3-s coated Ti implant (the inset shows aligned osteoblasts), while more fibrous tissue (FT) is observed adjacent to the α5β1-s coated implant.

In conclusion, our work shows the high potential of peptidomimetic ligands to generate bioactive surfaces for clinical applications. Both immobilizations to Ti via either thiol or phosphonic acid were proved efficient, confirming the versatility of the approach: by selecting the proper anchor unit, biomolecules suitable for different coating procedures or materials can be easily designed. Noteworthy, small, stable, and selective ligands could often attain the same cell response as complex full-length ECM proteins. We could demonstrate that the $\alpha v\beta 3$-selective surface fosters hMSCs osteogenesis in vitro and new bone formation in vivo, while the $\alpha 5\beta 1$ antagonist more efficiently promoted proliferation of cells in vitro. Moreover, mimetics are devoid of immunological response and stable to enzymatic cleavage, which makes these custom-made synthetic antagonists particularly suitable coating molecules for clinical implantable devices.

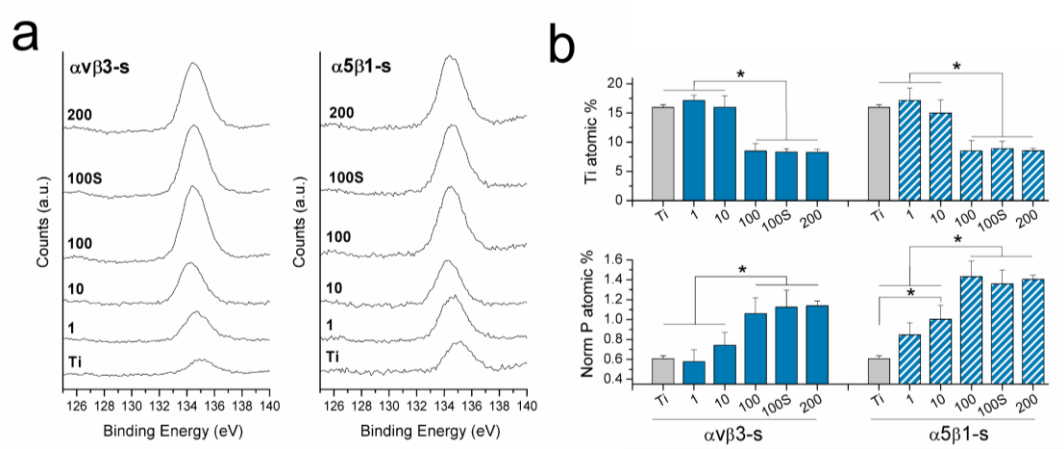

Fig 5. P 2p spectra (a) and Ti and P atomic percentage (b) of uncoated Ti (Ti) and mimetic-functionalized Ti at different coating concentrations (1 μM, 10 μM, 100 μM, 200 μM) and after an ultrasonication treatment to verify stability (100S). * means $p<0.05$. Atomic percentages of Ti and P decrease and increase, respectively, at increasing concentrations, reaching a plateau at 100 μM. Neither atomic percentages nor P spectra are modified by the ultrasonication treatment, confirming stability of the coating.

Experimental Section

Ti surface functionalization. Ti disks were obtained by turning cylindrical CP bars (10 mm in diameter, Technalloy S.A., Sant Cugat del Vallès, Spain). Polishing with silicon carbide girinding papers (Neuertek S.A., Eibar and Beortek S.A., Asua-Erandio, Spain) and with suspension of alumina particles (1 μm and 0.05 μm particle size) on cotton clothes was carried out to achieve a smooth mirror-like finish of the surface. After ultrasonically rinsing with cyclohexane, isopropanol, distilled water, ethanol, and acetone, samples were passivated with 65% (v/v) HNO_3 for 1 h. Afterwards, disks were silanized by immersion in 2% (v/v) APTES (3-(aminopropyl)-triethoxysilane, Sigma-Aldrich, St Louis, MO, USA) in anhydrous toluene (Sigma-Aldrich) in agitation at 70 ^{0}C for 1 h under nitrogen atmosphere. After rinsing samples with toluene, distilled water, ethanol, and acetone, a curing of the silane layer was performed at 120 ^{0}C for 5 min. To couple the crosslinking agent N-succinimidyl-3-maleimidopropionate (SMP) (Alfa Aesar, Karlsruhe, Germany), disks were immersed in disks in 7.5 M solution in agitation for 1 h at room temperature. For *in vitro* studies, peptidomimetics with thiol anchor were immobilized on Ti surface by dissolving the biomolecules in phosphate buffered saline (PBS) at 100 μM and pH 6.5, and then depositing 100 μL of these solutions overnight on Ti disk surfaces at RT. For *in vivo* studies peptidomimetics with phosphonic acid anchors were directly deposited on Ti samples (PBS, 100 μM, overnight, RT). VN and FN (both from Sigma-Aldrich) were coated on Ti at 50 μg/mL in PBS at pH 9.5 instead. Uncoated polished Ti disks were selected as negative controls (Ti).

Cell culture. All reagents were purchased from Sigma-Aldrich, unless otherwise noted. hMSCs (SCR 108, Merck Millipore) were cultured in Advanced Dulbecco's Modified Eagle's Medium (DMEM) supplemented with 10% (v/v) fetal bovine serum (FBS), 50 U/mL penicillin, 50 μg/mL streptomycin and 1% (w/v) L-glutamine. Cells were maintained at 37 °C, in a humidified atmosphere containing 5% (v/v) CO_2 and culture medium was changed twice a week. Upon reaching 70 % confluence, cells were detached by trypsin-EDTA and subcultured into a new flask. Cells at passages between 1 and 4 were used to carry out all the experiments. To evaluate cell attachment, hMSCs were plated at 10^4 cells/mL and incubated 37 °C and 5% (v/v) CO_2 containing atmosphere. After 6 h of incubation in serum-free medium, immunofluorescent staining of cell nuclei and actin fibers was performed to count attached cells. To study proliferation of cells on the substrates, 6×10^3 cells/mL were plated on samples in serum-free medium and incubated as previously explained.

Cell immunostaining and proliferation. After plating cells as previously described, and removing non-adherent cells by gently washing samples with PBS,

hMSCs were fixed with paraformaldehyde (PFA, 4% w/v in PBS) for 20 min, and permeabilized with 500 μL/disk of 0.05% (w/v) Triton X-100 in PBS for 20 min. The surface was blocked with 1% BSA (w/v) in PBS for 30 min, actin fibers and nuclei were stained by incubating with rhodamine-conjugated phalloidin (1:300, in Triton 0.05% (w/v) in PBS) for 1 h and with 4',6-diamidino-2-phenylindole (DAPI) (1:1000, in PBS-Glycine 20 mM) for 2 min at RT in the dark, respectively. Samples were rinsed three times with PBS-Glycine for 5 min between each step of the staining procedure. Ti disks were examined under a fluorescence inverted microscope (AF7000, Leica, Germany), and quantification of nuclei and cell projected area was done with the Fiji/Image-J package. For the cell proliferation assay, 6-hours post seeding, medium was aspired and replaced with complete medium. After 3, 6, and 8 days of incubation, cell number was evaluated with the Alamar Blue assay (Invitrogen Life Technologies, Merelbeke, Belgium): briefly, Alamar Blue-containing medium (10% (v/v)) was added for 1 h, and fluorescence of the dye was quantified according to the manufacturer instructions with a multimode microplate reader (Infinite M200 PRO, Tecan GroupLtd., Männedorf, Switzerland).

Cell differentiation. Gene expression was evaluated by RT-PCR analysis. 10^4 cells/well were plated on metallic disks and cultured for 7 days in basal medium. At harvest, cells were lysed and total RNA was extracted using RNeasy® Mini Kit (Qiagen, Hilden, Germany), according to manufacturer instructions. Total RNA was quantified with NanoDrop ND-1000 spectrophotometer (Thermo Scientific, Waltham, MA, USA). 200 ng of RNA were reverse transcripted to cDNA with QuantiTect Reverse Transcription Kit (Qiagen). A StepOnePlus Real-Time PCR System (Applied Biosystems, Foster City, CA, USA) with QuantiTect SYBR Green RT-PCR Kit (Qiagen) and gene-specific primers for runt-related transcription factor 2 (RUNX2 – primer sequences: FW: CGGAATGCCTCTGCTGTTAT, RV: TGGGGAGGATTTGTGAAGAC) and osteocalcin (OCN - primer sequences: FW: ATGAGAGCCCTCACACTCCT, RV: CTTGGACACAAAGGCTGCAC) were used, doing a 5 min incubation at 95 °C and 40 amplification cycles (10 sec at 95 °C and 30 sec at 60 °C), followed by a melt curve. Melting curve analysis was done to prove specificity and gene expression was normalized to β-actin (primer sequences: FW: AGAGCTACGAGCTGCCTGAC, RV: CGTGGATGCCACAGGACT).

***In vivo* implantation.** To test the ability of the biomolecule coating to induce bone growth *in vivo* a rat partial thickness calvarial defect was used. The protocol of housing, care, and experimentation was approved by the Animal Care and Use Committee at Dankook University, Republic of Korea. Eighteen 11 week-old, 250-300 g healthy male Sprague-Dawley rats were used. Animals were acclimatized for 7 days before implantation, and each rat was housed in a separate cage under

temperature- and humidity-controlled environment, exposed to a 12 h light-dark cycle, and had free access to water and food. Custom-made rod-type Ti implants (5.5 mm diameter, 5 mm long) were prepared and functionalized by immersion in the mimetics solution. After coating, samples were washed three times in sterile MQ water and sterilized by incubating in 70% ethanol for 30 min. Implant placement was performed under general anesthesia using an intramuscular injection of a mixture of ketamine (80 mg/kg) and xylazine (10 mg/kg). The animals were randomly allocated to one of three groups before implantation (n=6): Ti as the control group, avb3-selective mimetic-coated Ti, and a5b1-selective mimetic-coated Ti as study groups. After shaving over the cranial lesion, the surgical site was scrubbed with iodine and 70% ethanol, and a linear skin incision was made. A full thickness flap was retracted and the calvarial bone was exposed. Two 5.5 mm diameter partial thickness calvarial bone defect were prepared in each rat on each side of the parietal bone under cooling conditions with sterile saline buffer, using a dental handpiece and a 5.5 mm diameter LS-Reamer (Neobiotech, Seoul, South Korea). The implants were covered by 3D printed rigid polymer caps, and the cap and Ti constructs were secured to the calvarial bone using fixation screws via its anchoring rings. Rigid polymer caps (5.5 mm inner diameter and 5 mm height) were custom-made (Taulman 618 Nylon, Taulman 3D, Missouri, US) by 3D printing (NP-Mendel, Opencreators, South Korea). The subcutaneous tissues and periosteum was sutured with absorbable sutures (4-0 Vicryl®, Ethicon, Germany), and the skin was closed with non-absorbable suture material (4-0 Prolene, Ethicon, Germany). The animals were monitored daily for possible clinical signs of infection, inflammation, and any adverse reaction. After two and four weeks, the animals were euthanized by CO_2 inhalation and the tissue part of the calvarium surrounding the cap was harvested and fixed in 10% neutral buffered formalin for 24 hours at RT. The samples were then decalcified with RapidCalTM solution (BBC Chemical Co., Stanwood, WA), dehydrated and embedded in paraffin using standard procedures. Five serial sections (5 μm) were cut at the central of the defects, and the deparaffinized sections were subjected to hematoxylin & eosin (H&E) stain, and then imaged using a light microscope.

Statistical analysis. Statistical comparisons were based on analysis of variance (ANOVA) with Tukey post hoc test for pairwise comparisons and non-parametric Mann-Whitney test. Results are presented as mean + SEM.

Acknowledgements

The authors thank the Spanish Government for financial support through Project No. MAT2015-67183-R (MINECO-FEDER), co-funded by the European Union through

European Regional Development Funds. R.F. thanks the Government of Catalonia for financial support through a pre-doctoral fellowship. C.M.-M thanks the People Programme (Marie Curie Actions) of the European Union's Seventh Framework Programme (FP7-PEOPLE-2012-CIG, REA Grant Agreement No. 321985) for funding this project. Partial financial supports from Korea government are also acknowledged (grant no. 2009-0093829 &2015032163). Dr. M. Dominguez (CRNE, UPC) is acknowledged for conducting XPS measurements.

References

[1] J. Raphel, M. Holodniy, S. B. Goodman, S. C. Heilshorn, *Biomaterials* **2016**, *84*, DOI 10.1016/j.biomaterials.2016.01.016.

[2] R. Agarwal, C. González-García, B. Torstrick, R. E. Guldberg, M. Salmerón-Sánchez, A. J. García, *Biomaterials* **2015**, *63*, 137–145.

[3] J. Raphel, J. Karlsson, S. Galli, A. Wennerberg, C. Lindsay, M. G. Haugh, J. Pajarinen, S. B. Goodman, R. Jimbo, M. Andersson, et al., *Biomaterials* **2016**, *83*, 269–282.

[4] P.-Y. Wang, D. T. Bennetsen, M. Foss, T. Ameringer, H. Thissen, P. Kingshott, *ACS Appl. Mater. Interfaces* **2015**, *7*, 4979–4989.

[5] C. Mas-Moruno, R. Fraioli, F. Albericio, J. M. Manero, F. J. Gil, *ACS Appl. Mater. Interfaces* **2014**, *6*, 6525–6536.

[6] M. Dettin, A. Bagno, R. Gambaretto, G. Iucci, M. T. Conconi, N. Tuccitto, A. M. Menti, C. Grandi, C. Di Bello, A. Licciardello, et al., *J. Biomed. Mater. Res. A* **2009**, *90*, 35–45.

[7] M. Kantlehner, D. Finsinger, J. Meyer, P. Schaffner, A. Jonczyk, B. Diefenbach, B. Nies, H. Kessler, *Angew. Chemie - Int. Ed.* **1999**, *38*, 560–562.

[8] M. Pagel, R. Hassert, T. John, K. Braun, M. Wießler, B. Abel, A. G. Beck-Sickinger, *Angew. Chemie Int. Ed.* **2016**, n/a–n/a.

[9] T. A. Petrie, J. E. Raynor, C. D. Reyes, K. L. Burns, D. M. Collard, A. J. García, *Biomaterials* **2008**, *29*, 2849–57.

[10] J. E. Frith, R. J. Mills, J. J. Cooper-White, *J. Cell Sci.* **2012**, *125*, 317–27.

[11] S. Desseaux, H. Klok, *Biomaterials* **2015**, *44*, 24–35.

[12] K. A. Kilian, M. Mrksich, *Angew. Chemie - Int. Ed.* **2012**, *124*, 4975–4979.

[13] O. Fromigué, J. Brun, C. Marty, S. Da Nascimento, P. Sonnet, P. J. Marie, *J. Cell. Biochem.* **2012**, *113*, 3029–38.

[14] B. Elmengaard, J. E. Bechtold, K. Søballe, *Biomaterials* **2005**, *26*, 3521–6.

[15] C. Mas-Moruno, R. Fraioli, F. Rechenmacher, S. Neubauer, T. G. Kapp, H. Kessler,

Angew. Chemie Int. Ed. **2016**, 7048–7067.

[16] C. Dahmen, J. Auernheimer, A. Meyer, A. Enderle, S. L. Goodman, H. Kessler, *Angew. Chem. Int. Ed. Engl.* **2004**, *43*, 6649–52.

[17] S. Rahmouni, A. Lindner, F. Rechenmacher, S. Neubauer, T. R. A. Sobahi, H. Kessler, E. A. Cavalcanti-Adam, J. P. Spatz, *Adv. Mater.* **2013**, *25*, 5869–74.

[18] J. Klim, A. Fowler, A. Courtney, P. Wrighton, R. Sheridan, M. Wong, L. Kiessling, *ACS Chem. Biol.* **2012**, *7*, 518–525.

[19] F. Rechenmacher, S. Neubauer, J. Polleux, C. Mas-Moruno, M. De Simone, E. A. Cavalcanti-Adam, J. P. Spatz, R. Fässler, H. Kessler, *Angew. Chem. Int. Ed. Engl.* **2013**, *52*, 1572–5.

[20] R. Fraioli, F. Rechenmacher, S. Neubauer, J. M. Manero, J. Gil, H. Kessler, C. Mas-Moruno, *Colloids Surfaces B Biointerfaces* **2015**, *128*, 191–200.

[21] Z. Hamidouche, O. Fromigué, J. Ringe, T. Häupl, P. Vaudin, J.-C. Pagès, S. Srouji, E. Livne, P. J. Marie, *Proc. Natl. Acad. Sci. U. S. A.* **2009**, *106*, 18587–91.

[22] B. Keselowsky, L. Wang, Z. Schwarts, A. J. Garcia, B. D. Boyan, *J. Biomed. Mater. Res. Part A* **2007**, *80*, 700–710.

[23] M. Geetha, A. K. Singh, R. Asokamani, A. K. Gogia, *Prog. Mater. Sci.* **2009**, *54*, 397–425.

[24] E. L. S. Fong, C. K. Chan, S. B. Goodman, *Biomaterials* **2011**, *32*, 395–409.

[25] A. Caplan, *J. Cell. Physiol.* **2007**, 341–347.

[26] R. McBeath, D. M. Pirone, C. M. Nelson, K. Bhadriraju, C. S. Chen, *Dev. Cell* **2004**, *6*, 483–95.

[27] K. A. Kilian, B. Bugarija, B. T. Lahn, M. Mrksich, *Proc. Natl. Acad. Sci. U. S. A.* **2010**, *107*, 4872–7.

[28] J. Lee, A. a Abdeen, D. Zhang, K. a Kilian, *Biomaterials* **2013**, *34*, 8140–8148.

[29] C. Herranz-Diez, C. Mas-Moruno, S. Neubauer, H. Kessler, F. J. Gil, M. Pegueroles, J. M. Manero, J. Guillem-Marti, *ACS Appl. Mater. Interfaces* **2016**, *8*, 2517–2525.

[30] M. M. Martino, F. Tortelli, M. Mochizuki, S. Traub, D. Ben-David, G. a Kuhn, R. Müller, E. Livne, S. a Eming, J. a Hubbell, *Sci. Transl. Med.* **2011**, *3*, DOI 10.1126/scitranslmed.3002614.

[31] C. Mas-Moruno, P. M. Dorfner, F. Manzenrieder, S. Neubauer, U. Reuning, R. Burgkart, H. Kessler, *J. Biomed. Mater. Res. A* **2013**, *101*, 87–97.

[32] F. Rechenmacher, S. Neubauer, C. Mas-Moruno, P. M. Dorfner, J. Polleux, J. Guasch, B. Conings, H.-G. Boyen, A. Bochen, T. R. Sobahi, et al., *Chem. - A Eur. J.* **2013**, *19*, 9218–23.

[33] J. Guasch, B. Conings, S. Neubauer, F. Rechenmacher, K. Ende, C. G. Rolli, C. Kappel, V. Schaufler, A. Micoulet, H. Kessler, et al., *Adv. Mater.* **2015**, n/a–n/a.

[34] P. Roca-Cusachs, N. C. Gauthier, A. Del Rio, M. P. Sheetz, *Proc. Natl. Acad. Sci. U.*

S. A. **2009**, *106*, 16245–16250.

[35] D. Missirlis, T. Haraszti, C. v. C. Scheele, T. Wiegand, C. Diaz, S. Neubauer, F. Rechenmacher, H. Kessler, J. P. Spatz, *Sci. Rep.* **2016**, *6*, 23258.

[36] C. Mas-Moruno, F. Rechenmacher, H. Kessler, *Anticancer. Agents Med. Chem.* **2010**, *10*, 753–768.

[37] H. C. Kroese-Deutman, J. van den Dolder, P. H. M. Spauwen, J. A. Jansen, *Tissue Eng.* **2005**, *11*, 1867–75.

[38] B. Elmengaard, J. E. Bechtold, K. Søballe, *J. Biomed. Mater. Res. A* **2005**, *75*, 249–55.

[39] Y. Germanier, S. Tosatti, N. Broggini, M. Textor, D. Buser, *Clin. Oral Implants Res.* **2006**, *17*, 251–257.

[40] H. Daugaard, B. Elmengaard, J. E. Bechtold, T. Jensen, K. Soballe, *J. Biomed. Mater. Res. A* **2010**, *92*, 913–21.

Annex II

Paper V

Towards the cell-instructive bactericidal substrate: exploring the combination of nanotopographical and chemical cues on Ti surface

Engineering the interface between biomaterials and tissues is crucial to increase implant lifetime and avoid failures and revision surgeries. Ideally, permanent devices should enhance attachment and differentiation of stem cells, responsible for injured tissue replacement and repair, and simultaneously discourage bacterial colonization. To obtain such multifunctional surface we propose merging two strategies, topography- and chemistry-based. We coated bactericidal titanium (Ti) nanotopographies, which are not particularly eukaryotic cell-adhesive, with integrin-binding synthetic ligands that could rescue the adhesive capacity of the surfaces and instruct mesenchymal stem cell (hMSCs). Three different topographies were tested, coated alternatively with an $\alpha v\beta 3$-selective peptidomimetic, an $\alpha 5\beta 1$-selective peptidomimetic, or a RGD/PHSRN double-branched peptidic molecule. The effect of such combination of cues on hMSCs was studied. SEM observation revealed different cell attachment modes depending on the topography. Increased cell area, reduced circularity, more intense and larger focal adhesions were detected when the substrate was biomolecule-coated, irrespective of the substrate topography. Expression of osteogenic markers was also fostered on the $\alpha v\beta 3$-selective peptidomimetic-coated substrates. Finally, bacterial tests confirmed that topographies remain bactericidal in presence of the biomolecules. Such dual physicochemical approach to achieve multifunctional surfaces holds great promise for the design of novel cell-instructive biomaterial surfaces.

Authors: R. Fraioli, P.M. Tsimbouri, L.E. Fisher, A.H. Nobbs, B. Su, S. Neubauer, F. Rechenmacher, H. Kessler, M.J. Dalby, J. M. Manero, C. Mas-Moruno.

Format: full-paper.

Graphical abstract

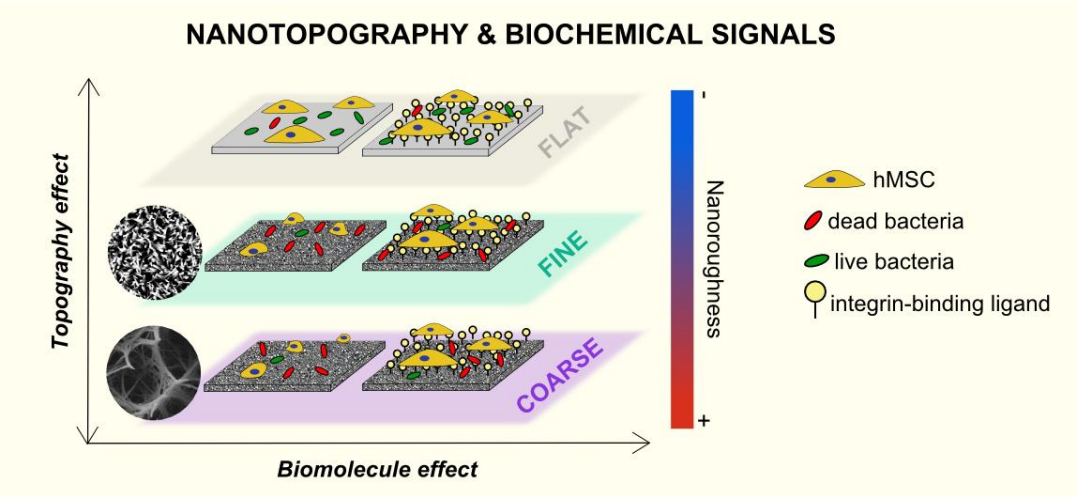

1. Introduction

According to a projection study through 2030, the burden of primary and revision joint arthroplasties is expected to increase significantly [1]: The number of hip replacement primary surgeries will grow by 174% by 2030 in the United States (from 208,600 in 2005 to 572,000), causing a growth for revision surgeries, which are expected to double by year 2026. Thus, despite a track record of positive outcomes, orthopedic implant failure will be a major clinical concern in the future as we strive to support the aging population. To address this problem, the two leading causes of implant failure should be taken into consideration: aseptic loosening and infection, which account for 18% and 20% of revision of total knee arthroplasty, respectively [2]. Though several causes for aseptic loosening exist, poor osseointegration is one of them. This highlights the importance of investigating on the design of multifunctional orthopedic coatings that are simultaneously antibacterial and osseoinductive [3,4]. With a few recent exceptions [5,6], most studies focus on either cell-guiding or antibacterial properties of the coating, ignoring the possibility of combined effects.

In the past ten years nanotopography has emerged as a potent tool to tune the response of human stem cells [7–9] and, more recently, to give antibacterial properties to the surface [10–12]. Topographical features of the surface at the nanometer scale have been shown to affect adhesion, proliferation and differentiation of mesenchymal stem cells, osteoprogenitor cells and osteoblasts [9]. Closely-packed hexagonal array nanotopography on tantalum has been demonstrated to foster osteogenesis and extracellular matrix (ECM) protein deposition of human mesenchymal stem cells (hMSCs) [13]. Osteogenic differentiation of hMSCs was also observed when cells were cultured on large titania nanotubes (100 nm diameter), compared to small nanotubes (30 nm diameter) [14]; this effect was ascribed by the authors to the increased cytoskeletal tension, which is

known to drive osteogenesis [15,16]. In a previous work we also demonstrated that the order of the nanometric features of the surface has a role in the induction of osteogenic differentiation [17]. A controlled degree of disorder of nanopits on poly(methyl methacrylate) (PMMA) promoted osteogenesis in absence of osteogenic soluble supplements, compared to a completely random and a fully-ordered substrates [17].

Following a biomimetic rationale, nanotopographies were also proved to be potentially antibacterial. Features similar to those of bactericidal insects' wings (the Clanger cicada (*Psaltoda claripennis*) [18,19] and the dragonfly *Diplacodes bipunctata* [20]) have been reproduced on the surface of artificial materials such as titanium and black silicon [10,20]. Both insects' wings present high aspect ratio surface nanometric features that have been demonstrated to be bactericidal. The needle-like features were found to effectively kill bacteria by imposing high deformational stresses to their membrane (leading to rupture or piercing) [18]. Such intrinsic bactericidal properties are particularly interesting for application in biomaterial surfaces since they are devoid of the limitations of numerous antibacterial coatings, such as silver- or antibiotic-releasing coatings, i.e. the initial burst release, which may be even cytotoxic to cells, the difficulty to control the release profile, the risk of developing antibiotic resistance and the limited lifespan, given the decreasing concentration of the released species.[4]

Despite their potential as antibacterial surfaces, such bio-inspired nanotopographies might not be optimal for eukaryotic cell-instructive purposes (e.g. osseointegration) and could even lead to a reduction in the cell adhesive properties of the surface. A viable solution to such issue is chemical functionalization to anchor cell receptor binding molecules on the surface. A family of biomolecules derived from the ECM, from the full-length proteins [21], to protein fragments encompassing the bioactive sequence of the protein [22], to small peptidic sequences [23–26], and

peptidomimetics ligands [27], have been used to create MSC-instructive substrates and thus can potentially be used to rescue the cell-instructive capacity of antibacterial nanotopographies. In doing so, multifunctional substrates that are simultaneously bactericidal and cell-instructive can be envisaged.

Herein we present a combined approach that merges bio-inspired high aspect ratio nanotopographical cues with the chemical grafting of integrin-binding peptidic ligands to engineer a bactericidal and osseoinductive titanium (Ti) surface. The rationale of this design is that biomolecule-coated metallic nanotopographies can simultaneously be bactericidal, due to the insect wing-inspired topography in our case, and cell-instructive, thanks to the presentation of cell receptor-binding cues at the surface. Two different nanotopographies generated by hydrothermal treatment were tested. Three different peptidic ligands were coupled to the topographies to verify the combination of topography and low molecular weight

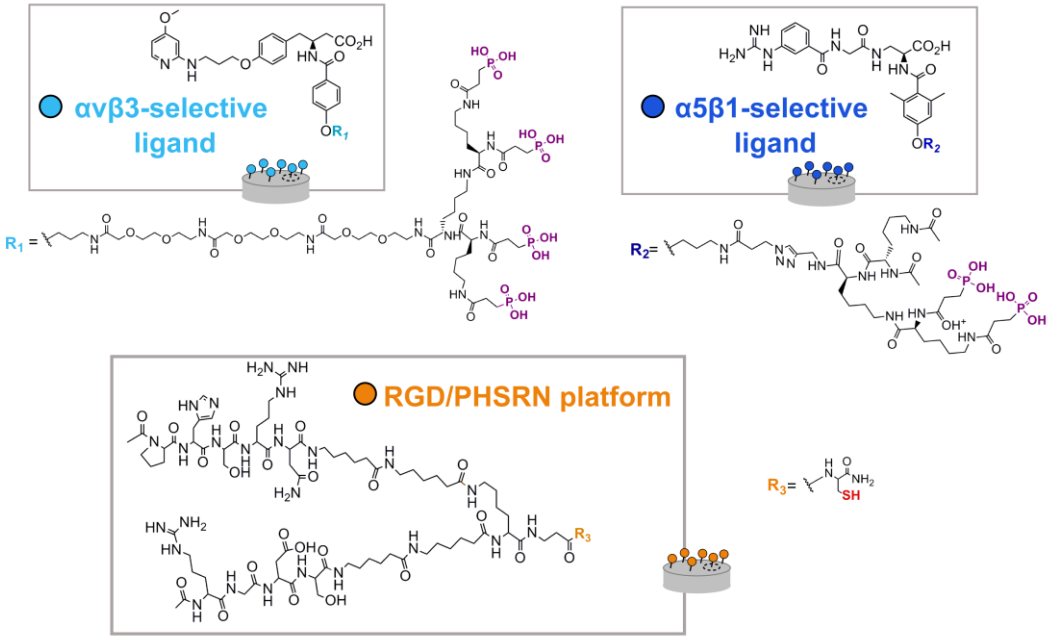

Figure 1. Chemical structure of the integrin-binding ligands: αvβ3-selective peptidomimetic (light blue), α5β1-selective peptidomimetic (dark blue), and RGD/PHSRN platform (orange). Phosphonic acid anchors are highlighted in purple and thiol anchor is highlighted in red.

receptor-binding ligands in supporting hMSC adhesion and differentiation and avoiding bacteria colonization. Two families of peptidic ligands were used: two integrin-selective peptidomimetics molecules, selective for integrin $\alpha v\beta 3$ or $\alpha 5\beta 1$ respectively, and a double-branched peptidic ligand containing the RGD and PHSRN sequences from fibronectin, recently synthesized in our laboratories (Fig. 1) [23,28]. We have previously demonstrated that both ligands families stimulate osteoblast-like cell attachment, cell spreading and osteogenic differentiation [23,29].

2. Materials and methods

2.1. Ti substrate preparation

Ti disks were prepared from a 0.9 mm thick ASTM grade 1 Ti sheet (Ti metals Ltd, UK). For the smooth control surfaces (denoted by FLAT), disks were polished to a mirror image and ultrasonically cleaned in water and ethanol. Nanotopographies were generated by an alkaline hydrothermal process, as previously described [10]. In brief, Ti disks were immersed in 1 M NaOH in a polytetrafluoroethylene (PTFE) lined steel vessel (Acid Digestion vessel 4748, Parr Instrument Company, USA) at 240 °C for either 2 h (denoted by FINE) or 3 h (denoted by COARSE). The vessel was removed after each time point from the oven and allowed to cool to room temperature (RT). The samples were rinsed in water and ethanol, sequentially, and then heat-treated at 300 °C for 1 h. To convert the sodium titanate layer generated during the process to TiO_2, samples were immersed in 0.6 M HCl for 1 h, rinsed in water and ethanol, and finally heat treated at 600 °C for 2 h.

2.2. Ligand conjugation to the metallic surface

All samples were preliminarily cleaned with nitric acid (1 h, RT) and rinsed with water, ethanol and acetone. Previously synthesized [23,28,30] integrin-selective molecules (Fig. 1) were covalently attached to the surface by dissolving the molecules in phosphate buffered saline (PBS) at 100 μM, and then depositing 100 μL of these solutions overnight on Ti disk surfaces at RT. The two integrin-selective peptidomimetics directly binded to Ti oxide via the anchoring phosphonate groups. The efficiency and stability of this coating method was proved in previous reports [31–33]. The $\alpha v\beta 3$-selective peptidomimetic was labeled V3, while the $\alpha 5\beta 1$-selective one was labeled 51. Alternatively, the peptidic RGD/PHSRN platform (labeled as P), which has a thiol group as anchoring group, required an extra step of silanization. In that case, Ti disks were exposed to silane vapor ((3-aminopropyl)triethoxysilane, APTES) in a vacuum chamber and kept at 100 °C for 30 min. Straight after silanization, the crosslinking agent N-succinimidyl-3-maleimidopropionate (SMP, 7.5 M in N,N-dimethylformamide (DMF)) (Alfa Aesar, Karlsruhe, Germany) was coupled by immersing the disks in DMF under agitation for 1 h at RT and rinsing with DMF, distilled water, ethanol and acetone. The peptidic platform was then anchored following the same protocol as the peptidomimetics molecules (100 μL drop, 100 μM in 6.5 pH PBS). The dissolving buffer for the platform is slightly acidic to prevent disulfide bond formation. Detailed characterization of this protocol has been reported elsewhere [29]. Experimental conditions were labeled according to the topography and the peptidic ligand grafted, such that FINE-V3 corresponds to the FINE topography coated with the $\alpha v\beta 3$-selective peptidomimetic. All reagents were from Sigma-Aldrich, unless otherwise stated.

2.3. Surface topography characterization

Ti topographies were mounted onto stubs and sputter coated with gold (high resolution sputter coater, Agar Scientific) for analysis on a Zeiss Sigma FE-SEM microscope. Height profile of the topographies was obtained by white light interferometric microscopy (Wyko NT9300 Optical Profiler, Veeco Instruments, New York, NY, USA) in vertical scanning interferometry mode. Data analysis was performed with Wyko Vision 4.10 software (Veeco Instruments).

2.4. Cell culture

hMSCs (Promocell, Germany) were cultured in Dulbecco's Modified Eagle Medium (DMEM) supplemented with 10% (v/v) fetal bovine serum (FBS), 200 mM L-glutamine (Invitrogen), 100 mM sodium pyruvate, 1% MEM NEAA (Gibco) and antibiotics (6.74 U/ml Penicillin-Streptomycin, 0.2 μg/ml Fungizone) at 37 °C in humidified atmosphere containing 5% (v/v) CO_2. Culture medium was changed twice a week, and cells used between passage 1 and 2 at the concentration of 5000 cells/well. For the PCR analysis 10000 cells/well were seeded. All reagents were from Sigma-Aldrich, unless otherwise stated.

2.5. SEM observation of cell morphology

After seeding hMSCs in serum-free conditions on Ti surfaces, 1% (v/v) FBS medium was added 6 h later to guarantee cell survival and cells kept in culture for 3 days. When the incubation time was over, samples were rinsed once with PBS, to remove floating cells, and remaining cells fixed in 2% glutaraldehyde in 0.2 M cacodylate buffer for 1 h at 4 °C. Ti disks were then immersed in 20, 40, 60 80 and 100% (v/v) ethanol, and 25, 50, 75 and 100% (v/v) hexamethylsilizane in ethanol. Afterwards, Ti disks were mounted onto a stub and sputter coated with gold (high resolution sputter

coater, Agar Scientific) for analysis on a Zeiss Sigma FE-SEM microscope. All reagents are from Sigma-Aldrich, unless otherwise stated.

2.6. Cell attachment and immunostaining

Cells were seeded and kept in serum-free medium for 6 h. The medium was then replaced with 1% (v/v) FBS medium and kept in culture for 18 h. At harvest (24 h incubation), surfaces were rinsed with PBS, and cells fixed in a 10% formaldehyde solution, permeabilized, and blocked in 1% (w/v) BSA/PBS. hMSCs were stained with 1:150 mouse anti-vinculin and 1:500 phalloidine-rhodamine in 1% (w/v) BSA/PBS for 1 h at 37 °C. After rinsing samples 3x5 min in 0.5% (v/v) Tween-20/PBS, 1:50 biotinylated anti-mouse secondary antibody (Vector Laboratories) was added in 1% (w/v) BSA/PBS and incubated again at 37 °C for 1 h. After washing, 1:50 FITC-conjugated streptavidin (Vector Laboratories) was added and incubated for 30 min at 4 °C. Finally, disks were washed and mounted using Vectashield mountant with DAPI nuclear stain (Vector Laboratories). All reagents are from Sigma-Aldrich, unless otherwise stated. Images from the immunostaining experiments were analyzed with the Fiji/Image-J package [34]. A self-made macro was used to quantify DAPI-stained nuclei, while characterization of cell-projected area, shape and focal adhesion length was done manually.

2.7. PCR analysis

After culturing cells for 21 days on Ti disks, total RNA was extracted using the RNeasy micro kit (Qiagen, Hilden, Germany) according to manufacturer instructions. A NanoDrop spectrophotometer (Thermo Scientific, Waltham, MA, USA) was used to quantify total RNA. RNA was reverse transcribed to cDNA using the QuantiTect Reverse Transcription Kit (Qiagen). Real time qPCR was carried out to quantify the expression of

osteocalcin (OCN) and osteopontin (OPN) genes with QuantiTect SYBR Green RT-PCR Kit (Qiagen) on a 7500 Real-Time PCR system (Applied Biosystems, Foster City, CA, USA). Primer sequences are reported in table 1. Melt curve analysis was used to validate the primer sequences for the genes. Gene expression was normalized to GAPDH expression, which was chosen as the housekeeping gene, and analyzed with the method.

Target Gene	Forward Sequence	Reverse Sequence
GAPDH	GTCAGTGGTGGACCTGACCT	ACCTGGTGCTCAGTGTAGCC
OPN	AGCTGGATGACCAGAGTGCT	TGAAATTCATGGCTGTGGAA
OCN	CAGCGAGGTAGTGAAGAGACC	TCTGGAGTTTATTTGGGAGCAG

Table 1. PCR primer sequences

2.8. Bacterial culture preparation

P. aeruginosa ATCC 27853 was grown aerobically for 16 h in 10 mL Luria-Bertani broth (LBB) in a 37 ºC shaker incubator set at 220 rpm. The bacterial suspension was then diluted in LBB to OD600 0.1 and further incubated until mid-exponential phase was reached. At this time bacterial cells were harvested by centrifugation (7 min, 5000 g), washed twice in 10 mM Tris-HCl buffer (2-amino-2-(hydroxymethyl)-1,3-propanediol, adjusted to pH 7 with hydrochloric acid), and suspended in Tris-HCl buffer to OD600 0.3 (approx. 10^7 cfu/mL).

2.9. Bacterial adhesion

The test surfaces and controls were placed into a 12-well microtiter plate and submerged in 2 mL of bacterial suspension. Plates were incubated for 1 h at 37 ºC under static conditions. After incubation, surfaces were rinsed to remove non-adherent bacteria by passing back and forth five times in a Universal container containing Tris-HCl buffer, repeated three times in total.

2.10. Live/Dead staining and fluorescence microscopy

Following rinsing, 1 mL of Live/Dead® BacLight™ bacterial viability stain (Invitrogen) was applied to the surfaces (as per manufacturers' instructions) and incubated in the dark for 15 min at RT. Surfaces were then rinsed in Tris-HCl buffer as explained above to remove excess stain. Surfaces were maintained in 1 mL of Tris-HCl buffer, and bacterial adhesion and viability was visualized by fluorescence microscopy. Image J software was used to calculate the number of cells with intact membranes (SYTO 9, green) and the number of cells with damaged membranes (propidium iodide, red) based on 5 images per surface. The average % kill was determined by (no. of damaged cells / total no. of cells) * 100. FLAT, FINE and COARSE with each peptide (12 total) were tested in one assay, which was repeated on three separate occasions using the same method each time.

2.11. Statistical analysis

Statistical comparisons were based on analysis of variance (ANOVA) with Tukey post hoc test for pairwise comparisons and non-parametric Mann-Whitney test. Results are presented as mean + SEM.

3. Results

3.1. Surface characterization

Two nanotopographies have been generated by applying a hydrothermal treatment to Ti samples for different reaction times. As shown in figure 2A, the length of the fibers increased with reaction time: the 2h treatment generates homogeneous fine spike-like structures (FINE); when reaction time is increased to 3h, these structures grow in length and merge to form much bigger pocket-like structures on the surface (COARSE). Geometrical features of these structures, obtained from the SEM image analysis, are summarized in Table 2 and the height profile is reported in Figure 2B.

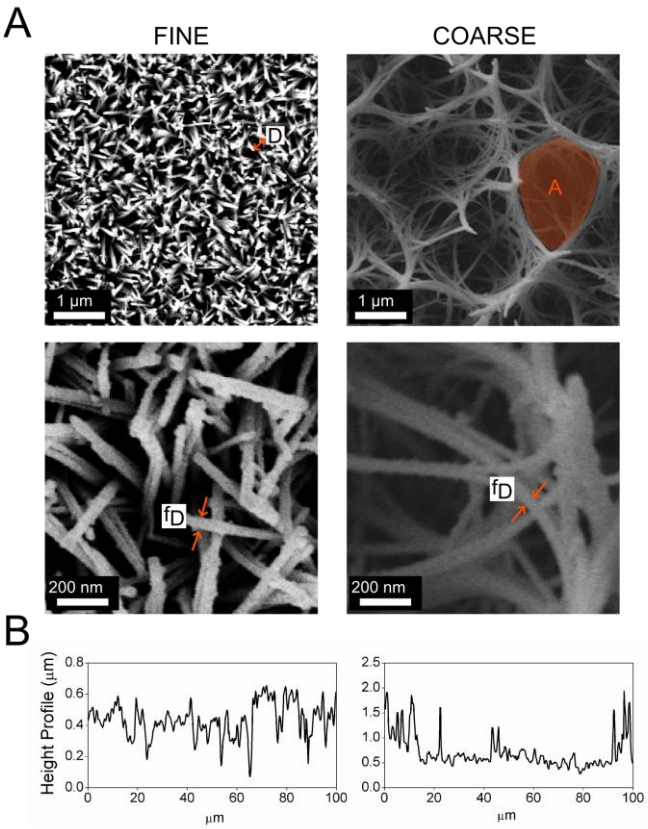

Figure 2. (A) SEM images of the nanotopographies. The labels tip-to-tip distance - D, "pocket" area - A, fiber diameter - f_D refer to the measured geometrical features of the nanostructure in table 2. (B) Height profile of the FINE (left) and COARSE (right) topographies.

Nanotopography	Geometrical feature	
FINE	D	(171.3 ± 48.3) nm
	f_D	(34.0 ± 6.5) nm
COARSE	A	(2.90 ± 1.80) μm^2
	f_D	(7.78 ± 2.56) nm

Table 2. Geometrical features of the nanotopographies. The labels (tip-to-tip distance - D, "pocket" area - A, fiber diameter - f_D) refer to the highlighted features of the structures in figure 2A. Values are reported as mean ± SD.

3.2. SEM observation of cell attachment reveals different attachment modes depending on the topography

Given the completely different topography presented to cells in the FLAT, FINE, and COARSE conditions, a difference in the way cells attach and probe the substrate is expected. SEM analysis has been carried out after incubating cells on the Ti substrates for 3 days. As shown in figure 3, cells spread more on the FLAT and FINE surfaces, while they look more rounded on the COARSE topography. Moreover, hMSCs probe the surface with cytoskeletal fiber extensions both on the smooth and on the FINE nanotopography. These extensions look thinner, less branched and more numerous on the FINE substrate. On the other hand, almost no elongation is observed on the COARSE topography. Both on the FINE and the COARSE topographies cells appear to have indentations (perhaps even piercings) throughout their lamellae by the spike-like structures of the surfaces.

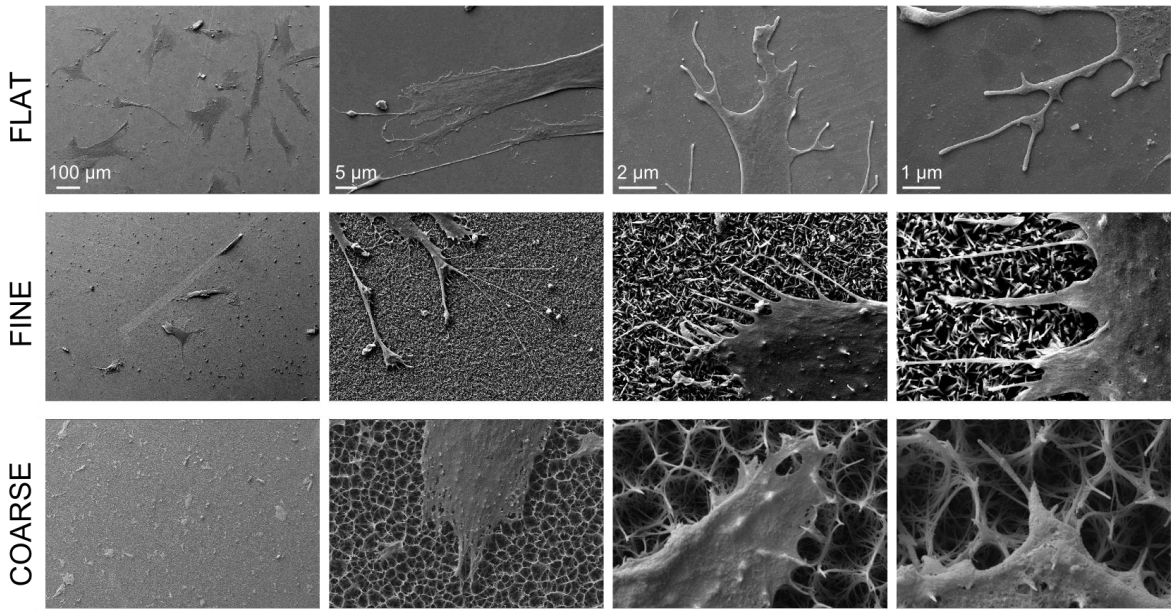

Figure 3. SEM images of hMSCs attaching on the flat Ti and Ti nanotopographies. Cells interact with the nanofeatures as can be seen by retraction fiber terminations and membrane indentations. This effect is most notable on the COARSE topography. Each column of images has the same magnification.

3.3. Effect of topography and ligand presentation on the number, area, and circularity of attached cells

For all cellular experiments including biomolecules, cell seeding has been done in serum-free conditions, in order to let cells attach to the surface mainly via the receptor-binding ligands, and avoiding unspecific interactions with serum proteins. Characterization of short-time cell response to the functionalized topographies was performed by incubating hMSCs for 24 h on the substrates and immunostaining nuclei and actin cytoskeleton. The number of cells attached to the FLAT and FINE Ti samples was not significantly affected by the presence of the synthetic ligands (figure 4A). Nonetheless, on the COARSE topography, where fewer cells adhered in the uncoated condition compared to the FLAT and FINE surfaces, the presence of the synthetic ligands generated an increase in cell

number, which was statistically significant in the case of the $\alpha 5\beta 1$-selective mimetic (COARSE-51) and the RGD/PHSRN platform (COARSE-P).

Though the presence of the receptor-binding ligands only affected attachment on the COARSE surface, hMSC projected area was increased by the addition of the biomolecules on all topographies (figure 4B). On the FLAT surfaces, this increase was statistically significant only for the $\alpha v\beta 3$-selective mimetic (FLAT-V3) and the RGD/PHSRN platform (FLAT-P). However, on the FINE and COARSE topographies, all biomolecules generated a significant increase in area compared to the uncoated sample of the same topography. Though cells appeared smaller on FINE and COARSE uncoated topographies compared to FLAT, no statistically significant difference in cell area was observed comparing the three uncoated topographies (not shown). Finally, quantification of cell circularity reveals that hMSC shape was unaffected by the presence of the peptide on the FLAT surface (figure 4C), where circularity attained low values in all conditions. Interestingly, a different outcome was observed on both nanotopographies: all ligands caused a statistically significant decrease in cell circularity. The increase in cell area and decrease in cell circularity when hMCSs are incubated on biomolecule-coated FINE and COARSE topographies, compared to their uncoated control, was also evident in the immunostained actin cytoskeleton in figure 5.

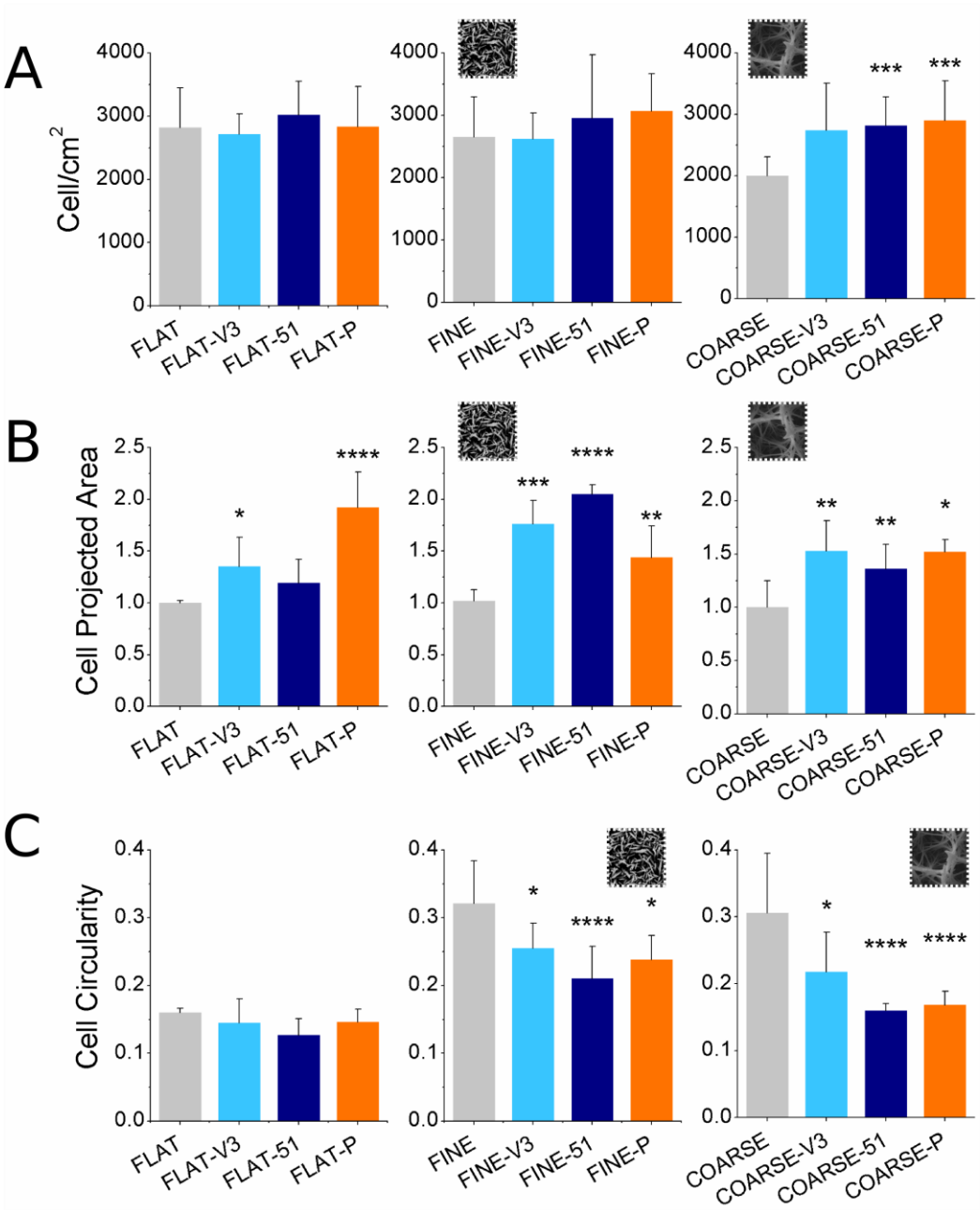

Figure 4. Number of attached cells (A), cell projected area (B), and cell circularity (C) on the FLAT (first column of graphs), FINE (second column of graphs), and COARSE (third column of graphs) surfaces with or without biomolecule coating. Cell projected area has been normalized to the uncoated condition in each graph (FLAT, FINE, and COARSE, respectively). Number of attached cells is not affected by the biomolecules on FLAT and FINE, while more cells adhere to the biomolecule-coated COARSE substrates. Cell area is significantly increased in presence of the biomolecule on all three topographies. While low circularity is observed on all FLAT conditions, the biomolecule-coated FINE and COARSE surfaces present lower circularity compared to the respective uncoated topography. * $p<0.05$, ** $p<0.01$, *** $p<0.001$, **** $p<0.0001$ vs. uncoated condition (FLAT, FINE and COARSE, respectively).

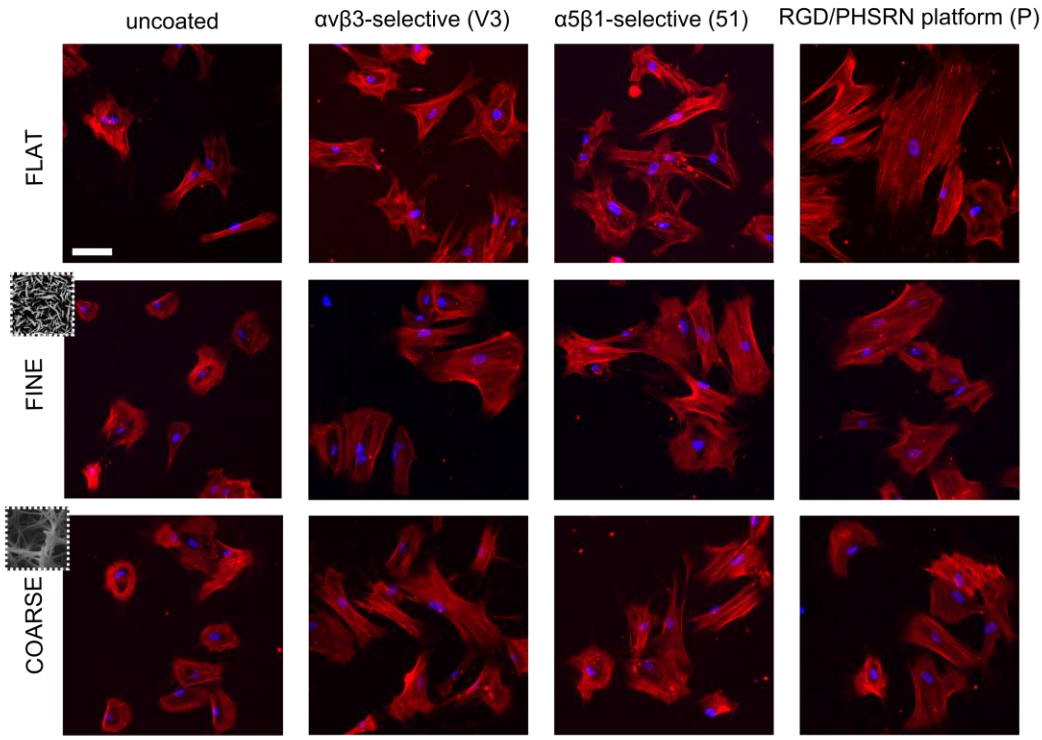

Figure 5. Immunostained actin fibers and DAPI-stained nuclei after 24 h of incubation. Cell spread more on the biomolecule-coated nanotopographies, compared to their uncoated control. A decrease in circularity was also evident on the COARSE and FINE substrates presenting integrin-binding ligands. Scale bar = 100 μm.

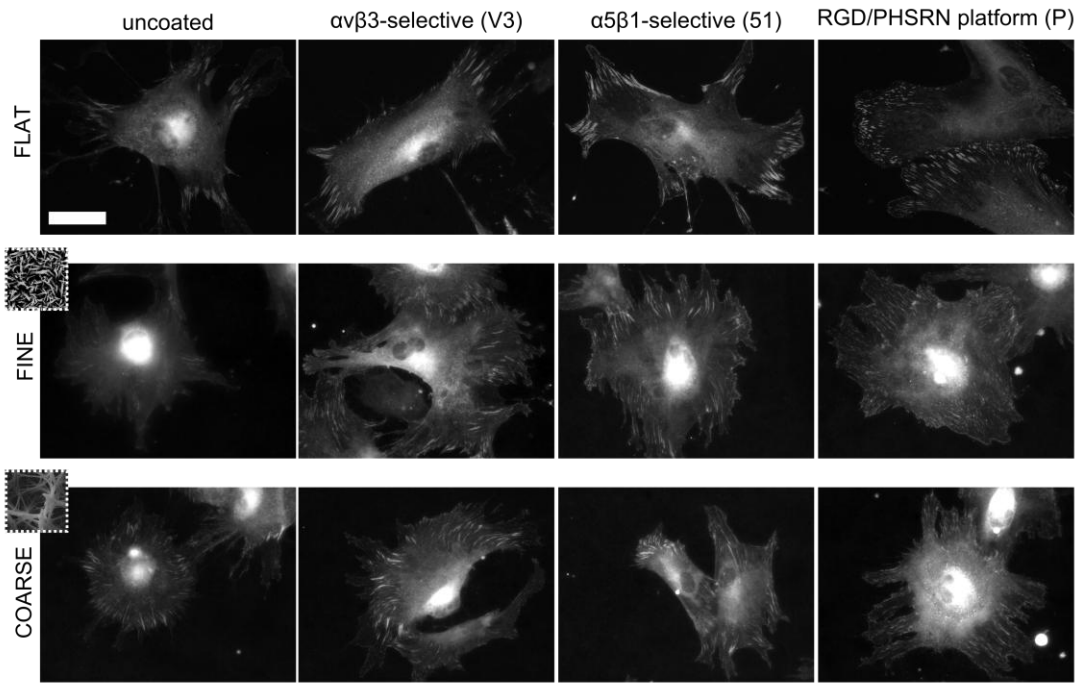

Figure 6. Immunostaining of vinculin after 24 h of incubation. Fluorescence intensity of vinculin adhesion sites on the biomolecule-coated substrate was increased when compared to the uncoated controls. Scale bar = 50 μm.

3.4. Focal adhesion dimension is both topography and chemistry-dependent

hMSCs cultured for 24 h on the coated and uncoated Ti samples were immunostained to visualize vinculin. This protein, which is part of the focal adhesion complex, is commonly used to label focal adhesions (FAs). As shown in figure 6, vinculin staining was more intense when cells adhere to the functionalized surfaces, compared to when they attached to their uncoated counterparts. This is observed on all three topographies and it is particularly evident on the FINE nanotopography, where vinculin staining had very low intensity on the uncoated condition. By means of image analysis, the dimension of focal contacts was quantified (figure 7). Focal contact dimension appeared to be influenced by both the topography and the chemistry of the substrate. The effect of both nanotopographies (FINE and COARSE) was to produce an overall reduction in the distribution of FA area, compared to the FLAT surface. However, the effect of the biomolecules was to generate a shift towards larger focal adhesions, compared to the uncoated topographies. This increase in FA area is statistically significant on the FINE-51, COARSE-V3 and COARSE-51 surfaces, compared to their uncoated controls (FINE and COARSE, respectively).

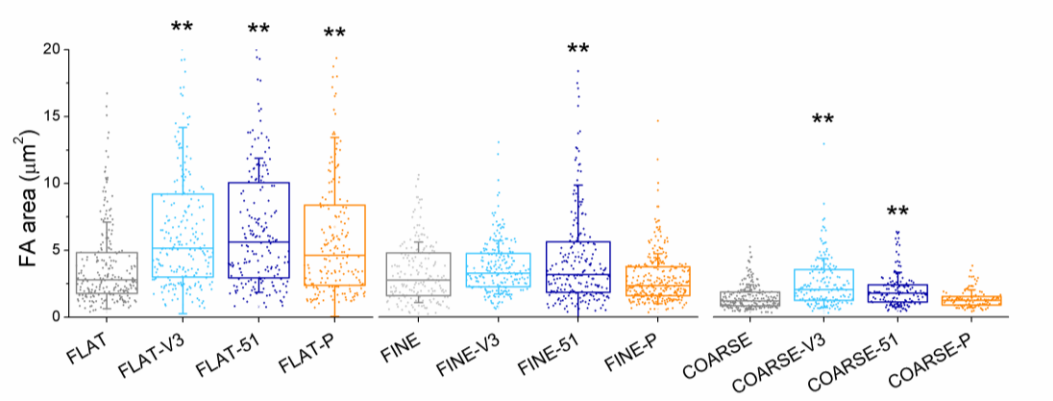

Figure 7. Focal adhesion area on FLAT, FINE, and COARSE topographies after 24 h incubation. Passing from the smooth Ti to FINE and COARSE surfaces, FA area was reduced. However, upon grafting biomolecules, the dimension of the FA was increased compared to the uncoated condition of each topography. ** $p<0.01$ vs. uncoated condition (FLAT, FINE and COARSE, respectively).

3.5. Expression of osteogenic genes

Quantitative PCR analysis of gene expression was carried out after 21 days of incubation in basal medium on the uncoated and biomolecule-coated topographies. The expression of the late osteogenic markers OCN and OPN was evaluated in order to monitor the progression of hMSCs into the osteoblastic lineage (figure 8). The trend for expression of both genes was very similar on all topographies: though not statistically significant, the $\alpha v\beta 3$-selective peptidomimetic stimulated the highest expression of both OCN and OPN on FLAT, FINE and COARSE Ti topographies, while the $\alpha 5\beta 1$-selective peptidomimetic and the RGD/PHSRN peptidic platform did not change gene expression significantly on all topographies. The increase caused by the $\alpha v\beta 3$-selective peptidomimetic was particularly evident on the COARSE topography, and it was significantly higher compared to the uncoated control and the other peptidic coatings in the case of OCN. No significant difference has been observed among topographies (not shown).

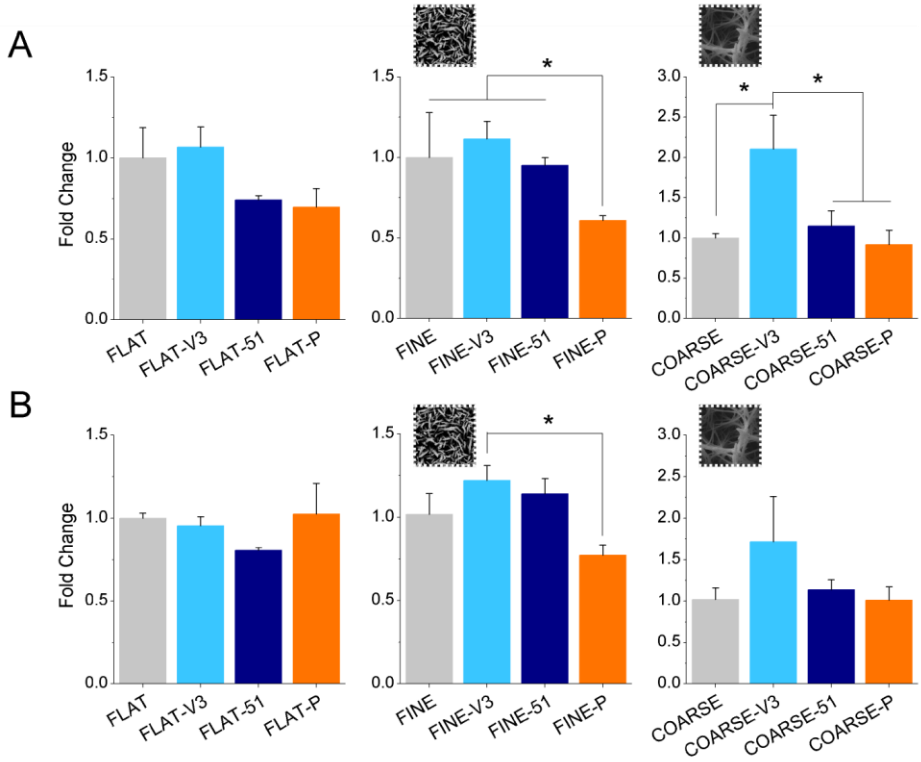

Figure 8. Expression of the osteogenic markers osteocalcin (A) and osteopontin (B). A clear trend towards higher marker expression on the $\alpha v\beta 3$-selective peptidomimetic (V3) is visible, though statistically significant only on the COARSE topography. Data have been normalized to the uncoated condition of the respective topography. * $p<0.05$ vs. uncoated condition (FLAT, FINE and COARSE, respectively).

3.6. Topography dictates bacterial attachment

In order to check the effect of topography and ligands on the bactericidal properties of the surfaces, bacterial attachment (*P. aeruginosa*) assays were carried out on the substrates. Compared to the polished Ti surfaces (FLAT), both topographies (FINE and COARSE) presented a higher number of dead cells, as shown in figure 9. No effect of the grafted ligands was observed irrespectively of the topography of the substrate, since no variation of the percentage of dead cells was detected compared to the uncoated condition of each topography (figure 9B).

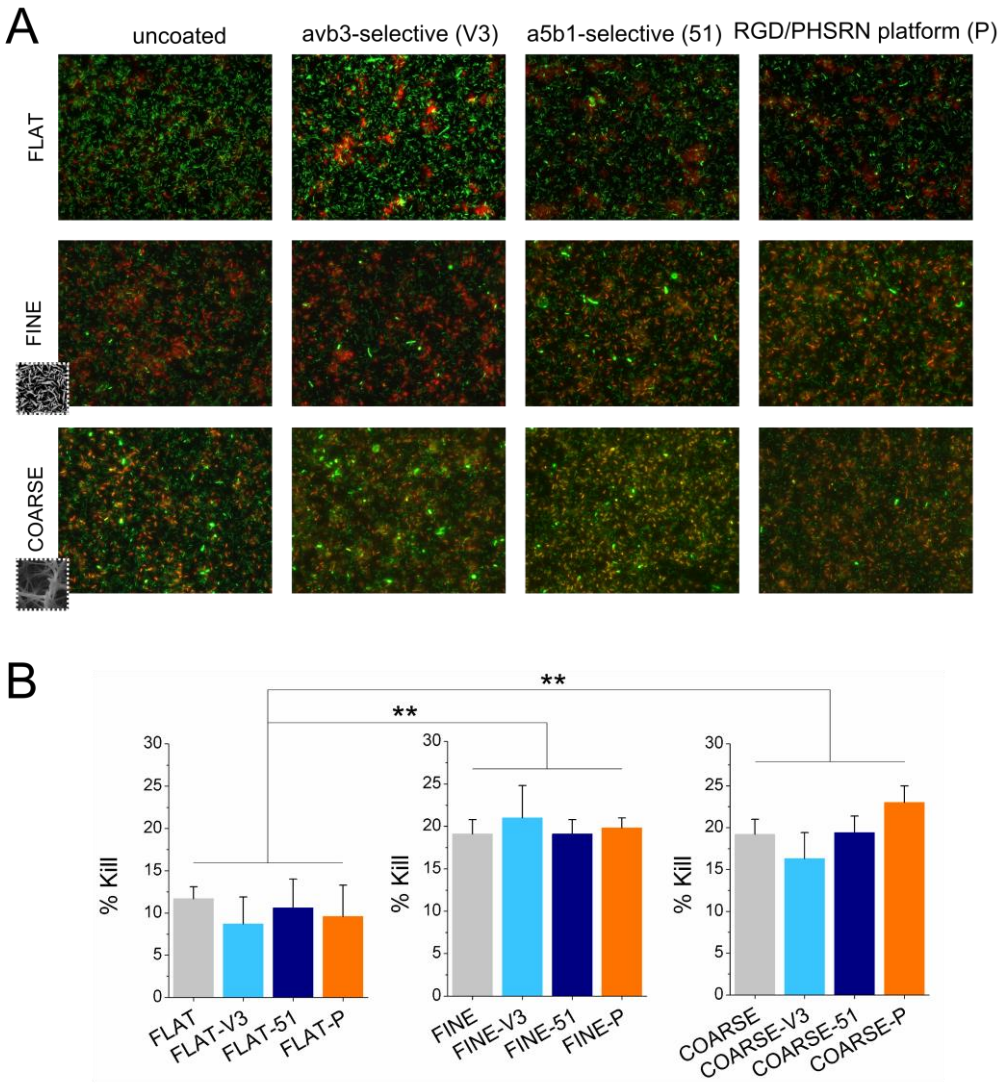

Figure 9. Representative fluorescence microscopy images (A) of *P. aeruginosa* stained with Live/Dead viability stain and percentage of dead cells (B). Live cells are stained green, while dead cells appear red. Increase in the %kill was observed on both nanotopographies, compared to the FLAT Ti surface. No effect of the biomolecules is visible. ** $p<0.01$ vs. uncoated condition (FLAT, FINE and COARSE, respectively).

4. Discussion

A plethora of metallic materials have been optimized to serve as biomaterials for joint replacement implants [35]. Several alloys, especially Ti-based, have been generated to meet the structural requirements of orthopedic implants. Nonetheless, premature failure still occurs, mainly due to aseptic loosening or infection. In the quest for an optimized integration with the surrounding tissues and reduction of bacterial colonization, the focus is at the tissue-implant interface: physicochemical modifications can convert biocompatible inert surfaces into bioactive ones, which actively discourage infection and foster osseointegration [4].

With the aim of creating a multi-functional Ti surface that is simultaneously osseoinductive and antibacterial, we propose merging two classical surface functionalization strategies, namely topographical and chemical modification of the surface. The hydrothermal treatment described in this study allows for the generation of Ti substrates with nanoscale, high aspect ratio topographical features and does not require any constraint on the shape and dimension of the sample. The rationale behind the generation of such topographies is the biomimesis of natural bactericidal surface, such as the wings of the Clanger cicada (*Psaltoda claripennis*) [10,18,19] and the dragonfly *Diplacodes bipunctata* [20]. To simultaneously enhance the cell adhesive properties of the topographies, which were reduced compared to the flat Ti surface, we combined the bio-inspired substrates with low molecular weight integrin-binding molecules. Previous studies from our group already reported stimulation of osteoblast-like cell attachment, increased cell spreading and osteogenic differentiation, exerted by the three ligands used in the present work [23,29].

As observed in the lowest magnification SEM images, fewer hMSCs adhere and spread on the nanotopographies, compared to the flat polished

Ti surface. The fact that cells also look slightly detached from the nanotopographies suggests that binding to the surface is weaker, compared to the polished FLAT Ti surface. Similarly, immunostaining of actin cytoskeleton reveals that cell shape is much more circular on both the FINE and COARSE topographies compared to the flat surface, with the formation of less and smaller cytoskeletal elongations. However, adhesive capacity of the nanotopographies is rescued after grafting integrin-binding peptides: presenting receptor-binding cues on the nanowires fosters spreading of cells, which also present a much less circular shape. Interestingly, the effect of the biomolecules is much more evident on the less adhesive nanotopographies, than on the polished surface. hMSCs are more prone to attach and spread on the FLAT Ti surface, where they reach low values of circularity, even in absence of any ligand on the surface. On the contrary, on FINE and COARSE topographies, where cell spreading is less fostered and cells stay mostly rounded, the presence of the integrin ligands is crucial.

Focal adhesions are also affected by the integrin-binding molecules: vinculin-staining is much more intense and focal adhesion area is increased on all surfaces, including the polished control, in presence of the ligands. This might be due to the exposure of integrin-binding cues on the surface, which stimulate the formation of bigger adhesions by recruiting cell surface receptors. Though few studies combined topographical stimulation and biochemical signals, an enhancing effect in terms of cell adhesion was previously observed on RGD-functionalized nanoporous alumina membranes [36] and sandblasted Ti6Al4V disks [32].

Since both nanotopography and biochemical signals are known to ultimately alter gene expression by inducing nuclear structural changes and activating specific signaling cascades, hMSC differentiation was expected to change on our functionalized topographies. A trend towards higher expression of osteogenic markers (OCN and OPN) is detected on the

Ti surfaces coated with the $\alpha v\beta 3$-selective peptidomimetic, though gene expression statistically increases only on the least-adhesive COARSE topography, compared to the uncoated control of this nanotopography. The positive effect of this integrin subtype on osteogenic differentiation of osteoblasts and MSCs has been previously reported [37,38]. From these observations, it seems that the more $\alpha 5\beta 1$-selective surfaces, both the peptidomimetic one and the FN-inspired, are less effective in stimulating osteogenesis on these substrates. Osteogenesis is known to require development of large, super-mature, adhesions supporting increasing cytoskeletal tension [15,16,39]. Integrin subtype $\alpha v\beta 3$ is selective for vitronectin, which has been implicated in increased adhesion bridging compared to FN (which preferentially binds integrin $\alpha 5\beta 1$) [40]. Potentially, such bridging would facilitate increased adhesion between topographical features [9].

Finally, nanotopography-related bactericidal properties of the samples were tested with *P. aeruginosa* attachment assays. Similar surfaces were previously reported to be bactericidal [10]. However, surfaces were not tested in presence of biomolecules. As expected, both FINE and COARSE nanotopographies were more effective than flat Ti in inducing bacteria death due to the mechanical effect of their high aspect ratio nanofeatures. Coating of the substrates with the integrin-binding ligands did not affect the bactericidal properties of the nanostructured substrates, thereby indicating that such antibacterial effect is merely caused by the topography of the surface, rather than by biochemical signals. This mechanical bactericidal effect has been observed before on artificial surfaces presenting similar bio-inspired nanotopography [20].

5. Conclusions

The design of multifunctional coatings has increasing relevance, especially to solve multiple issues, such as infection and impaired osseointegration of joint-replacement implants. In this work, we proposed merging topographical and biochemical cues on the surface of a clinically relevant material such as Ti. Compared to other methods, the bactericidal effect given by the topography is particularly interesting for application in the orthopedic field as it circumvents the problems associated with the systemic release of antibacterial agents. By grafting cell receptor-binding ligands on nanotopographies, we could simultaneously take advantage of the topography-induced inhibition of bacteria colonization and improve the adhesive properties of the nanostructured substrates. While integrin-binding molecules did not affect antibacterial properties of the nanotopographies, they fostered cell attachment, spreading, focal contacts formation and, in some cases, differentiation of hMSCs on Ti. This study offers an example of how combination of very different strategies can be a straightforward method to obtain multifunctional biomaterial surfaces.

Acknowledgments

The authors thank the Spanish Government for financial support through Project No. MAT2015-67183-R (MINECO/FEDER), co-funded by the European Union through European Regional Development Funds. R.F. and C.M.-M thank the Government of Catalonia for financial support through a pre-doctoral and post-doctoral fellowship, respectively. R.F. also thanks the European Molecular Biology Organization (EMBO) for a short-term fellowship award. C.M.-M also thanks the People Programme (Marie Curie Actions) of the European Union's Seventh Framework Programme (FP7-PEOPLE-2012-CIG, REA Grant Agreement No. 321985) for funding this project. PMT, BS, LEF, AHN, and MJD are funded by EPSRC grants (EP/K034898/1 and EP/K035142/1).

References

[1] Kurtz S, Ong K, Lau E, Mowat F, Halpern M. Projections of primary and revision hip and knee arthroplasty in the United States from 2005 to 2030. J Bone Joint Surg Am 2007;89:780–5. doi:10.2106/JBJS.F.00222.

[2] Bozic KJ, Kurtz SM, Lau E, Ong K, Chiu V, Vail TP, et al. The epidemiology of revision total knee arthroplasty in the united states. Clin Orthop Relat Res 2010;468:45–51. doi:10.1007/s11999-009-0945-0.

[3] Neoh KG, Hu X, Zheng D, Kang ET. Balancing osteoblast functions and bacterial adhesion on functionalized titanium surfaces. Biomaterials 2012;33:2813–22. doi:10.1016/j.biomaterials.2012.01.018.

[4] Raphel J, Holodniy M, Goodman SB, Heilshorn SC. Multifunctional Coatings to Simultaneously Promote Osseointegration and Prevent Infection of Orthopaedic Implants. Biomaterials 2016;84. doi:10.1016/j.biomaterials.2016.01.016.

[5] Rocas P, Hoyos-Nogués M, Rocas J, Manero JM, Gil J, Albericio F, et al. Installing Multifunctionality on Titanium with RGD-Decorated Polyurethane-Polyurea Roxithromycin Loaded Nanoparticles: Toward New Osseointegrative Therapies. Adv Healthc Mater 2015;4:1956–60. doi:10.1002/adhm.201500245.

[6] Wang L, Chen J, Cai C, Shi L, Liu S, Ren L, et al. Multi-biofunctionalization of titanium surface with mixture of peptides to achieve excellent antimicrobial activity and biocompatibility. J Mater Chem B 2014. doi:10.1039/C4TB01318B.

[7] Lv L, Liu Y, Zhang P, Zhang X, Liu J, Chen T, et al. The nanoscale geometry of TiO 2 nanotubes influences the osteogenic differentiation of human adipose-derived stem cells by modulating H3K4 trimethylation. Biomaterials 2015;39:193–205.

[8] Sjöström T, Dalby MJ, Hart A, Tare R, Oreffo ROC, Su B. Fabrication of pillar-like titania nanostructures on titanium and their interactions with human skeletal stem cells. Acta Biomater 2009;5:1433–41. doi:10.1016/j.actbio.2009.01.007.

[9] Dalby MJ, Gadegaard N, Oreffo ROC. Harnessing nanotopography and integrin-matrix interactions to influence stem cell fate. Nat Mater 2014;13:558–69. doi:10.1038/nmat3980.

[10] Diu T, Faruqui N, Sjöström T, Lamarre B, Jenkinson HF, Su B, et al. Cicada-inspired cell-instructive nanopatterned arrays. Sci Rep 2014;4:7122. doi:10.1038/srep07122.

[11] Puckett SD, Taylor E, Raimondo T, Webster TJ. The relationship between the nanostructure of titanium surfaces and bacterial attachment. Biomaterials 2010;31:706–13. doi:10.1016/j.biomaterials.2009.09.081.

[12] Flint SH, Brooks JD, Bremer PJ. Properties of the stainless steel substrate, influencing the adhesion of thermo-resistant streptococci. J Food Eng 2000;43:235–42. doi:10.1016/S0260-8774(99)00157-0.

[13] Wang P-Y, Bennetsen DT, Foss M, Ameringer T, Thissen H, Kingshott P. Modulation of Human Mesenchymal Stem Cell Behavior on Ordered Tantalum Nanotopographies Fabricated Using Colloidal Lithography and Glancing Angle Deposition. ACS Appl Mater Interfaces 2015;7:4979–89. doi:10.1021/acsami.5b00107.

[14] Oh S, Brammer KS, Li YSJ, Teng D, Engler AJ, Chien S, et al. Stem cell fate dictated solely by altered nanotube dimension. Proc Natl Acad Sci U S A 2009;106:2130–5. doi:10.1073/pnas.0813200106.

[15] McBeath R, Pirone DM, Nelson CM, Bhadriraju K, Chen CS. Cell shape, cytoskeletal tension, and RhoA regulate stem cell lineage commitment. Dev Cell 2004;6:483–95. doi:10.1016/S1534-5807(04)00075-9.

[16] Kilian KA, Bugarija B, Lahn BT, Mrksich M. Geometric cues for directing the differentiation of mesenchymal stem cells. Proc Natl Acad Sci U S A 2010;107:4872–7. doi:10.1073/pnas.0903269107.

[17] Dalby MJ, Gadegaard N, Tare R, Andar A, Riehle MO, Herzyk P, et al. The control of human mesenchymal cell differentiation using nanoscale symmetry and disorder. Nat Mater 2007;6:997–1003. doi:10.1038/nmat2013.

[18] Ivanova EP, Hasan J, Webb HK, Truong VK, Watson GS, Watson JA, et al. Natural bactericidal surfaces: Mechanical rupture of pseudomonas aeruginosa cells by cicada wings. Small 2012;8:2489–94. doi:10.1002/smll.201200528.

[19] Hasan J, Webb HK, Truong VK, Pogodin S, Baulin VA, Watson GS, et al. Selective bactericidal activity of nanopatterned superhydrophobic cicada Psaltoda claripennis wing surfaces. Appl Microbiol Biotechnol 2013;97:9257–62. doi:10.1007/s00253-012-4628-5.

[20] Ivanova EP, Hasan J, Webb HK, Gervinskas G, Juodkazis S, Truong VK, et al. Bactericidal activity of black silicon. Nat Commun 2013;4:2838–44. doi:10.1038/ncomms3838.

[21] Felgueiras HP, Evans MDM, Migonney V. Contribution of fibronectin and vitronectin to the adhesion and morphology of MC3T3-E1 osteoblastic cells to poly(NaSS) grafted Ti6Al4V. Acta Biomater 2015;28:225–33. doi:10.1016/j.actbio.2015.09.030.

[22] Agarwal R, González-García C, Torstrick B, Guldberg RE, Salmerón-Sánchez M, García AJ. Simple coating with fibronectin fragment enhances stainless steel screw osseointegration in healthy and osteoporotic rats. Biomaterials 2015;63:137–45. doi:10.1016/j.biomaterials.2015.06.025.

[23] Mas-Moruno C, Fraioli R, Albericio F, Manero JM, Gil FJ. Novel peptide-based platform for the dual presentation of biologically active peptide motifs on biomaterials. ACS Appl Mater Interfaces 2014;6:6525–36. doi:10.1021/am5001213.

[24] Fromigué O, Brun J, Marty C, Da Nascimento S, Sonnet P, Marie PJ. Peptide-based activation of alpha5 integrin for promoting osteogenesis. J Cell Biochem 2012;113:3029–38. doi:10.1002/jcb.24181.

[25] Frith JE, Mills RJ, Cooper-White JJ. Lateral spacing of adhesion peptides influences human mesenchymal stem cell behaviour. J Cell Sci 2012;125:317–27. doi:10.1242/jcs.087916.

[26] Maia FR, Bidarra SJ, Granja PL, Barrias CC. Functionalization of biomaterials with small osteoinductive moieties. Acta Biomater 2013;9:8773–89. doi:10.1016/j.actbio.2013.08.004.

[27] Mas-Moruno C, Fraioli R, Rechenmacher F, Neubauer S, Kapp TG, Kessler H. $\alpha v\beta 3$- or $\alpha 5\beta 1$-Integrin-Selective Peptidomimetics for Surface Coating. Angew

Chemie Int Ed 2016:7048–67. doi:10.1002/anie.201509782.

[28] Rechenmacher F, Neubauer S, Polleux J, Mas-Moruno C, De Simone M, Cavalcanti-Adam EA, et al. Functionalizing αvβ3- or α5β1-selective integrin antagonists for surface coating: a method to discriminate integrin subtypes in vitro. Angew Chem Int Ed Engl 2013;52:1572–5. doi:10.1002/anie.201206370.

[29] Fraioli R, Rechenmacher F, Neubauer S, Manero JM, Gil J, Kessler H, et al. Mimicking bone extracellular matrix: Integrin-binding peptidomimetics enhance osteoblast-like cells adhesion, proliferation, and differentiation on titanium. Colloids Surfaces B Biointerfaces 2015;128:191–200. doi:10.1016/j.colsurfb.2014.12.057.

[30] Neubauer S, Rechenmacher F, Brimioulle R, Di Leva FS, Bochen A, Sobahi TR, et al. Pharmacophoric Modifications Lead to Superpotent αvβ3 Integrin Ligands with Suppressed α5β1 Activity. J Med Chem 2014;57:3410–7. doi:10.1021/jm500092w.

[31] Rechenmacher F, Neubauer S, Mas-Moruno C, Dorfner PM, Polleux J, Guasch J, et al. A molecular toolkit for the functionalization of titanium-based biomaterials that selectively control integrin-mediated cell adhesion. Chem - A Eur J 2013;19:9218–23. doi:10.1002/chem.201301478.

[32] Mas-Moruno C, Dorfner PM, Manzenrieder F, Neubauer S, Reuning U, Burgkart R, et al. Behavior of primary human osteoblasts on trimmed and sandblasted Ti6Al4V surfaces functionalized with integrin αvβ3-selective cyclic RGD peptides. J Biomed Mater Res A 2013;101:87–97. doi:10.1002/jbm.a.34303.

[33] Auernheimer J, Zukowski D, Dahmen C, Kantlehner M, Enderle A, Goodman SL, et al. Titanium implant materials with improved biocompatibility through coating with phosphonate-anchored cyclic RGD peptides. Chembiochem 2005;6:2034–40. doi:10.1002/cbic.200500031.

[34] Schindelin J, Arganda-Carreras I, Frise E, Kaynig V, Longair M, Pietzsch T, et al. Fiji: an open-source platform for biological-image analysis. Nat Methods 2012;9:676–82. doi:10.1038/nmeth.2019.

[35] Geetha M, Singh AK, Asokamani R, Gogia AK. Ti based biomaterials, the ultimate choice for orthopaedic implants – A review. Prog Mater Sci 2009;54:397–425. doi:10.1016/j.pmatsci.2008.06.004.

[36] Leary Swan EE, Popat KC, Desai TA. Peptide-immobilized nanoporous alumina membranes for enhanced osteoblast adhesion. Biomaterials 2005;26:1969–76. doi:10.1016/j.biomaterials.2004.07.001.

[37] Schneider GB, Zaharias R, Stanford C. Osteoblast integrin adhesion and signaling regulate mineralization. J Dent Res 2001;80:1540–4. doi:10.1177/00220345010800061201.

[38] Kilian KA, Mrksich M. Directing Stem Cell Fate by Controlling the Affinity and Density of Ligand-Receptor Interactions at the Biomaterials Interface. Angew Chemie 2012;124:4975–9. doi:10.1002/ange.201108746.

[39] Biggs MJP, Richards RG, Gadegaard N, Wilkinson CDW, Oreffo ROC, Dalby MJ. The use of nanoscale topography to modulate the dynamics of adhesion formation in primary osteoblasts and ERK/MAPK signalling in STRO-1+ enriched skeletal stem cells. Biomaterials 2009;30:5094–103. doi:10.1016/j.biomaterials.2009.05.049.
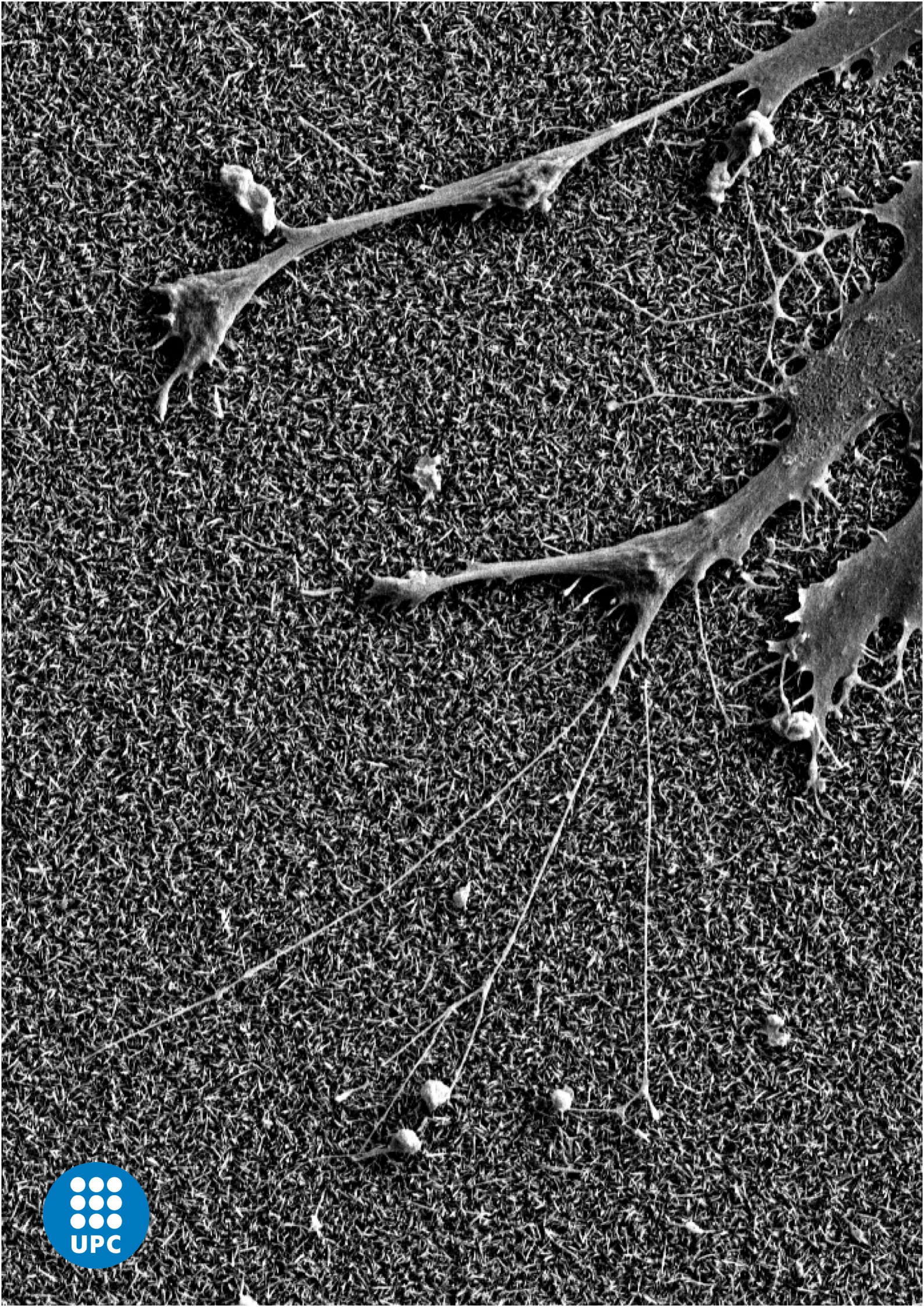
[40] Malmstroöm J, Lovmand J, Kristensen S, Sundh M, Duch M, Sutherland DS. Focal complex maturation and bridging on 200 nm vitronectin but not fibronectin patches reveal different mechanisms of focal adhesion formation. Nano Lett 2011;11:2264–71. doi:10.1021/nl200447q.